การประยุกต์ใช้ถังปฏิกิริยาฟลูอิดไดซ์เบดแบบไร้อากาศที่มีการจัดรูปแบบใหม่ในการบำบัดน้ำเสียประเภทต่างๆ

นางสาวพัชรียา รุ่งกิจวัฒนานุกูล

วิทยานิพนธ์นี้เป็นส่วนหนึ่งของการศึกษาตามหลักสูตรปริญญาวิศวกรรมศาสตรดุษฎีบัณฑิต
สาขาวิชาวิศวกรรมสิ่งแวดล้อม ภาควิชาวิศวกรรมสิ่งแวดล้อม
คณะวิศวกรรมศาสตร์ จุฬาลงกรณ์มหาวิทยาลัย
ปีการศึกษา 2559

The Various Applications of a Novel Configuration Anaerobic Fluidized Bed Reactor for Wastewater Treatment

Miss Phatchariya Rungkitwatananukul

A Dissertation Submitted in Partial Fulfillment of the Requirements
for the Degree of Doctor of Philosophy Program in Environmental Engineering
Department of Environmental Engineering
Faculty of Engineering
Chulalongkorn University
Academic Year 2016

Thesis Title	
By	Miss Phatchariya Rungkitwatananukul
Field of Study	Environmental Engineering
Thesis Advisor	Assistant Professor Chaiyaporn Puprasert, Ph.D.
Thesis Co-Advisor	Associate Professor Wiboonluk Pungrasmi, Ph.D.

Accepted by the Faculty of Engineering, Chulalongkorn University in Partial Fulfillment of the Requirements for the Doctoral Degree

.....Dean of the Faculty of Engineering
(Associate Professor Supot Teachavorasinskun, D.Eng.)

THESIS COMMITTEE

.....Chairman
(Associate Professor Sutha Khaodhiar, Ph.D.)

.....Thesis Advisor
(Assistant Professor Chaiyaporn Puprasert, Ph.D.)

.....Thesis Co-Advisor
(Associate Professor Wiboonluk Pungrasmi, Ph.D.)

.....Examiner
(Assistant Professor Sarun Tejasen, Ph.D.)

.....Examiner
(Associate Professor Tawan Limpiyakorn, Ph.D.)

.....Examiner
(Assistant Professor Benjaporn Suwannasilp, Ph.D.)

.....External Examiner
(Professor TAKASHI YAMAGUCHI, Ph.D.)

พัชรียา รุ่งกิจวัฒนานุกูล : การประยุกต์ใช้ถังปฏิกิริยาฟลูอิดไดซ์เบดแบบไร้อากาศที่มีการจัดรูปแบบใหม่ในการบำบัดน้ำเสียประเภทต่างๆ (The Various Applications of a Novel Configuration Anaerobic Fluidized Bed Reactor for Wastewater Treatment) อ.ที่ปรึกษาวิทยานิพนธ์หลัก: ผศ. ดร.ชัยพร ภู่ประเสริฐ, อ.ที่ปรึกษาวิทยานิพนธ์ร่วม: รศ. ดร.วิบูลย์ ลักษณ์ พึ่งรัศมี, 190 หน้า.

งานวิจัยนี้เป็นการศึกษาสมรรถนะของถังปฏิกิริยาฟลูอิดไดซ์เบดแบบไร้อากาศที่มีการจัดรูปแบบใหม่ ในการบำบัดน้ำเสียประเภทต่างๆ โดยการใช้เม็ดยางเป็นวัสดุตัวกลางในถังปฏิกิริยาฟลูอิดไดซ์เบดที่ช่วยลดค่าความเร็วไหลขึ้น (Up-flow velocity) ทำให้การควบคุมสภาวะฟลูอิดไดซ์เซชั่นในระบบทำได้โดยการป้อนน้ำเสียให้มีค่าความเร็วไหลขึ้นมากพอ เพื่อทดแทนการเวียนน้ำเสียภายในระบบ จึงทำให้สามารถเดินระบบได้โดยไม่จำเป็นต้องหมุนเวียนน้ำเสียภายใน ซึ่งให้ข้อดีในแง่ของการประหยัดพลังงานเมื่อเปรียบเทียบกับการเดินระบบฟลูอิดไดซ์เบดแบบดั้งเดิม อย่างไรก็ตามการเดินระบบด้วยการป้อนน้ำเสียที่มีค่าอัตราไหลขึ้นสูง ส่งผลให้ค่าระยะเวลากักเก็บน้ำเสียมีค่าลดต่ำลงมาก ดังนั้นเพื่อทดสอบสมรรถนะของถังปฏิกิริยาฟลูอิดไดซ์เบดที่มีการจัดรูปแบบใหม่จึงแบ่งการทดลองออกเป็นสามส่วน โดยการทดลองส่วนที่หนึ่ง เป็นการหารูปแบบการไหลของน้ำเสียในถังปฏิกิริยารูปแบบใหม่นี้ ซึ่งพบว่าเป็นการไหลของน้ำเสียภายในถังปฏิกิริยารูปแบบใหม่นี้ มีลักษณะเป็นแบบถัง CSTR 22 – 30 ถังต่อกันแบบอนุกรม ซึ่งใกล้เคียงกับถังปฏิกิริยาแบบท่อ (Plug flow reactor) การทดลองส่วนที่สองเป็นการศึกษาสมรรถนะของถังปฏิกิริยารูปแบบใหม่นี้ ในการบำบัดน้ำเสียที่มีค่าซีโอดีต่ำโดยมีค่าระยะเวลากักเก็บน้ำเสียเท่ากับ 50 นาที โดยการบำบัดแบบไร้อากาศ ซึ่งพบว่าระบบมีประสิทธิภาพการกำจัดซีโอดีสูงสุด เมื่อเดินระบบที่มีค่าอัตราภาระสารอินทรีย์เท่ากับ 5.6 ก.ซีโอดี/ล.-วัน โดยมีค่าการกำจัดซีโอดีเท่ากับร้อยละ 86 ± 6 การทดลองส่วนที่สามเป็นการศึกษาสมรรถนะของถังปฏิกิริยารูปแบบใหม่นี้ ในการกำจัดไนเทรตด้วยกระบวนการดีไนทริฟิเคชัน เพื่อบำบัดน้ำเสียที่มีค่าอัตราส่วนซีโอดีต่อไนเทรต เท่ากับ 1:1 2:1 3:1 5:1 และ 10:1 โดยควบคุมระยะเวลากักเก็บน้ำเท่ากับ 50 นาทีตลอดการทดลอง ซึ่งพบว่าเมื่อเดินระบบที่มีค่าอัตราส่วนซีโอดีต่อไนเทรต เท่ากับ 3:1 ระบบมีประสิทธิภาพการกำจัดไนเทรตและซีโอดีสูงสุด น้ำที่ผ่านการบำบัดแล้วมีค่าไนเทรตและซีโอดีต่ำ นอกจากนี้ในงานวิจัยยังได้ศึกษาการเปลี่ยนแปลงกลุ่มประชากรจุลินทรีย์ด้วยเทคนิค MiSeq Illumina Sequencing เพื่อศึกษาความสัมพันธ์ระหว่างประสิทธิภาพของระบบในการบำบัดน้ำเสีย และประชากรจุลินทรีย์ที่มีความโดดเด่นในการเดินระบบบำบัดน้ำเสียด้วยกระบวนการไร้อากาศและกระบวนการดีไนทริฟิเคชัน

ภาควิชา	วิศวกรรมสิ่งแวดล้อม	ลายมือชื่อนิสิต .....
สาขาวิชา	วิศวกรรมสิ่งแวดล้อม	ลายมือชื่อ อ.ที่ปรึกษาหลัก .....
ปีการศึกษา	2559	ลายมือชื่อ อ.ที่ปรึกษาร่วม .....

5471445021 : MAJOR ENVIRONMENTAL ENGINEERING
KEYWORDS: FLUIDIZED BED REACTOR / LOW STRENGTH WASTEWATER / DENITRIFICATION PROCESS / RESIDENCE TIME DISTRIBUTION / ANAEROBIC TREATMENT / MISEQ ILLUMINA SEQUENCING

PHATCHARIYA RUNGKITWATANANUKUL: The Various Applications of a Novel Configuration Anaerobic Fluidized Bed Reactor for Wastewater Treatment. ADVISOR: ASST. PROF. CHAIYAPORN PUPRASERT, Ph.D., CO-ADVISOR: ASSOC. PROF. WIBOONLUK PUNGRASMI, Ph.D., 190 pp.

In this research, the performance of a novel configuration anaerobic fluidized bed reactor (FBR) was studied for various wastewater treatment applications. According to the use of low density material as supporting media, granular rubber, providing a very low up-flow velocity for inducing fluidization state. The fluidization state inside this reactor was controlled by only feeding with wastewater flowrate. Consequently, this reactor operated without internal recirculation that provided an advantage in term of energy conservation. However, high feeding flow rate was result in a very low hydraulic retention time (HRT). Therefore, the performance of a novel configuration anaerobic FBR should be investigated. There were three experimental parts in this research. In the first part, due to the reactor configuration was modified, liquid flow pattern should be studied. The hydrodynamic behavior was investigated in a novel FBR using a residence time distribution (RTD) experiment. The RTD experimental result showed that the liquid flow pattern was closed to tanks of CSTR (22 – 30 tanks) in series or plug flow behavior. In wastewater treatment application, the novel FBR was performed under low hydraulic retention time (HRT) operation (without internal recirculation), and its performance should be further studied. To evaluate the performance of the reactor, there are two experimental approaches in this research. The first approach, a novel FBR was evaluated for low strength anaerobic wastewater treatment under 50 min of HRT. The novel FBR achieved 86 ± 6% of COD removal efficiency at an organic loading rate (OLR) of 5.6 g COD/L-d. In the second approach, a novel FBR, was performed for treating nitrate with a denitrification process at COD:NO_3^- - N of 1:1, 2:1, 3:1, 5:1 and 10:1. The highest nitrate removal efficiency was obtained at 99 ± 1%, with COD:NO_3^- - N ratio of 3:1. The effluent contained low COD and nitrate concentration. The results have confirmed that a novel FBR achieved high performance as anaerobic and denitrification reactor. Moreover, to investigate the relationships between the distribution of microbial community and reactor performance in different reactor operation, this study performed 16S rRNA gene sequencing analysis from granular sludge. The results showed that different OLRs and COD to nitrate ratios affected to dominant microbial community distribution.

Department:	Environmental Engineering	Student's Signature	.....
Field of Study:	Environmental Engineering	Advisor's Signature	.....
Academic Year:	2016	Co-Advisor's Signature	.....

ACKNOWLEDGEMENTS

First of all, I would like to thank to my advisor, Asst. Prof. Chaiyaporn Puprasert, and my co-advisor, Assoc. Prof. Wiboonluk Pungrasmi, my deepest gratitude and respect. I feel honored and very fortunate to be their student. Without them, I would not have been able to complete a dissertation of this quality and depth. I received insightful academic guidance from them, and learnt much from their endless passion and rigorous attitude towards research. I really appreciate their patience and understanding when I face difficulties in my research and personal life.

I am very thankful for the support and advice from all the members of my dissertation committee: Prof. Yamaguchi Takashi, Assoc. Prof. Sutha Khaodhiar, Asst. Prof. Saran Tejasen, Assoc. Prof. Tawan Limpiyakorn and Assist. Prof. Benjaporn Suwannasilp. Each of them brought a unique set of experiences and ideas, and my dissertation has greatly benefited from this cooperation.

I would like to acknowledge Assoc. Prof. Hatamoto Masashi and Mr. Hirakata Yuga from Aqua & Soil Environmental Laboratory, Department of Environmental Systems Engineering, Nagaoka University of Technology, Japan for fulfill my dissertation.

I am equally grateful for the help and friendship of my colleagues and stuffs of Department of Environmental Engineering, Faculty of Engineering, Chulalongkorn University and member of Aqua & Soil Environmental Laboratory, Department of Department of Environmental Systems Engineering, Nagaoka University of Technology, Japan.

Last but not least, thank you my dear parents, raising me, loving me and teaching me the wisdom of life. Your support has allowed me to face all challenges bravely and never give up my dreams.

CONTENTS

Page

THAI ABSTRACT iv

ENGLISH ABSTRACT v

ACKNOWLEDGEMENTS vi

CONTENTS vii

List of Tables XII

List of Figures XIV

CHAPTER 1 RESEARCH RATIONALE 1

1.1 Introduction 1

1.2 Overall research outline 2

1.3 Research hypotheses 5

1.4 Research objectives 5

CHAPTER 2 RESEARCH BACKGROUND 7

2.1 Fluidized bed reactor 7

2.1.1 Minimum fluidization velocity 7

2.1.2 Terminal fluidization velocity 11

2.1.4 Anaerobic fluidized bed reactor 12

2.1.5 The advantage and disadvantage of anaerobic fluidized bed 15

2.1.6 Supporting media for fluidized bed reactor 15

2.2 Anaerobic process 17

2.2.1 Low strength wastewater 19

2.2.2 Anaerobic treatment for low strength wastewater 20

2.2.2.1 Substrate concentration 20

Page

2.2.2.2 Methane production 21
2.2.3 Effect of environmental parameters on anaerobic treatment 22
2.2.4 Anaerobic fluidized bed reactor using crumb rubber granule as a media 23
2.2.5 Bacteria and archaea community in wastewater treatment 24
2.3 Biological denitrification process 25
2.3.1 Nitrate-rich wastewater 29
2.3.2 External carbon source for denitrification 29
2.3.3 Factor controlling denitrification 31
2.3.4 Denitrification fluidized bed reactor using crumb rubber granule as a media 32
2.3.5 Denitrifying bacteria 34
CHAPTER 3 HYDRODYNAMIC BEHAVIOR STUDY IN A NOVEL ANAEROBIC FBR USINGRESIDENCE TIME DISTRIBUTION (RTD) 36
3.1 Introduction 36
3.2 Research scope 37
3.3 Materials and Methods 38
3.2.2 Reactor configuration and operation 38
3.2.1 Supporting media in a novel FBR 41
3.2.3 Experimental determination of residence time distribution (RTD) 42
3.3 Results and discussion 43
3.4 Conclusion 46
CHAPTER 4 A NOVEL ANAEROBIC FLUIDIZED BED REACTORS USING RUBBER GRANULE AS A MEDIA FOR LOW STRENGTH WASTEWATER TREATMENT 47

Page

4.1 Introduction 47

4.2 Research objectives 49

4.3 Research approaches 49

4.4 Experimental scope 49

4.5 Material and Methods 50

4.5.1 Reactor configuration and experimental set-up 50

4.5.1 Synthetic wastewater preparation and operational conditions 53

4.5.2 Process parameters 54

4.5.3 Microbial community analysis 55

4.6 Results and discussions 58

4.6.1 Start-up period for biofilm formation 58

4.6.2 Performance of a novel FBR for low-strength anaerobic wastewater treatment 58

4.6.2.1 COD removal efficiency 58

4.6.2.2 Methane gas production 60

4.6.2.3 ORP, pH, volatile fatty acid and total alkalinity 61

4.6.2.3 Suspended solid 63

4.6.3 COD removal profiles and process parameters along the reactor height in the novel FBR for treating low-strength wastewater 64

4.6.4 Microbial community distribution analyzed using MiSeq Illumina technique 67

4.7 Conclusions 73

CHAPTER 5 A NOVEL FBR USING RUBBER GRANULE AS A MEDIA FOR DENITRIFICATION PROCESS AT DIFFERENT COD TO NITRATE RATIOS 74

Page

5.1 Introduction 74

5.2 Research objectives 76

5.3 Research approaches 76

5.4 Experimental scope 76

5.5 Material and Methods 77

5.5.1 Reactor configuration and operation 77

5.5.2 Supporting media 81

5.5.3 Operational conditions 81

5.5.4 Synthetic wastewater preparation 82

5.5.5 Liquid samples 83

5.5.6 Granular sludge samples 84

5.5.7 Microbial community analysis 85

5.6 Results and Discussion 87

5.6.1 Performance of a novel FBR for denitrification at different COD:NO_3^--N ratios 88

5.6.1.1 Nitrate and COD removal efficiency 88

5.6.1.2 pH, volatile fatty acid and total alkalinity 93

5.6.1.3 Total suspended solid 95

5.6.1.4 Nitrite and ammonia accumulation 96

5.6.1.5 Profiles of nitrate and COD removal at several levels along the reactor height at different COD:NO_3^--N ratios 97

5.6.1.6 Relationship between environmental parameters and microbial community distribution along the reactor height at different COD:NO_3^--N ratios. 99

Page

5.6.2 Performance of a novel FBR under a carbon step feeding concept 107
5.6.2.1 The performance of a novel FBR in initial state 108
5.6.2.3 Effect of low carbon source on the performance of a novel FBR 109
5.6.2.4 Performance of the novel FBR in carbon source step feeding.... 111
5.6.2.5 Effect of carbon step feeding on the performance of the novel FBR 114
5.6.2.6 Profiles of substrate concentration and process parameters at several levels along the reactor height: a comparison between before and after carbon step feeding condition..... 116
5.7 Conclusions 122
Chapter 6 CONCLUSIONS AND RECOMMENDATIONS 124
6.1 Conclusions 124
6.2 Recommendations 125
REFERENCES 127
APPENDIX 138
Appendix A 139
Appendix B 143
Appendix C 159
VITA 190

List of Tables

Page

Table 2.1 Examples of process operating conditions and performance for anaerobic FBRs. 13

Table 2.2 Studies of anaerobic fluidized bed treatment on laboratory/pilot scale. ... 14

Table 2.3 Classification of wastewater strength and examples. 20

Table 3.1 The parameters values used for calculating minimum and terminal fluidizing velocity. 39

Table 3.2 Properties of granular rubber used in this study. 41

Table 3.3 The condition and model analysis results of a novel configuration FBR. 46

Table 4.1 The parameters values for calculating minimum and terminal fluidizing velocity. 51

Table 4.2 The compositions of synthetic wastewater in denitrification and anaerobic treatment. 54

Table 4.3 Analytical methods and sensors or meters used. 55

Table 4.4 The reactor performance of a novel configuration anaerobic FBR for treating low strength wastewater. 60

Table 4.5 Average (±SD) of process parameter results from a novel FBR for treating low-strength wastewater under anaerobic treatment. 62

Table 4.6 Biomass yields and effluent suspended solid at different OLRs 64

Table 5.1 The parameters values for calculating minimum and terminal fluidizing velocity. 78

Table 5.2 Properties of crumb rubber granule used in this study. 81

Table 5.3 The composition of synthetic nitrate-rich wastewater 83

Table 5.4 Analytical methods and sensors or meters used. 84

Table 5.5 Average values of substrate concentrations and removal efficiencies at different COD:NO_3^--N ratios. 90

Table 5.6 The performance of the novel FBR and the conventional FBR (with recirculation) using crumb rubber granule as a media. 91

Table 5.7 pH, Total alkalinity and Total VFA in a novel FBR for treating various COD to nitrate ratios wastewater 94

Table 5.8 Yield and suspended solid at different COD : NO_3^- - N ratios. 96

Table 5.9 Nitrite and ammonia concentration at COD : NO_3^--N ratios of 1:1, 2:1, 3:1, 5:1 and 10:1 97

Table 5.10 Process parameter values at initial state 108

Table 5.11 Average value of process parameter results at COD/NO_3^- -N as 1:1 111

Table 5.12 Average parameter results at different COD:NO_3^- -N as 3.6:1 113

List of Figures

Page

Figure 1.1 Flow chart of overall research approaches..... 4

Figure 2.1 The two force that influence to the carrier particle in fluid. 8

Figure 2.2 Exponent m in correlation for bed expansion (McCabe et al. (1993a) 12

Figure 2.3 Steps of organic digestion in anaerobic process. (Modified from Metcalf & Eddy, 2003)..... 18

Figure 2.4 Fraction of methane production which is lost as dissolved in the effluent, as a function of the influent COD (Takayuki, 1994). 21

Figure 2.5 The change in nitrogen oxidation state during nitrification and denitrification. Modified from *(Cloete and Muyima, 1997)* 26

Figure 2.6 The electron transport system under oxic and anoxic conditions using O_2 and NO_3^- as electron acceptor. Modified from *(Cloete and Muyima, 1997)*..... 27

Figure 2.7 Phylogenetic tree of the major phyla of wastewater denitrifying bacteria constructed by the neighbor-joining method on the basis of 1003 partial 16S rDNA sequences (> 500 bp) retrieved from GenBank. Special carbon assimilating populations: - Methanol; x - Acetate; o - Glycerol; Δ - Methane (DeSantis *et al.*, 2006b; Letunic and Bork, 2011a; Lu *et al.*, 2014). 34

Figure 3.1 Framework of hydrodynamic behavior in a novel configuration anaerobic FBR. 38

Figure 3.2 Side view and top view of a novel configuration anaerobic FBR used in this study. 40

Figure 3.3 Schematic diagram of a novel configuration anaerobic FBR for RTD experiment. 41

Figure 3.4 Pictures of granular rubber used as a media in a novel configuration anaerobic FBR. 42

Figure 3.5 The variation of experimental exit age distribution in a novel configuration anaerobic FBR, (a) 50 L/d, (b) 60 L/d and (c) 70 L/d..... 44

Figure 4.1 Framework of experimental study for low strength anaerobic wastewater treatment. 50

Figure 4.2 Side view and top view of a novel configuration anaerobic FBR used in this study. 52

Figure 4.3 Schematic diagram of a novel FBR for low strength anaerobic wastewater treatment, (a) performance of the reactor study, (b) profiling of substrate removed study and (c) distribution of microbial community study..... 53

Figure 4.4 Steps of DNA extraction and PCR analysis for sludge samples from low-strength anaerobic wastewater treatment 57

Figure 4.5 Influent and effluent COD at OLR of 18.6, 9.4, and 5.6 g COD/L-d. 59

Figure 4.6 Influent and effluent quality with operation time at various OLR operation. 63

Figure 4.7 Profiling of COD concentration, pH and ORP at several levels along the reactor height, OLR 5.6 g COD/L-d (a), OLR 9.4 g COD/L-d (b), and OLR 18.6 g COD/L-d (c). 66

Figure 4.8 Microbial distribution in a novel FBR for treating low-strength wastewater at various OLRs, (a) Phylum level and (b) Class level. 67

Figure 4.9 Microbial diversity and distribution in a novel FBR at different OLRs. Circle sizes relate to abundance rate, as shown in the bottom of the figure..... 71

Figure 4.10 Redundancy analysis of microbial community and environmental analysis in sludge sample at different COD:NO_3^- -N ratios. 72

Figure 5.1 Framework of denitrification process at different COD:NO_3^- - N ratios. 77

Figure 5.2 Side view and top view of a novel anaerobic FBR used in this study. 79

Figure 5.3 Schematic diagram of a novel FBR for denitrification process, (a) performance of the reactor study, (b) profiling of substrate removed study and (c) microbial community distribution study.....80

Figure 5.4 Picture of crumb rubber granule used as media in the new configuration fluidized bed reactor. 81

Figure 5.5 Steps of DNA extraction and PCR analysis for sludge samples from low-strength anaerobic wastewater treatment. 86

Figure 5.6 Granular rubber bed (without biofilm) and biofilm formation after start-up period. 88

Figure 5.7 Influent and effluent nitrate concentration and nitrate removal efficiencies at different COD:NO_3^- - N ratios. 89

Figure 5.8 Influent and effluent COD concentration and COD removal efficiencies at different COD:NO_3^- - N ratios. 90

Figure 5.9 Removed and remained substrate concentration at different COD to nitrate ratios. Data are shown as the mean ± 1SD. 93

Figure 5.10 Effluent suspended solid from different COD:NO_3^- - N ratios. 95

Figure 5.11 The profiles of nitrate and COD concentrations at different levels along the reactor height.....98

Figure 5.12 Profiles of (a) nitrate removal, (b) COD removal, (c) pH, (d) ORP, (e) total VFA and, (f) alkalinity from sampling ports P1, P2, P6, and P10 at different COD:NO_3^--N ratios.....100

Figure 5.13 Relative abundance of (a) predominant phyla and (b) microorganism classes at different COD:NO_3^--N ratios. 102

Figure 5.14 Microbial diversity and distribution in the novel FBR at different COD:NO_3^--N ratios. Circle sizes relate to abundance rate. 104

Figure 5.15 Principal component analysis plots of microbial community in the (A) Order level, (B) Family level, and (C) OTU level.....105

Figure 5.16 Redundancy analysis of microbial community and environmental analysis in sludge sample at different COD:NO3- - N ratios. 106

Figure 5.17 process parameter results at COD:NO_3^- -N as 1:1 110

Figure 5.18 The novel FBR with carbon step feeding concept for treating different COD/NO_3^- -N ratios (a) influent and effluent nitrate and (b) influent and effluent COD..... 112

Figure 5.19 COD and nitrate removal efficiencies for treating different COD:NO_3^- -N ratios and for the carbon step feeding to the novel FBR. 115

Figure 5.20 Total suspended solid in the novel FBR for treating different COD:NO_3^- -N ratios and for the carbon feeding concept. 116

Figure 5.21 Profiles of substrate concentration at several levels along the reactor height at (a) COD:NO_3^- -N of 3:1 and (b) COD:NO_3^- -N of 3.6:1 (carbon step feeding condition). 117

Figure 5.22 Microbial distribution in phylum level from different operational conditions (a) COD:NO_3^- - N ratio of 3:1 and (b) carbon step feeding. 119

Figure 5.23 Microbial distribution in class level from different operational conditions (a) COD:NO_3^- - N ratio of 3:1 and (b) carbon step feeding. 121

CHAPTER 1
RESEARCH RATIONALE

1.1 Introduction

Fluidized Bed Reactor (FBR) can be classified as an attached growth bioreactors. Small materials are used as fluidized media for microbial attachment and keep active biomass inside the reactor. Generally, biomass content is in a range of 15 to 30 g VSS/L. The FBR has many advantages, such as high stability for treating wastewater under extreme condition and needs small space for the treatment system. Moreover, FBR can be operated under low hydraulic retention time (HRT) due to high amount of active microorganisms and high internal recirculating flow rate. The operation of FBR has main disadvantage in terms of more energy consumption for controlling the fluidization state. In conventional FBR, feeding velocity combining with internal recirculating velocity are used for inducing fluidization state inside the reactor. High up-flow velocity is needed to provide dilution of substrate near the inlet, but it also reduces benefits of a plug-flow regime (Rittmann and McCarty, 2001). The selection of supporting media is an important factor to achieve high performance of FBR. Size and density of material affect the control of fluidization state. Higher density or larger particle size causes high up-flow velocity for internal recirculating, resulting in high energy consumption.

The performance of the FBR using various supporting media has been studied (Borja *et al.*, 1995; Kida *et al.*, 1990b). The results showed that rough surface media provided higher performance than smooth surface media, and high specific surface area did not relate to the reactor performance. However, the key factor is the selection of light density material as media, which provide optimum surface area for microbial adhesion.

Rubber granule is an alternative material used as media in FBR. It has low density and has been proved as the optimum media in anaerobic wastewater

treatment. Moreover, previous research has found that rubber granule can be used as media in a conventional anaerobic and denitrifying FBRs. The fluidization state can be controlled under low up-flow velocity when using rubber granule as media. The result showed high performance in term of COD and nitrate removal efficiencies under low COD to nitrate ratios (Horkam, 2011; Sirinukulwattana *et al*., 2013). This idea leads to the development of new configuration anaerobic FBR (without internal recirculation). The reactor operation occurred when the feeding flow increased as high as the recirculating flow. Thus, the recirculating pump is unnecessary for this reactor and only feeding pump will be operated to control the fluidization state inside the reactor. The application of feeding pump is for feeding substrate and inducing the fluidized media bed. This type of reactor is called a novel FBR. Due to the change of the reactor configuration, hydrodynamic behavior is examined to study the liquid flow pattern in the reactor used in this research. Although a novel FBR has advantage for its low energy consumption, the reactor must be operated under a very low HRT. Thus, the performance in wastewater treatment application was investigated. A novel FBR was evaluated in two applications. The first is low-strength anaerobic wastewater treatment and the second is nitrate reduction by denitrification process.

1.2 Overall research outline

For the performance in wastewater treatment, this research approach consists of three experimental parts. The first experimental part was to examine the hydrodynamic behavior of a novel FBR. The second part was to study the performance of a novel FBR using rubber granule as media for treating low-strength wastewater under anaerobic condition. The third part was to study the performance of a novel FBR for denitrification process. The overall research outline is shown in Figure 1.1.

Part 1: Hydrodynamic behavior study.

This experiment was set to study different liquid flow rate. In this part, residence time distribution (RTD) was a tool to examine the liquid flow pattern, mixed flow volume, plug flow volume and dead zone volume.

Part 2: Low-strength anaerobic wastewater treatment.

The experiment consisted of the start- up period of anaerobic FBR with enrichment culture to promote anaerobic bacteria adhered on the supporting media. After steady state, the performance of a novel FBR was investigated for treating low-strength wastewater. Wastewater with various COD concentrations was fed to examine substrate removal efficiency at low HRT. The COD removal was focused on at different part of the reactor column by determining the substrate concentration at several ports along the reactor height. Moreover, the distribution of microorganisms was studied via MiSeq Illumina technique.

Part 3: Nitrate reduction at different COD to nitrate ratios.

In this part, the reactor was set-up to promote the bacterial growth on supporting media. After steady state, wastewater with various COD:NO_3^- - N ratios was fed to the reactor. To study the performance of a novel FBR for denitrification, various concentrations of external carbon source were fed to study the optimum concentration that appropriates for the nitrate content in wastewater. Glucose was selected as external carbon source and sodium nitrate chosen as nitrate source. In this experiment, the performance of FBR was investigated at different ratios of COD to nitrate. The COD and nitrate removal was examined at different parts along the reactor height. Moreover, the distribution of microorganisms was studied via MiSeq Illumina technique.

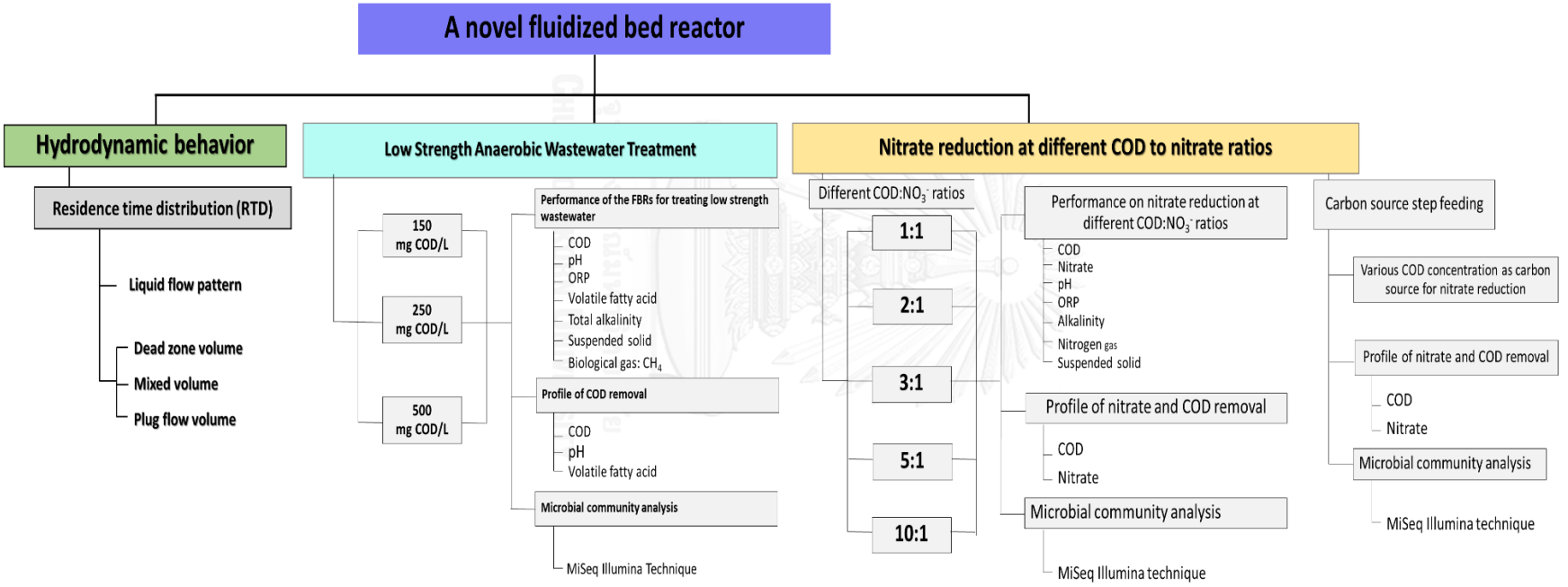

Figure 1.1 Flow chart of overall research approaches.

1.3 Research hypotheses

1) The novel configuration anaerobic FBRs using rubber granule as media can control the fluidization state without internal recirculation.
2) The novel configuration anaerobic FBRs can provide high performance in low-strength wastewater treatment under a very short hydraulic retention time.
3) The novel configuration anaerobic FBRs can provide high nitrate removal efficiency by attached growth denitrifying bacteria under low carbon concentration.
4) The novel configuration anaerobic FBRs can result in different microbial distribution at different levels of the reactors under low-strength wastewater treatment.
5) The novel configuration anaerobic FBRs can result in different microbial distribution at different levels of the reactors under different COD to nitrate ratios.

1.4 Research objectives

1) To study the hydrodynamic behavior of a novel configuration anaerobic FBR using RTD experiment.
2) To evaluate the performance of a novel configuration anaerobic FBR in term of COD removal efficiency for treating low-strength wastewater.
3) To study the profile of COD removal and microbial community distribution in a novel configuration anaerobic FBR under different OLR operation.
4) To evaluate the performance of a novel configuration anaerobic FBR in terms of COD and nitrate removal efficiencies for treating wastewater with different COD:NO_3^--N ratios.

5) To study the profile of COD and nitrate removal and microbial community distribution inside a novel configuration anaerobic FBR for treating wastewater with different COD:NO_3^--N ratios.

CHAPTER 2
RESEARCH BACKGROUND

2.1 Fluidized bed reactor

A fluidized bed reactor (FBR) contains small media, such as sand or granular activated carbon, which is a supporting material for bacterial adhesion. FBR differs from the packed-bed reactor due to its high bed expansion and wastewater up-flow velocity. Bed expansion is created to provide large pore space that reduces clogging and short-circuiting inside the reactor. Moreover, it can increase contact opportunity between microorganism and wastewater. The smaller supporting media size provides higher specific surface area. This results in a good performance of fluidized bed reactors.

In wastewater treatment, FBR is used for both aerobic and anaerobic processes. It can control the fluidization state by maintaining the up-flow velocity. There are three forces that occurring in the fluidization state: drag forces, buoyant force and up-flow velocity of liquid (as shown in Figure 2.1)

To control the fluidization state, there are two forms of up-flow velocity: minimum fluidization velocity and terminal fluidization velocity. The description of them is as shown below.

2.1.1 Minimum fluidization velocity

The minimum fluidization velocity is a crucial parameter needed for the design of any fluidization operation. The resulting minimum fluidization velocity depends upon fluidized media, including shape, size and density. The density, for example, directly alters the net gravitational force acting on the media, and hence the minimum drag force, or velocity, needed to lift the media. The shape alters not only the relationship between the drag force and velocity, but also the packing properties of the fixed bed and the associated void spaces and velocity of fluid through them.

The minimum fluidization velocity can be basically calculated by balancing all forces that react to the supporting media. Generally, the carrier media are contained in the fluid, which have two forces, gravity force and drag force, acting on them (McCabe *et al.*, 1993b) (as shown in Figure 2.1).

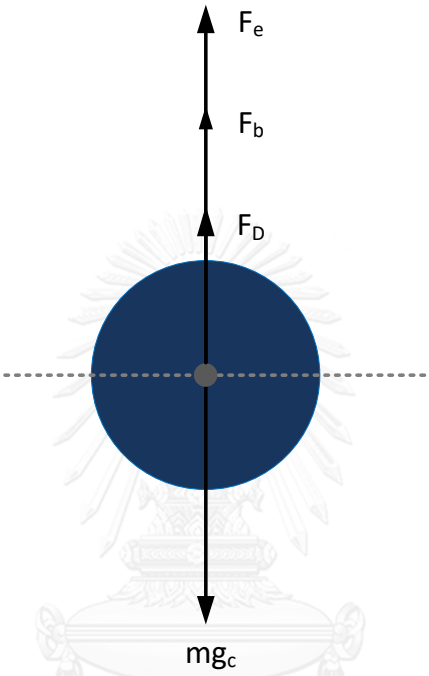

Figure 2.1 The two force that influence to the carrier particle in fluid.

If the liquid flow through media, the force will effect to the body showed in Eq. (2.1)

$$\frac{m}{g_c}\frac{du}{dt} = F_e + F_b + F_D \qquad 2.1$$

Where,

m = mass of immerse body

g_c = Newton's-law proportionality factor (32.174 ft-bl/bl$_f$-s^2)

F_e = External force (N)

F_b = Buoyant force (N)

F_D = Drag force (N)

F_e, F_b , and F_D we can find from the Eq. (2.2), (2.3), and (2.4), respectively.

$$F_e = \frac{ma_e}{g_c} \quad (2.2)$$

$$F_b = \frac{m\rho a_e}{\rho_p g_c} \quad (2.3)$$

$$F_D = \frac{C_D u_0^2 \rho A_p}{2g_c} \quad (2.4)$$

Where,

a_e = Acceleration of particle from external force, m/s^2

ρ = density of fluid, g/m^3

ρ_p = density of particle, g/L

C_D = Drag coefficient, dimentionless

u_0 = Velocity of approaching steam, m/s

A_p = Projected area of particle, m^2

An equation for the minimum fluidization velocity can be obtained by setting the pressure drop across the bed. It's equal to the weight of the bed per unit area of cross section that allows the buoyant force of the displaced fluid. The Ergun's equation

for pressure drop in packed beds in Eq. (2.5) can be rearranged to Eq. (2.6) (McCabe *et al.*, 1993b).

$$\frac{\Delta\rho}{L} = \frac{150\bar{V}_0\mu}{g_c\emptyset_S^2 D_p^2}\frac{(1-\varepsilon)^2}{\varepsilon^3} + \frac{1.75\rho\bar{V}_0^2}{g_c\emptyset_S D_p}\frac{1-\varepsilon}{\varepsilon^3} \quad (2.5)$$

$$\frac{150\mu\bar{V}_{0M}}{\emptyset_S^2 D_p^2}\frac{(1-\varepsilon)}{\varepsilon_M^3} + \frac{1.75\rho\bar{V}_{0M}^2}{\emptyset_S D_p}\frac{1}{\varepsilon_M^3} = g(\rho_p - \rho) \quad (2.6)$$

The equation derived for the minimum fluidizing velocity is applied to liquids as well as to gases. However, $\bar{V}_{0M}$ of fluidized bed with liquid or gas are quite different. Fluidizing sand with water, the particles will move farther apart and their motion becomes more vigorous as the velocity increases. However, the average bed density at a given velocity is the same in all sections of the bed. This condition is called "particulate fluidization".

In this research, crumb rubber granule is chosen as the media. Therefore, from Eq. (2.6), the minimum fluidization velocity and terminal fluidization velocity can be calculated as below:

The quantities needed are:

μ = Absolute viscosity (0.01 cm^3/s)

$\Delta\rho$ = Density difference (1.2 – 1.0 = 0.2 g/cm^3)

D_p = diameter of spherical particle (0.043 cm)

ε_M = minimum porosity for fluidization (0.4)

$\emptyset_s$ = Sphericity, defined by $\frac{S_p}{v_p} = \frac{6}{\emptyset_s D_p}$

v_p = Volume of single particle, ft^3 or m^3

S_p = Surface area of single particle, m^2 or ft^2

g = Gravitational acceleration, m/s^2 or ft/s^2 (9.80 m/s^2)

Bed expansion = 50 percent

2.1.2 Terminal fluidization velocity

The terminal fluidizing velocity can be calculated by the finding of maximum porosity of fluidization as shows in (2.7) and Eq. (2.8).

$$L = L_M \frac{1-\varepsilon_M}{1-\varepsilon} \tag{2.7}$$

$$\left(\frac{\varepsilon}{\varepsilon_M}\right)^m = \frac{V_0}{V_{0m}} \tag{2.8}$$

Where,

L = Total height of fluidized bed at the terminal fluidizing velocity

L_M = Bed height at incipient fluidization

ε_M = minimum porosity for fluidization

ε = maximum porosity

$\nu_\circ$ = Terminal fluidizing velocity

The expanded bed height may be obtained from ε and the values of L and ε_M (incipient fluidization), using the Eq. (2.8). So, the ε is 0.6.

From the Stoke's law, the Reynold's numbers can be approached by the Eq. (2.9).

$$N_{Re,p} = \frac{D_p V_{0M} \rho_p}{\mu} \quad (2.9)$$

When, $N_{Re,p}$ = Reynold's numbers

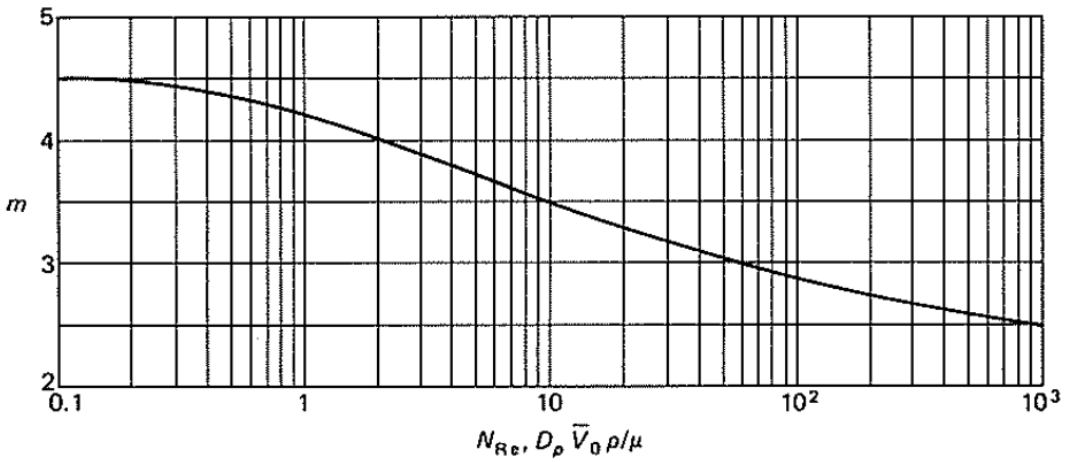

Figure 2.2 Exponent m in correlation for bed expansion (McCabe et al. (1993a)

2.1.4 Anaerobic fluidized bed reactor

The design of attached growth anaerobic fluidized bed reactor (FBR) is similar to physical design for up-flow expanded bed reactor. The FBR is operated at high up-flow velocity of approximately 20 m/h (using sand as a media) to provide 100 percent of bed expansion. Normally, to keep the stability of fluidization state, 150 percent of the bed expansion is recommended.

Activated carbon has been considered as media in FBRs. The mean diameter of the granular activated carbon particle is recommended at 0.6 - 0.8 mm, providing the up-flow velocity of 20 to 24 m/h. However, the limitation of using activated carbon is the cost (Metcalf & Eddy, 2003). Anaerobic FBR performance data with various types of wastewater is presented in Table 2.1. Summary of carrier particle studied for various industrial and synthetic wastewater is shown in Table 2.2.

Table 2.1 Examples of process operating conditions and performance for anaerobic FBRs.

Wastewater	Temperature (°C)	COD loading (kg/m^3-d)	HRT (hour)	COD removed (%)
Citric acid	35	42	24	70
Starch, whey	35	8.2	105	99
Milk	35	3-5	12-18	71-85
Molasses	35	12-30	3-8	50-95
Glucose	35	10	12	95
Sulfide, pulp	35	3-18	3-62	60-80

Metcalf & Eddy, 2003

Table 2.2 Studies of anaerobic fluidized bed treatment on laboratory/pilot scale.

		Reactor			Carrier			Operating condition					Methane gas		
Type of wastewater	Diameter (m)	Height (m)	volume (m^3)	Volume of fluidized bed (%)	type	Diameter (mm)	Feed concentration (mg/L)	COD loading rate (kgm^3/day)	Superficial Velocity (m/hr)	Temperature (° C)	pH	HRT (hour)	COD removal (%)	Biogas rate m^3	Methane
Glucose	0.08	1	).0015x10	33	Perlite	0.968	12500	3.27-5.75	8.64	35	6.5-7.0	20-32	85-90	0.0026	-
Sucrose	0.066	0.75	0.002	25	Biolite	0.3	2500	25	10	35	7	4.8-72	80	-	70
Vinasse	0.115	1.5	0.015	15-70	Granular Pozzolana	0.3-0.45	2500	20-32	15-Jun	35	6.7-7.0	4	70-75	-	-
Brewery wastewater	0.16	3	0.06	0.06	Sand	0.5	90000	8-14	30	35	6.8-7.4	4.8-33	75	0.35	78-88
Fruit process wastewater	0.001	-	0.001	-	Saponite	0.4-0.8	5100	0.0025	-	35	7-7.6	60-300	97.7-99.2	1.95	-
Municipal wastewa	0.05	0.55	0.002	75	Sand	0.2	1600	4-24	50	35	7	May-68	75	0.365	-

Modified from (Saravanane and Muthy, 2000)

2.1.5 The advantage and disadvantage of anaerobic fluidized bed

The FBR gives many potential advantages over other high rate anaerobic reactors such as up-flow anaerobic sludge blanket (UASB) reactor, filter reactor and down-flow stationary fixed film reactor (DSFF). The details are as followed,

- High sludge activity
- High treatment efficiency
- No clogging of reactors
- No problems of sludge retention
- Less chance for organic shock loads and gas hold up
- Small area requirements

Certain reviews have found that the major disadvantages were high energy consumption due to very high liquid re-circulation ratio and high investment cost for liquid distribution in order to obtain uniform fluidization especially in a large scale plant.

2.1.6 Supporting media for fluidized bed reactor

In order to control the fluidization conditions, adequate flow is needed to induce and maintain fluidization state. From the calculation of minimum fluidization velocity (as shown in Eq. (2.6)), it can be seen that the velocity is depended on the size and density of the carrier particle.

The settling velocity of bioparticles (media and biofilm) will later decrease when the thickness of biofilm increases. The larger particles will initially move to the top of the reactor where the surrounding contains low substrate concentration. This phenomenon leads to the decrease in their size. Finally, it will move downward (as density increases) into a region of higher substrate concentration. Bioparticles with thin biofilms, in contrast, move toward the bottom of the bed, where they are exposed to high substrate concentrations causing more rapid growth and increase in size. The

resulting situation is unstable, including motion within the bed which will lead to ultimately uniform bioparticle size throughout the bed.

Bioparticles built up from low-density carrier particles are similar to the biofilm itself. The fluidized bed tends to stratify because the density of carrier particles does not significantly change as the biofilm grows, only the diameter changes. This is true for bioparticles without supporting materials, such as UASB granules. In that case, larger particles have a higher settling velocity, causing them to move to the bottom of the bed, where they are exposed to higher substrate concentration, leading them to grow even larger. On the other hand, smaller particles move to the top where they are exposed to less substrate, which causing the biofilm to grow more slowly or decreases in size due to decay and shear on the surface. Consequently, bed stratification is a common occurrence. The above analysis is based on the assumption of a uniform carrier particle size. In reality, however, there can be significant differences in carrier particle size. As a consequence, larger particles are forced to stay at the bottom where they accumulate biofilm beyond the optimum thickness, while smaller carrier particles migrate to the top where they can be ineffectually cycled through the biomass wastage device. For this reason, it is important for FBRs to have a uniform particle size.

In the past, sand and activated carbon were popular media for the reactor. The recommended size is in the range of 0.4 to 0.5 mm. Up-flow velocity of 30-36 m/h could be obtained when sand was used as a media (Metcalf&EddyInc., 2003). The recommended surface area is about 1000 m^2/m^3 of reactor volume, which was greater than other fixed film packing process.

However, the limitation of successful application of FBR technology is the control of biofilm attachment on supporting carrier media. Therefore, supporting media is an important factor for achieving high-efficiency wastewater treatment reactor.

There are many research works focusing on the optimum media in FBRs (for anaerobic wastewater treatment), such as cristobalite, zeolite, vermiculite, granular active carbon, granulated clay, pottery stone, volcanic ash and slag. Results indicated that rough surface media (cristobalite) could provide higher performance than high

specific surface area (for example granular activated carbon) with smooth surface area (Kida *et al.*, 1990b). Using kaoline, pozzolana and biolite as media provided similar COD removal efficiencies. This study shows that the rough surface carrier particle encourages microbial adhesion (Calderon *et al.*, 1996).

Crumb rubber granules has been proved as a good media that can be used as bacterial supporting particle in anaerobic treatment process. It has suitable surface and non-toxic for microbial adhesion (Park et al., 2006). Moreover, crumb rubber granules have been proved as a good media in anaerobic FBR for treating high organic loading rate (OLR) and for denitrification. The results showed that the rubber granules have endured 2-year reactor operation without cracking (Horkam, 2011; Rungkitwatananukul, 2010).

2.2 Anaerobic process

Anaerobic digestion occurs in an oxygen-absent condition. Substrates are converted to gases which release to the atmosphere. There are 4 steps in anaerobic process: hydrolysis, acidogenesis, acetogenesis and methanogenesis (as illustrated in Figure 2.3).

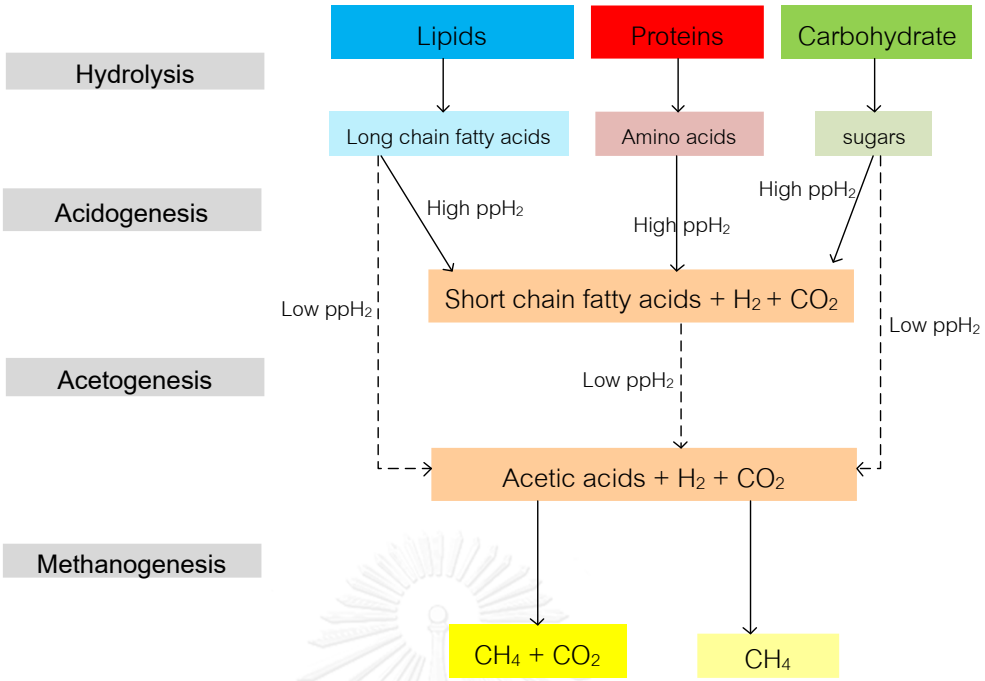

Figure 2.3 Steps of organic digestion in anaerobic process.
(Modified from Metcalf & Eddy, 2003).

1) Hydrolysis is a process that transforms large complex and undissolved substrates (for example carbohydrates, proteins and lipids) to small dissolved organic compounds (sugar, amino acid and long chain fatty acids), which capable of passing through cell walls and membranes of fermentative bacteria.

2) Acidogenesis state, where the dissolved compounds present in cells of fermentative bacteria are converted into simple compounds. Acid is produced, depending on hydrogen partial pressure. In the low hydrogen partial pressure, the products are acetic acid, hydrogen and carbon dioxide as shown in Eq. (2.10), while propionic acid is produced under the high hydrogen partial pressure (Eq. (2.11)).

$$C_6H_{12}O_6 + 2H_2O \rightarrow 2CH_3COOH + 2CO_2 + 4H_2 \quad (2.10)$$

$$C_6H_{12}O_6 \rightarrow CH_3CH_2COOH + CH_3COOH + 2CO_2 + H_2 \quad (2.11)$$

3) Acetogenesis, where obligate hydrogen-producing acetogenic bacteria convert the digested products into acetate, carbondioxide and hydrogen, as shown in Eq. (2.12) and (2.13).

$$CH_3CH_2COOH + H_2O \rightarrow CH_3COOH + CO_2 + 3H_2 \quad (2.12)$$

$$CH_3CH_2CH_2COOH + H_2O \rightarrow 2CH_3COOH + 2H_2 \quad (2.13)$$

4) Methanogenesis, which converts acetate to biological gas (methane, and carbon dioxide) by two pathways; (1) methane can be produced by acetoclastic methanogen using acetate as a substrate, as shown in Eq. (2.14) and (2) methane is produced by hydrogen-utilizing methanogen using carbon dioxide as a substrate, as shown in Eq. (2.15).

$$CH_3COOH \rightarrow CH_4 + CO_2 \quad (2.14)$$

$$CO_2 + 4H_2 \rightarrow CH_4 + H_2O \quad (2.15)$$

2.2.1 Low strength wastewater

The definition of wastewater can be classified as low, medium or high strength base on BOD (or degradable COD concentration). Table 2.3 shows the range of BOD concentrations associated with classification and provided examples of wastewater sources.

Low strength wastewater can be contained a variety of biodegradable compounds such as short-chain volatile fatty acid (VFA), alcohol, carbohydrate and protein. The examples of low strength wastewater are effluent from alcohol and soft drink bottling industries, papermaking mills and paper recycling, fruit and vegetable canneries.

Table 2.3 Classification of wastewater strength and examples.

Waste water Strength	BOD Range (mg/l)	Example of Sources
Low	<1,000	Municipal, agricultural (including flushed manures), pulp and paper.
Medium	1,000-10,000	Food processing, canning, citrus processing, dairy processing, juice processing, brewery.
High	10,000-200,000	Ethanol production, distilleries, biodiesel production, petrol chemical, slaughterhouse

2.2.2 Anaerobic treatment for low strength wastewater

2.2.2.1 Substrate concentration

Low substrate concentration in the reactor result in low activity of microorganism in anaerobic sludge. This phenomenon can be described by Monod kinetics. The model is generally used to describe the conversion rate in anaerobic treatment of soluble substrate. According to the Monod kinetics, the specific growth rate (μ) and the specific of sludge activity (V) depend on the substrate concentration (S). The saturation constant (Ks) defines the affinity of a microorganism for the limiting substrate. The higher Ks value result in the lower of the affinity. The Ks is corresponding to the half of the maximum activity. The expressions for μ and V as a function of S are given by the Eq. (2.16) and Eq. (2.17).

$$\boldsymbol{\mu = \frac{\mu_{max} \cdot S}{K_s + S}} \tag{2.16}$$

$$\boldsymbol{V = \frac{V_{max} \cdot S}{K_s + S}} \tag{2.17}$$

The relationship between both rate is given by the cell yield (Y), as shown in Eq. (2.18).

$$\mu = \boldsymbol{Y} \cdot \boldsymbol{V} \tag{2.18}$$

It is mean that the optimized treatment performance should have high specific growth rate in reactor sludge and Ks should be very low. However, the true values of K_s depend on the substrate type that utilized by specific microorganism.

2.2.2.2 Methane production

In anaerobic treatment, 70% to 80% of the biogas production is methane that can be used as energy and fuel. According to Henry's law, however, the solubility of methane for such a biogas composition would result in 65 to 75 mg COD/L of dissolved methane at 30 °C in equilibrium. This leads to the dissolved methane can leave from the reactor without being biogas collected. The loose of methane gas to become small at the influent COD concentration higher than 750 mg/L (Takayuki, 1994).

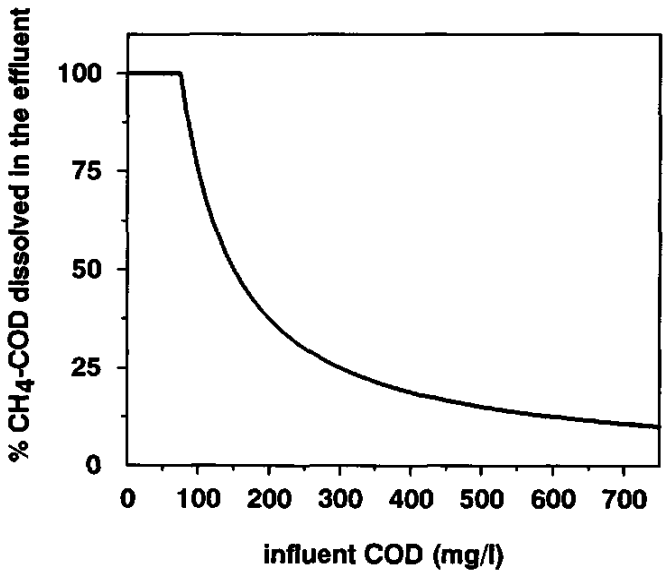

Figure 2.4 Fraction of methane production which is lost as dissolved in the effluent, as a function of the influent COD (Takayuki, 1994).

The fraction of methane production which is lose as dissolved in the effluent with a function of the influent COD, as shown in Figure 2.4. Normally, the anaerobic treatment reactors are operated under mesophilic conditions, the treatment of low strength wastewater would lose considerable amounts of possible useful energy.

2.2.3 Effect of environmental parameters on anaerobic treatment

- Temperature

The increasing of reaction rate relates to the increase of temperature. In biological system, there are two optimal range for methane production; 1) 30 to 40 °C that represent the mesophilic range (15 to 40 °C) and 2) 50 to 60 °C that represent the thermophilic range (above 40 °C). Methane can be produced at temperature below 10 °C. However, the temperature should be maintained above 20 °C for reasonable rate of methane production.

- pH, volatile fatty acid and alkalinity

The non-methanogenic bacteria can survive such strong sensitivity in environmental condition and are able to function in a range of pH from 5 to 8.5. However, optimum pH range of 6.6 to 7.6 is allowed for the methane producing bacteria. The pH drop can cause by the accumulation of volatile fatty acid. Generally, anaerobic process can operate over a wide range of volatile fatty acid concentrations (from less than 100 mg/L to over 5,000 mg/L). To maintain the proper pH in the reactor, the accumulation of acids in the bioreactor must be neutralized by carbon dioxide-bicarbonate buffering. Therefore, excess alkalinity or ability to control pH must be present to guard against the accumulation of excess volatile fatty acid. The three major chemical sources of alkalinity are lime, sodium bicarbonate, and sodium carbonate.

- Mixing

Mixing is an important factor in pH control and maintain of environmental condition uniform. The advantages of mixing are the distribution of buffering agents throughout the reactor and prevent the occurring of high intermediate concentration metabolic products that may inhibited to methanogens.

- Nutrient requirements

The low growth yields of anaerobic microbe are result in low nutrient requirements, compared to aerobes. Normally, $C_5H_7O_2N$ is assumed as the composition of microorganisms in both of aerobic and anaerobic. In anaerobic process, sludge is produced with 20% less than aerobic process. Thus, nitrogen and phosphorus requirements should decrease proportionately. The COD to nitrogen ratio has been observed to be as high as 700:5. However, a ratio of 250:5 is reasonable for highly loaded processes (0.8 – 1.2 kg COD/kg VSS-d. The trace element required for achievement of anaerobic process (Speece, 1996).

2.2.4 Anaerobic fluidized bed reactor using crumb rubber granule as a media

In the previous research, conventional fluidized bed reactors (with internal recirculation) using rubber granule as a media were investigated on COD removal efficiencies under anaerobic condition. The result showed the performance of a conventional FBR for treating high strength wastewater (COD concentration 2,500 to 10,000 mg/L), at the OLR of 5-20 g COD/L-d. Under high HRT as 12 h, the reactor performed 80 to 95% of COD removal efficiencies and the highest methane content in biogas was performed as 55.3% at the OLR of 15 g COD/L-d (Rungkitwatananukul, 2010).

Moreover, the FBR was modified by without internal recirculation for medium strength wastewater treatment. At OLR of 30 g COD/L-d (equal to 1,045 mg/L of COD

concentration). The results showed 95% COD removal efficiencies (Sirinukulwattana *et al.*, 2013).

2.2.5 Bacteria and archaea community in wastewater treatment

- Bacteria

In wastewater treatment plant, quantitative changes between autotrophic and heterotrophic bacteria are affected by wastewater characteristics, type and operation of technological system or geographic location (Cydzik-Kwiatkowska *et al.*, 2012; Ma *et al.*, 2013; Zhang *et al.*, 2012). In municipal WWTPs, Betaproteobacteria belonged to Proteobacteria (21–65 %), which is the most abundant class, largely responsible for organic and nutrient removal; subdominant phyla are *Bacteroidetes*, *Acidobacteria*, and Chloroflexi (Hu *et al*., 2012; Nguyen *et al.*, 2011; Nielsen *et al*., 2010; Wan *et al.*, 2011; Wang *et al*., 2012). The report of a survey found that the most numerous bacterial genera were *Tetrasphaera*, *Trichococcus*, *Candidatus Microthrix*, *Rhodoferax*, *Rhodobacter, Hyphomicrobium*, belonging to *Firmicutes* and *Chloroflexi* phyla (McIlroy *et al.*, 2015), while the predominant phylum within Archea was *Euryarcheota.*

- Archaea

Archaea are also capable of attaching to biotic and abiotic surfaces and developing biofilms. The members of the archaeal in the phyla *Euryarchaeaota*, *Crenarchaeota*, *Korarchaeota* and *Thaumarchaeota* are well documented in extreme habitats. And, they have relationship to biofilm formation in the environment (Jones *et al.*, 2012; Reysenbach *et al.*, 2000; Sauder *et al.*, 2011; Weidler *et al.*, 2008). The methanogenic process is an exclusive feature of a group of prokaryotes classified in the Phylum *Euryarchaeota*, which is currently divided into six orders: *Methanobacteriales*, *Methanococcales*, *Methanomicrobiales*, *Methanosarcinales*, *Methanopyrales* and *Methanocellales* (Liu and Whitman, 2008; Sakai *et al.*, 2008).

Despite their ample phylogenetic, morphological and physiological diversity, methanogens only use a limited number of substrates to obtain energy. Most

methanogens are restricted to use hydrogen and carbon dioxide (H_2 + CO_2) or formate (Liu and Whitman, 2008) as substrate. Moreover, some members of the *Methanomicrobiales* use secondary alcohols, while *Methanosarcinales* that comprise acetoclastic methanogens such as *Methanosarcina* spp. and *Methanosaeta* spp, are able to degrade methyl group-containing compounds (Angelidaki *et al.*, 2011; Liu and Whitman, 2008).

2.3 Biological denitrification process

Denitrification is one of process to reduce nitrate in water and wastewater. Denitrifying bacteria are dominant microorganism in this system. The microorganisms which perform in denitrification process are facultative aerobe. Denitrifying bacteria can survive under incomplete anaerobic condition (Tiedje, 1988).They can reduce nitrogen oxide under oxygen limited condition (Rittmann and McCarty, 2001). Nitrogen removal from wastewater is based on the conversion of organic and inorganic nitrogen (NH_4^+, NO_3^-, NO_2^-) into nitrogen gas (released to the atmosphere). Nitrogen compounds are also eliminated due to assimilation into biomass. Generally, conventional nitrogen removal consists of two steps, nitrification and denitrification. The change in nitrogen oxidation state during nitrification and denitrification are shown in Figure 2.5.

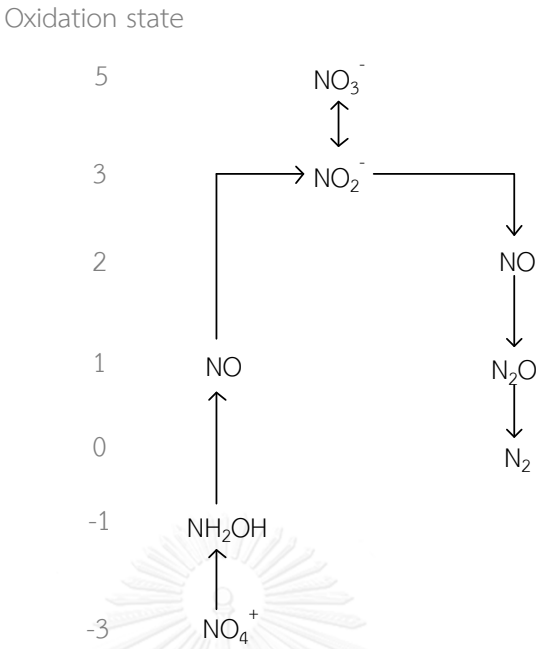

Figure 2.5 The change in nitrogen oxidation state during nitrification and denitrification. Modified from *(Cloete and Muyima, 1997)*

As shown in Figure 2.5, the oxidation state of nitrogen can reduce biochemically. Since, nitrogen reduction is incorporated into new synthesized biomass, the process is called “assimilation nitrate reduction”. Beside this process, nitrate is reduced to elementary nitrogen and serves as an electron accepter in the electron transfer system (ETS) as show in Figure 2.6. The process is known as denitrification process, describing formally by Eq. (2.19).

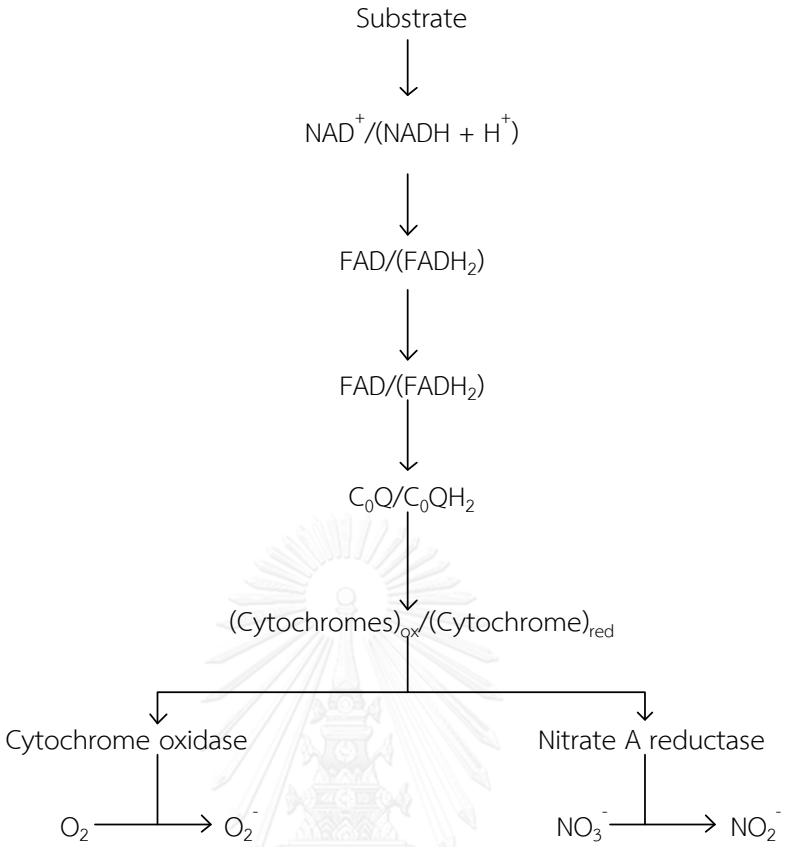

Figure 2.6 The electron transport system under oxic and anoxic conditions using O_2 and NO_3^- as electron acceptor. Modified from *(Cloete and Muyima, 1997)*.

$$8(H^+ + e^-) + H^+ + NO_3^- \rightarrow NH_4^+ + OH^- + 2H_2O \quad (2.19)$$

The activated hydrogen donors are predominately external biodegradable substrate or organic storage products. The specific yield of free energy released in the ETS under anoxic conditions is about 5 percent less than under oxic condition when the final electron acceptor is oxygen.

Denitrification occurs under anoxic condition. Nitrate and sulfate normally are the main electron accepters in this system. Overall reaction for biological growth is a conservation of electron in this process. Electron donor is oxidized, generating

electrons and carbon dioxide which are used for energy production and biomass synthesis. The occurring of denitrification process is as shown in the Eq (2.20).

$$Electron\ donor + NO_3^- \rightarrow Biomass + N_2 + CO_2 \quad (2.20)$$

Denitrification process can be divided into 4 steps as followed,

- Nitrate reduction

In nitrate reduction, nitrate is converted to nitrite by a reductase enzyme that produced by bacteria as shown in Eq. (2.21).

$$NO_3^- + 2e^- + 2H^+ \rightarrow NO_2^- + H_2O \quad (2.21)$$

- Nitrite reduction

In nitrite reduction state, nitrite is reduced to nitric oxide, as presented in Eq. (2.22). Nitrite reductase enzyme is catalyst in this step.

$$NO_2^- + e^- + 2H^+ \rightarrow NO + H_2O \quad (2.22)$$

- Nitric oxide reduction

Nitric oxide oxidation is reaction to reduce nitric oxide to nitrous oxide by Nitric oxide reductase as catalyst (as shown in Eq. (2.23)).

$$NO + e^- + H^+ \rightarrow 0.5N_2O + 0.5H_2O \quad (2.23)$$

- Nitrous reduction

Nitrous oxide reductase enzyme is a catalyst in this step. Nitrous oxide is reduced to nitrogen gas as shown in Eq. (2.24). The overall reaction in denitrification process can be described by Eq. (2.25). It can be seen that 1 molecule of nitrate can provide 5 molecules of electron during denitrification.

$$N_2O + e^- + H^+ \rightarrow N_2 + 0.5H_2O \quad (2.24)$$

$$NO_3^- + 5e^- + 6H^+ \rightarrow 0.5N_2O + 3H_2O \quad (2.25)$$

2.3.1 Nitrate-rich wastewater

Generally, industrial wastewater and sewage contain high nitrogen compounds. After aerobic treatment, ammonia is oxidized to nitrite and nitrate, which is released to natural water resources, causing problems to both the environment and to human, for example, causing eutrophication, lowering water quality, and posing potential hazard to human health. For instance, consumption of water containing high nitrate can cause blue baby syndrome in children. In addition, nitrate and nitrite have the potential to form N-nitrous compounds, which are carcinogenic. The main sources of nitrate-rich wastewater are nitrogenous fertilizer, animal waste, septic system and other sources, depending on the urban development (Ford and Tellam, 1994).

2.3.2 External carbon source for denitrification

Normally, the external carbon source is necessary for biological denitrification process. Heterotrophic bacteria need carbon substrate as electron donor. Methanol has normally been used as carbon source for denitrification process due to its inexpensive price (Her and Huang, 1995; Wen *et al*., 2003). However, some studies report that the use of methanol as a sole carbon source showed very small amount of nitrate reduction or needed a very long adaptation period (Akunna *et al.*, 1993). In addition, the use of methanol as a carbon source affects the diameter, size distribution

and stability of the granular sludge system. Granular sludge are loosened and become large particle that moves to the top of the reactor in colloidal manner (Jin *et al.*, 2012a).

When comparing between the use of methanol and acetate, the result shows that acetate can provide higher growth rate as well as denitrification rate than the one using methanol as carbon source (Lee and Welander, 1996).

Xie et al. (2012) studied the effect of carbon source and COD:NO_3^-- N ratio on denitrification. Their results showed that the COD:NO3- - N ratio in a range of 7 to 8 were the critical ratio for the system, when using glucose and cassava stillage as carbon sources.

Glucose is one of a popular external carbon sources for high nitrate wastewater. Comparing with other carbon sources, glucose is easily biodegradable substrate. The stoichiometric reaction when using glucose as electron donor is shown in the Eq. (2.26).

$$5C_6H_{12}O_6 + 24NO_3^- + 24H^+ \rightarrow 42H_2O + 30CO_2 + 12N_2 \qquad (2.26)$$

In the Eq. (2.26), it can be seen that 24 mole of nitrate nitrogen is consumed concomitantly with 5 moles of glucose. If this reaction occurs in a suitable condition, the substrate will be converted to 30 moles of carbon dioxide and 12 moles of nitrogen gas.

2.3.3 Factor controlling denitrification

- Temperature

Similar to other heterotrophs, the kinetics of denitrifying bacteria is affected by temperature based on the Arrhenius equation, as shown in Eq. (2.27) and Eq. (2.28).

$$k = Ae^{-Ea/RT} \quad (2.27)$$

$$k = k_2\theta^{T_1-T_2} \quad (2.28)$$

Where k is the specific denitrification rate at temperature T (mg NO_3^--N/mg VSS/d), A is the prefactor, Ea is the activation energy in J/mol, R is the ideal gas constant (8.314 J/mol/K), T is the absolute temperature, and θ is the temperature coefficient (dimensionless).

Denitrification rate is obtained at the optimum temperature in the range of 20 to 60 ℃. The declining rate occurs rapidly at lower or higher temperature than this range.

- pH

Alkalinity is produced during denitrification, 3.57 g alkalinity (as $CaCO_3$) is generated per gram of nitrate-nitrogen reduced to nitrogen gas. Denitrification may occur at a pH up to 11 in wastes, however, the optimum pH for denitrification was found in the range of 7 to 9. Denitrification activity reduces sharply outside this region, which may be attributed to the inhibitory effects of hydrogen ion or hydroxide ion on denitrification enzyme, such as N_2O reductase (Berks et al., 1993).

- Oxygen

Oxygen inhibits denitrification by providing a better electron acceptor for denitrifying species to generate energy. The Gibbs standard free energy of water-oxygen

is -78.73 KJ/e-equivalent and that for nitrate-nitrogen is -72.20 KJ/e-equivalent (Rittmann and McCarty, 2001), making oxygen a more favorable electron acceptor.

The threshold oxygen-inhibiting concentration is around 0.2 mg O_2/L (Knowles, 1982). In practice, the oxidation reduction potential (ORP), which is a measure of the activity or strength of oxidizers and reducers in relation to their concentration in wastewater, has been used to indicate aerobic, anoxic and anaerobic state of the system. The ORP generally shows a strong response to DO especially at low oxygen concentrations, and is a better monitoring and controlling parameter under anoxic and anaerobic conditions than using DO concentration. In general, ORP value lower than -200 mV indicates anaerobic conditions, while between -200 to +200 mV is for anoxic condition and higher than +200 mV is for aerobic condition.

- Nitrogen species

Nitrite inhibition on bacterial growth has long been recognized for both pure and mixed cultures (de Almeida *et al.*, 2007). The 2 possible mechanisms for nitrite-mediated inhibition in nitrate reduction include: 1) the competition for NADH between nitrate and nitrite reductase; and 2) the internal accumulation of toxic nitrite resulted from high rate of nitrate reduction. Several studies have suggested that instead of nitrite, the inhibition is actually caused by the non-dissociated nitrous acid (HNO_2). The threshold inhibitory concentration of HNO_2 varies upon the culture condition, pH and carbon availability (Abeling and Seyfried, 1992; Baumann *et al.*, 1997).

Similar to nitrite, nitric oxide (NO) is able to inhibit nitrite reductase as well as the nitrous oxide reductase. No inhibition effects have been reported for nitrous oxide on any of the denitrification steps so far.

2.3.4 Denitrification fluidized bed reactor using crumb rubber granule as a media

In the previous research, the conventional fluidized bed reactors (with internal recirculation) using rubber granule as a media were investigated on nitrate removal

efficiency. Four different COD to nitrate ratio of 2:1 5:1 10:1 and 15:1 were fed into the reactors. Fixed nitrated concentration of 100 mg/l and hydraulic retention time of 8 h were conducted and controlled throughout the experiment. From this research, the results clearly indicated that the rubber granule, the media derived from waste-tires, can be used as a media in fluidized bed reactor, provided acceptable reactor performance. The result revealed that the nitrate removal efficiency was obtained about 95 96 96 and 96%, respectively while the COD removal efficiency was achieved as 78 78 73 and 75 %, respectively. In this system, the COD to nitrate ratio of 2:1 was chosen for nitrate removal since it uses the lowest amount of organic substance. Whereas the nitrate removal efficiency was nearly the same as other COD to nitrate ratio. The microbial community analysis by PCR-DGGE technique were clearly revealed that denitrifying bacteria were the major population in all fluidized bed reactors performed. The variety species of denitrifying bacteria increased when COD to nitrate ratio increased (Wanida Horkam, 2011).

2.3.5 Denitrifying bacteria

Microorganism in denitrification process consist of bacteria and archaea, and the diversity in wastewater treatment process is indicated via 16S rRNA gene-based studies as shown in Figure 2.7.

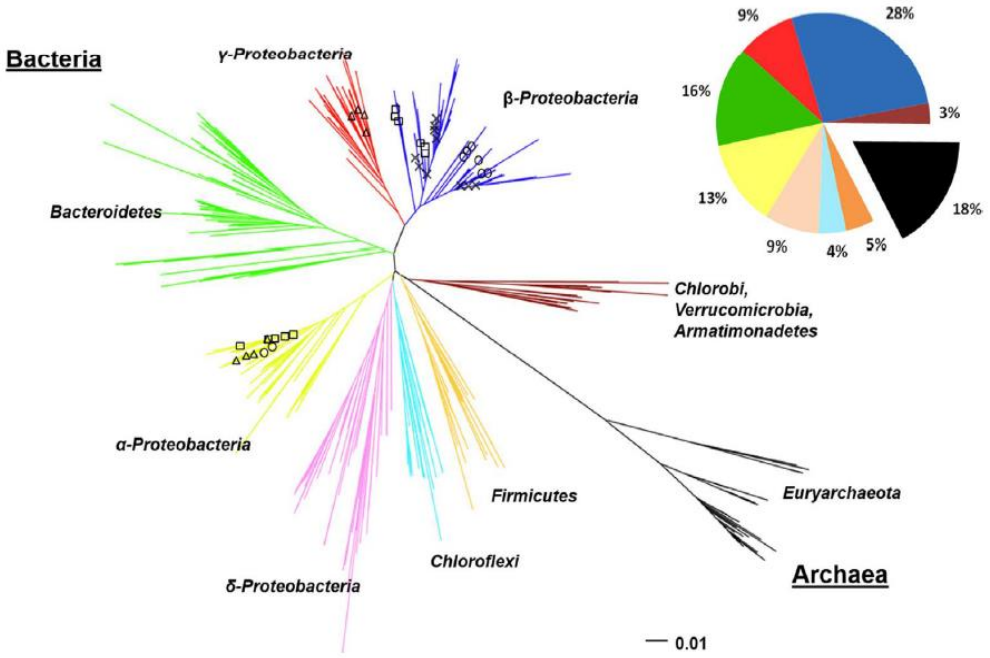

Figure 2.7 Phylogenetic tree of the major phyla of wastewater denitrifying bacteria constructed by the neighbor-joining method on the basis of 1003 partial 16S rDNA sequences (> 500 bp) retrieved from GenBank. Special carbon assimilating populations:□ - Methanol; x - Acetate; o - Glycerol; Δ - Methane (DeSantis *et al.*, 2006b; Letunic and Bork, 2011a; Lu *et al.*, 2014).

Denitrifying bacteria can be classified into 2 groups: heterotrophic and autotrophic bacteria. However, heterotrophic bacteria play an important role in denitrification process in wastewater treatment.

1) Heterotrophic denitrifying bacteria

Heterotrophic denitrifying bacteria are a group of microorganisms that use organic carbon as energy and carbon source for growth. Microorganisms belonging to

the heterotrophic denitrifying bacteria can be found in various genus such as Achromobacter, Acinetobacterium, Agrobacterium, Alcaligenes, Arthrobacter, Bacillus, Chromobacterium, Corynebacterium, Flavobacterium, Halobacterium, Hypomicrobinm, Methanomonas, Moraxella, Neisseria, Paracoccus, Propionibacterium, Psedomonas, Rhizobium, Rhodopseudomonas, Spirillum and Vibrio.

2) Autotrophic denitrifying bacteria

Autotrophic denitrifying bacteria use inorganic carbon as carbon source and use inorganic compound as electron donor. Microorganisms belonging to autotrophic denitrifying bacteria consist of *Paracoccus ferrooxidans, Paracoccus denitrificans, P.pantotrophus,* and *P.versutus.* They can use ferrous ion (Fe^{2+}) and hydrogen sulfide (H_2S) as electron donors and nitrate as electron accepter.

Heterotrophic denitrifying bacteria require an electron donor such as influent BOD, and other carbon source for respiration and growth. As an initial BOD may not be sufficient, external carbon source is an important electron donor for reducing nitrate and phosphorus in wastewater treatment. Generally, external carbon source is added for nitrate removal in nitrate-rich wastewater. Methanol and acetate are wildly used as the source of carbon for denitrification (Akunna *et al.*, 1993; Burghate and Ingole, 2013; Wen *et al.*, 2003). Certain research, however, has found that the use of methanol as a sole carbon source provides low nitrate and nitrite reduction and methanol was not significantly consumed (Akunna *et al.*, 1993).

CHAPTER 3
HYDRODYNAMIC BEHAVIOR STUDY IN A NOVEL ANAEROBIC FBR USINGRESIDENCE TIME DISTRIBUTION (RTD)

3.1 Introduction

Anaerobic technology has been widely used for wastewater treatment due to the energy conservation in reactor operation. Recovering energy from biological gas production under anaerobic treatment and sludge digestion is more cost effective than the aerobic treatment. Nowadays, many researches focus on the design of anaerobic reactors in order to achieve high performance for substrate removal efficiency with low operating costs (Chen *et al.*, 2014; Leyva-Diaz *et al.*, 2016). Anaerobic fluidized bed reactor is an attached-growth wastewater treatment reactor which offers various advantages, such as high efficiency for substrate removal due to the enhancement of contact between microbes adhering on carrier media and the wastewater steam, rapid recovery of system stability with the change in operating condition, and the ability to operate under low hydraulic retention time (HRT) due to the internal recirculation flow rate. However, high up-flow velocity (caused by the recirculation) is needed to fluidize media bed in the conventional FBR, leading to the high reactor operation costs. Use of low density material as supporting media should be one of the alternative ways to conserve energy in the conventional FBR.

In this research, a novel configuration FBR has been developed using low density material as media. Granular rubber is a low-density material, and has already been proved as useable media in wastewater treatment system. It is a non-toxic material for microorganisms in wastewater treatment under anoxic and anaerobic conditions (Park *et al.*, 2006). A novel FBR can operate effectively without internal recirculation. The recirculating pump is not required, but feeding flow rate must be increased to replace the missing recirculating flow rate. This leads to the operation of reactor under very low HRT. Thus, the reactor configuration was modified by increasing

the column height to prolong HRT for biological treatment. Reactor configuration of this novel FBR make it different from the conventional one. The hydrodynamic behavior should therefore be investigated for further analysis.

Among various experimental methodologies, residence time distribution (RTD) is widely used for describing the phenomenon and liquid flow pattern not only in chemical reactors but also in biological reactors (Hu *et al.*, 2012; Saravanathamizhan *et al.*, 2008; Sendhil *et al.*, 2012). The RTD measurement is an effective tool that can help understanding and determining hydrodynamic parameters (Essadki *et al.*, 2011). Moreover, the RTD has been of interest in the study of hydrodynamic flow characteristics and dead volume in biological treatment reactors (Kostov *et al.*, 2011; Krishna *et al.*, 2009). There are many researches that have studied the liquid flow pattern in the reactors using RTD measurement. They found the difference in liquid flow pattern in different parts of the reactor, as described by RTD measurement (Dhaouadi *et al.*, 1997; Essadki *et al.*, 2011; Gavrilescu and Tudose, 1999). In general, RTD measurement can be achieved by using tracer experiments, which consists of an impulse response method. Tracer injection occurs at the inlet of a reactor and an observation probe is located at the outlet. Flow model is then selected to explain the liquid flow behavior of the reactor. Therefore, the objective of this work is to determine the hydrodynamic behavior of a novel FBR at different flow rates.

3.2 Research scope

The novel configuration FBRs and its equipment were set-up at the 1st floor of Department of environmental engineering building. There are experimental scopes as follows,

1) Tap water was fed into a novel configuration anaerobic FBR with different water flowrate as 50 L/d, 60 L/d and 70 L/d. To investigate the liquid flow pattern inside the reactor, a tracer (5 mL of 70 g/L KCl) was injected to the reactor via pulse injection method. Overall research framework is illustrated in Figure 3.1.

2) A novel configuration anaerobic FBR was made from transparent plastic tube with 0.03 m of diameter and 300 cm of the height. The active volume was 1.6 L.
3) Rubber granule was used as a carrier media with 0.43 mm of effective size and 1.2 g/cm^3 of density.
4) HRT was controlled at 50 min in every condition.

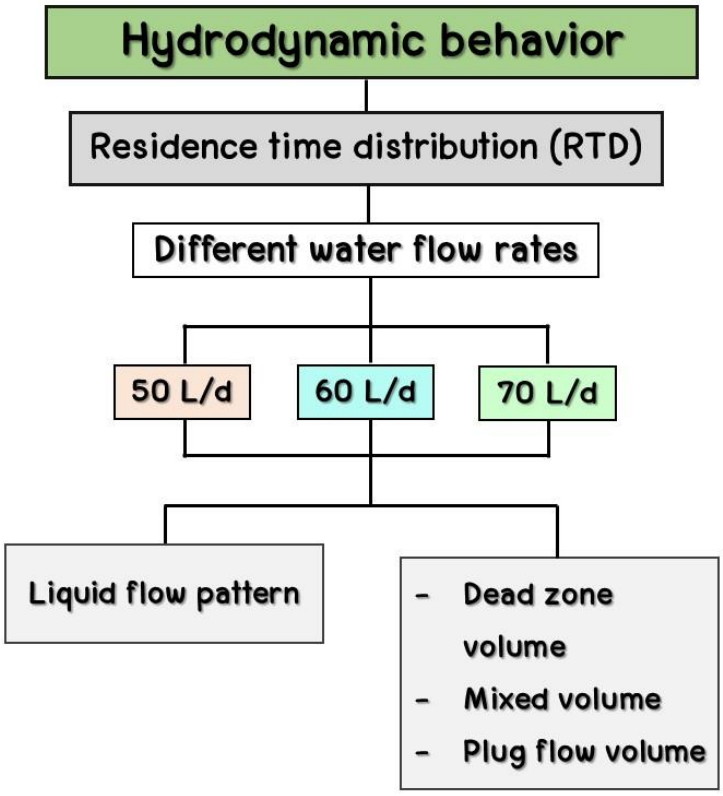

Figure 3.1 Framework of hydrodynamic behavior in a novel configuration anaerobic FBR.

3.3 Materials and Methods

3.2.2 Reactor configuration and operation

It was covered at the top by a released cap, which is a 3 phase separation equipment with 10 cm inner diameter, and 37.5 cm height to prevent sludge back wash from the reactor and to make the 3 phase separation. The main function of the

3 phase separator design was to facilitate the return of bio-particles without external energy and control device. Moreover, it provides enough gas-water interface inside the gas dome as well as sufficient settling area outside the dome to control surface overflow rate and to allow proper return of solid back to the reactor.

The feeding flow rate was calculated from minimum fluidization velocity and terminal fluidization velocity using Eq. (2.6). The values of each parameter are shown in Table 3.1. The minimum fluidization velocity (V_{0m}) was 1.16 m/h and the terminal fluidization velocity (V_0) was 7.19 m/h. It can be seen that the fluidization state of the rubber granule can be controlled by using low up-flow velocity.

Table 3.1 The parameters values used for calculating minimum and terminal fluidizing velocity.

Parameter	Value
D_p	0.43 cm
ρ	1 g/cm^3
ρ_p	1.2 g/cm^3
φ	1
ε_m	0.40
μ	0.008 cm^3/s
L	1.5 cm
L_m	1.0 cm
G	981 cm/s^2

As illustrated in Figure 3.3, feeding medium stored in the influent tank was pumped into inlet port of the reactor by peristaltic pump with average flow rate of 60 L/d. The biological gas was then measured by gas volume counter. The effluent flowed

out of the reactor through the effluent port. This reactor only needed one pump for feeding and controlling the fluidization state of the reactor.

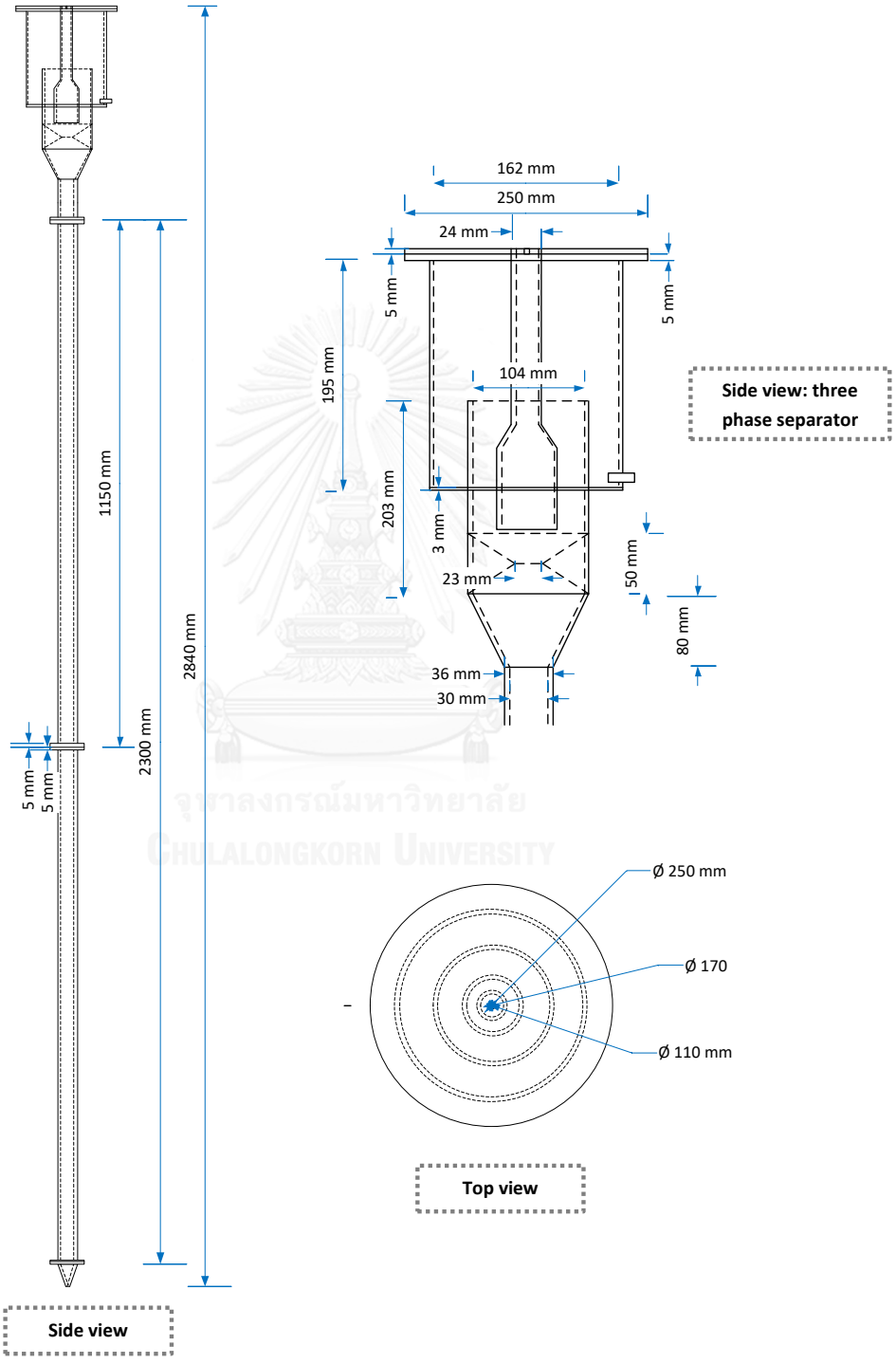

Figure 3.2 Side view and top view of a novel configuration anaerobic FBR used in this study.

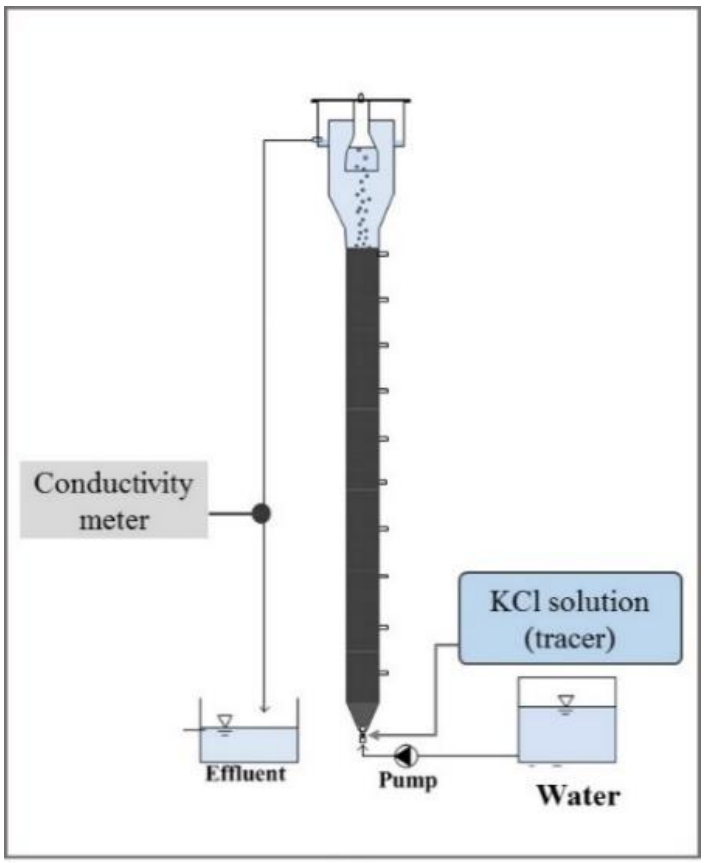

Figure 3.3 Schematic diagram of a novel configuration anaerobic FBR for RTD experiment.

3.2.1 Supporting media in a novel FBR

Granular rubber is a low density material. The properties of granular rubber used in this research is presented in Table 3.2 and its pictures are shown in Figure 3.4.

Table 3.2 Properties of granular rubber used in this study.

Properties	**Value**
Effective size	0.43 mm
Density	1.2 g/cm^3
Specific surface area	0.025 m^2/g
Uniformity coefficient	1.53

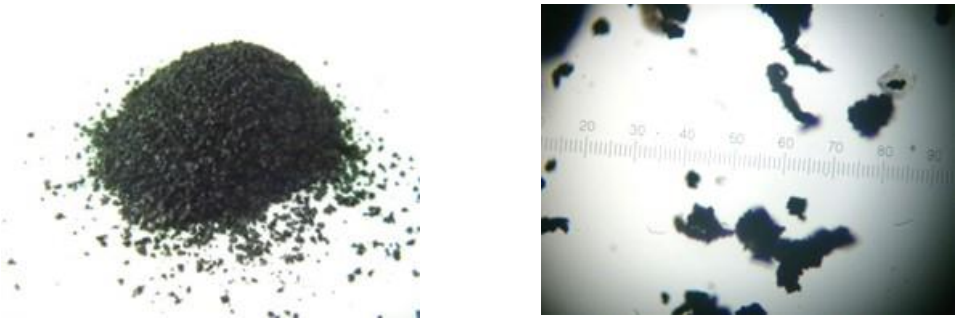

(a) real photo b) under microscope 10X

Figure 3.4 Pictures of granular rubber used as a media in a novel configuration anaerobic FBR.

3.2.3 Experimental determination of residence time distribution (RTD)

The RTD experiments were conducted at different water flow rates of 50 L/d (minimum flow rate), 60 L/d (average flow rate) and 70 L/d (maximum flow rate). A tracer (5 mL of 70 g/L KCl) was injected through the three-way port located at the inlet of the reactor. As shown in Figure 3.3, the KCl concentration was measured as a function of time at the sampling port located by the exit port. The concentration of tracer was measured by a conductivity probe (SevenGo Duo pro, METTLER TOLEDO, Switzerland).

The exit age distribution (E) was determined using the tracer method with a pulse regime, which is presented by the following Eq. (3.1) (Levenspiel, 1999)).

$$\int_0^\infty E\, dt = 1 \qquad (3.1)$$

The variance of the curve and dead space in the reactor were calculated according to a model (Levenspiel, 1999)) as present in Eq. (1.2), Eq (1.3), and Eq. (1.4).

Normalized mean:

$$u_a = \frac{\int_0^\infty x \cdot \int(x)dx}{\int_0^\infty \int(x)dx} \qquad (3.2)$$

Variance: $$\sigma^2 = \frac{\int_0^\infty (x-u_a)^2 \cdot \int(x) \cdot dx}{\int_0^\infty \int x \cdot dx} \quad (3.3)$$

Dead space: $$V_d = (1 - v_a \mu_a) \cdot V \quad (3.4)$$

where V_d is the volume of dead space in the reactor (L), V is the theoretical working volume of the reactor (L), and v_a is the fraction of tracer.

3.3 Results and discussion

Hydrodynamic behavior in the novel FBR

Three different water flow rates were studied: 50 L/d, 60 L/d and 70 L/d. From RTD experiments, it was found that the tracer was detected in the effluent from 16 to 20 min after the tracer injection. The results from RTD experiments are shown in Figure 3.4. A high sharp peak of tracer was present at the exit age at around 32, 28, and 22 min for water flow rate of 50, 60, and 70 L/d, respectively.

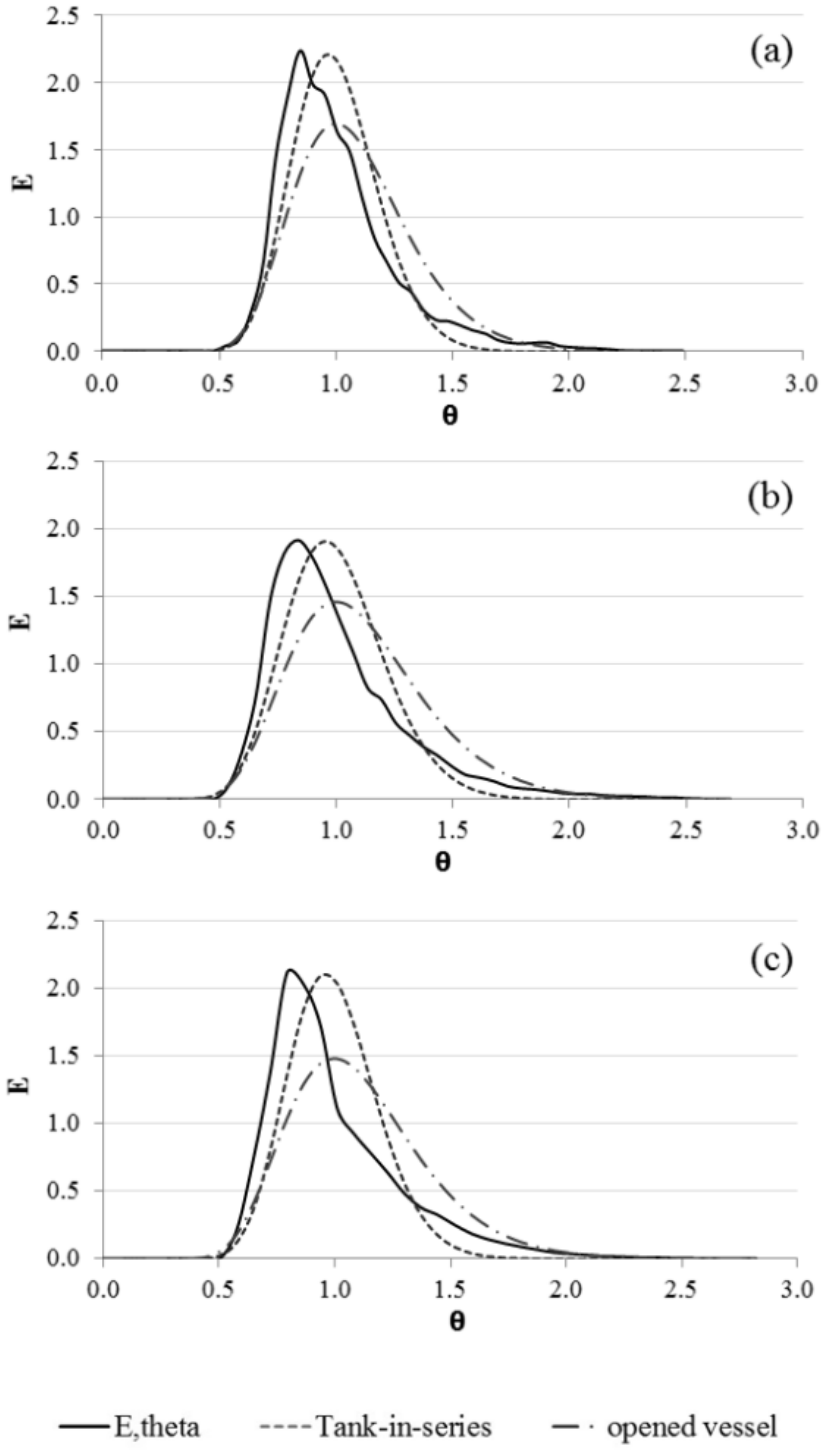

Figure 3.5 The variation of experimental exit age distribution in a novel configuration anaerobic FBR, (a) 50 L/d, (b) 60 L/d and (c) 70 L/d.

Figure 3.5 (a), (b) and (c) experimental exit age with flow rates of 50, 60 and 70 L/d, respectively. It can be observed that the relations of E(t) at each flow rate were positively skewed distributions. According to the compartment model, it implied that the liquid flow pattern inside the reactor were theoretical plug flow with mixed flow. Table 3.3 shows that a small volume of mixed flow reactor can be found with 12 to 17 percent of the total volume of the reactor. The highest flow rate provided the highest mixed flow volume. As flow rate increased, the mixed flow volume also increased, which referred to the increase in recirculation in the reactor. It implied that the liquid flow was more turbulent and resulted in the increase in the fluidization state.

Unlike the mixed flow volume, dead volume did not relate to the liquid flow rate. At the flow rate of 70 L/d, 16.3 percent dead volume was obtained. This was higher than that of the flow rate of 60 L/d. The lowest dead volume occurred at the flow rate of 60 L/d, which was 13.1 percent, while the highest dead volume was found at a flow rate of 50 L/d, which was 18.1 percent. Hydrodynamic studies showed that 22 to 65 percent of the dead volume were found in a fixed-bed reactor, depending on the volumetric flow rate (Méndez-Romero *et al.*, 2011). Whereas in the high flow rate reactor the percentages of dead volume of 7.1 to 19.5 percent were presenting in an expanded granular sludge bed (EGSB) at different flow velocities (Zheng *et al.*, 2012).

As illustrated in Figure 3.4, the experimental graphs were close to the modified tank-in-series model. The results were similar to many tanks of CSTR in each flow rate. It means that liquid flow patterns in a novel FBR reached that of the plug flow reactor. The volume of plug flow regimes at each flow rate was in the range of 1.07 to 1.11 L, which made up the majority of the total volume of reactor, 1.6 L. Conversely, a small volume of mixed flow reactor was found.

Table 3.3 The condition and model analysis results of a novel configuration FBR.

Flow rate (L/d)	Design HRT (min)	Tank in series, N	Dead volume (L)	Plug flow volume (L)	Mixed flow volume (L)
50	46.08	30	0.29 (18.1%)	1.11	0.20
60	38.40	22	0.21 (13.1%)	1.17	0.22
70	32.91	27	0.26 (16.3%)	1.07	0.27

In previous research, there were reports of hydrodynamic behavior in RTD experiments in a conventional FBR using light beads as a media. It was found that the liquid flow was defined as a combination of plug flow and ideal mixing reactor (Kostov *et al.*, 2011).

3.4 Conclusion

From the overall results, it can be concluded that the hydrodynamic behavior of liquid flow in the novel FBR was close to a plug flow reactor. The increase in liquid flow rate induced a mixed flow regime. At a flow rate of 60 L/d, the results showed the smallest volume of dead zone inside the reactor. This result can be used to modify and explain the novel FBR for further applications.

CHAPTER 4
A NOVEL ANAEROBIC FLUIDIZED BED REACTORS USING RUBBER GRANULE AS A MEDIA FOR LOW STRENGTH WASTEWATER TREATMENT

4.1 Introduction

Anaerobic technology is widely used in various wastewater treatment applications, not only high-strength wastewater treatment but also low-strength wastewater treatment. The use of anaerobic process becomes a very attractive option due to low capital and operational costs. Moreover, anaerobic reactor is suitable for treating wastewater produced by seasonally operating agro-industrial or tourist area, because these units can be maintained for long period of time without substrate feeding (Manariotis and Grigoropoulos, 2002). Moreover, anaerobic process provides many advantages greater than that of the aerobic reactor, such as low production of biological solid wastes, low nutrient requirement, no energy requirement for aeration and production of energy in a form of methane gas. Although anaerobic wastewater treatment is recommended for treating high-strength wastewater, anaerobic treatments have also been responsible for low-strength wastewater for more than two decades (Lucena et al., 2011; Manariotis and Grigoropoulos, 2002; Verstraete and Vandevivere, 1999).

Anaerobic bioreactors have been proved for low-strength wastewater treatment, such as anaerobic filter (AF), up-flow anaerobic sludge blanket (UASB), anaerobic fluidized bed (FBR) or expanded bed reactor (EBR) and anaerobic baffled reactor (ABR) (Krishna *et al.*, 2009). Among various high-rate anaerobic reactors, UASB is well known for treating low-strength wastewater, especially domestic wastewater (Lucena *et al.*, 2011). Anaerobic fluidized bed reactor (AFBR) is one of the high-rate anaerobic bioreactors. It is classified as an attached growth wastewater treatment. Due to the small supporting media contained inside the reactor, AFBR has ability to keep large mass of microorganisms in the system. The excellent functions of AFBR include

low operating cost, large amount of mass transfer rate and uniform mixing (Andalib et al., 2014).

The key factor to achieve high efficiency AFBR is the supporting media selection. Supporting media in AFBR provide more surface area for microbial adhesion than other attached growth bioreactor, for example, packed bed bioreactor (Grady *et al.*, 1999). Granular rubber has been proven as suitable media in conventional AFBR (Horkam, 2011; Rungkitwatananukul, 2010) and in modified configuration of AFBR (Sirinukulwattana et al., 2013). Granular rubber is a low density material, non-toxic for microbial growth and has suitable surface for microbial adhesion (Park *et al.*, 2006). Moreover, previous research has successfully used granular rubber as carrier media in FBR without internal recirculation for anaerobic wastewater treatment (Sirinukulwattana *et al.*, 2013).

In this research, the configuration of FBR was modified from the conventional one. The FBR was operated without internal recirculation, called a novel configuration anaerobic FBR. According to the reactor operation without internal recirculation, a novel configuration anaerobic FBR must be operated under a very low hydraulic retention time (HRT). There is no report about the use of a novel configuration FBR for low-strength anaerobic wastewater treatment under a very low HRT. Therefore, in this study, performance of a novel configuration anaerobic FBR was investigated for the treatment of low-strength wastewater under anaerobic condition and with HRT less than an hour. The research objective was to evaluate COD removal efficiency at different organic loading rate (OLR) operations. Moreover, microbial community distribution and COD removal profiles were evaluated at several levels along the reactor height. To investigate the relationships between microbial community distribution and reactor performance, this study performed 16S rRNA gene sequencing analysis via MiSeq Illumina technique.

4.2 Research objectives

- To evaluate the performance of a novel anaerobic FBR in term of COD removal efficiency for treating low-strength wastewater under a very low HRT.
- To examine the profile of COD concentrations in a novel configuration anaerobic FBRs under different OLR conditions.
- To monitor the microbial community distribution in a novel configuration anaerobic FBRs under different OLR conditions.

4.3 Research approaches

In this part, there were three main approaches as indicated in Figure 4.1.

(1) The performance of a novel configuration anaerobic FBR for treating low COD concentration wastewater.

(2) The substrate removal pattern of a novel configuration anaerobic FBR at different OLR operations.

(3) The distribution of microbial community in a novel configuration anaerobic FBRs.

4.4 Experimental scope

The novel configuration FBRs and its equipment were set-up at the 1st floor of Department of Environmental Engineering building. The experimental scopes were as follows,

1) Synthetic wastewater was prepared from tap water using glucose as carbon source and sufficient trace elements were added. Wastewater with different COD concentrations at 150, 250, and 500 mg/L were fed to evaluate performance of the reactor, as well as profiling the COD removal and microbial distribution at several levels along the reactor height. Overall research scope is illustrated in Figure 4.1.

2) HRT was controlled at 50 min in every condition.
3) A novel anaerobic FBR was made from transparent plastic tube with 0.03-m diameter and 300-cm height. The active volume was 1.6 L.
4) Rubber granule was used as carrier media with 0.43 mm of effective size and density of 1.2 g/cm^3.
5) Inoculum was prepared from seed sludge of anaerobic filter reactor that was located in the Faculty of Engineering, Chulalongkorn University.

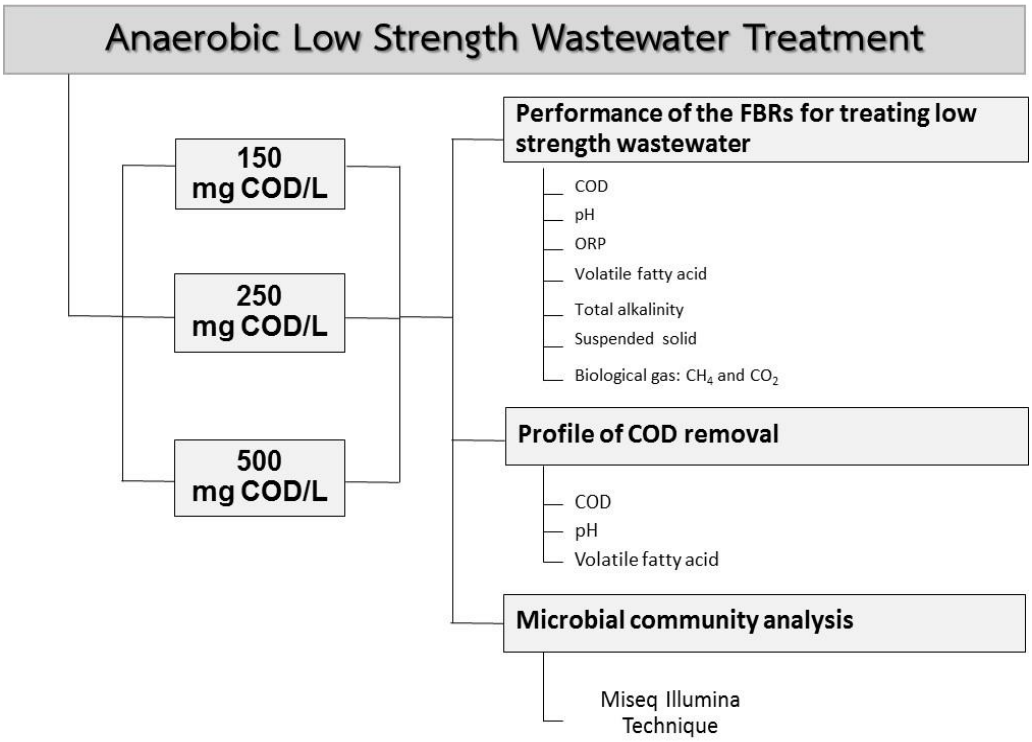

Figure 4.1 Framework of experimental study for low strength anaerobic wastewater treatment.

4.5 Material and Methods

4.5.1 Reactor configuration and experimental set-up

The FBR column was made of transparent plastic with 3 mm thickness, 0.03 m inner diameter, and 2.30 m column height. Granular rubber was made from spent-tire waste and had average size of 0.43 mm, 1.2 g/cm^3 density, 0.025 m^2/g specific surface

area, and 1.53 uniformity coefficient. The upper part of the reactor was 0.35 m in height, the three phase separator was installed to prevent sludge wash out from the reactor and enhance gas-solid-liquid separation. The schematic diagram of the fluidized bed reactor is shown in Figure 4.2.

The feeding flow rate was calculated from minimum fluidization velocity and terminal fluidization velocity using Eq. (2.6). The parameter values are shown in Table 4.1. The minimum fluidization velocity (V0m) was 1. 16 m/ h and the terminal fluidization velocity (V_0) was 7.19 m/h. It can be seen that the fluidization state of the rubber granule can be controlled by low up-flow velocity.

Table 4.1 The parameters values for calculating minimum and terminal fluidizing velocity.

Parameter	Value
D_p	0.43 cm
ρ	1 g/cm^3
ρ_p	1.2 g/cm^3
φ	1
ε_m	0.40
μ	0.008 cm^3/s
L	1.5 cm
L_m	1.0 cm
G	981 cm/s^2

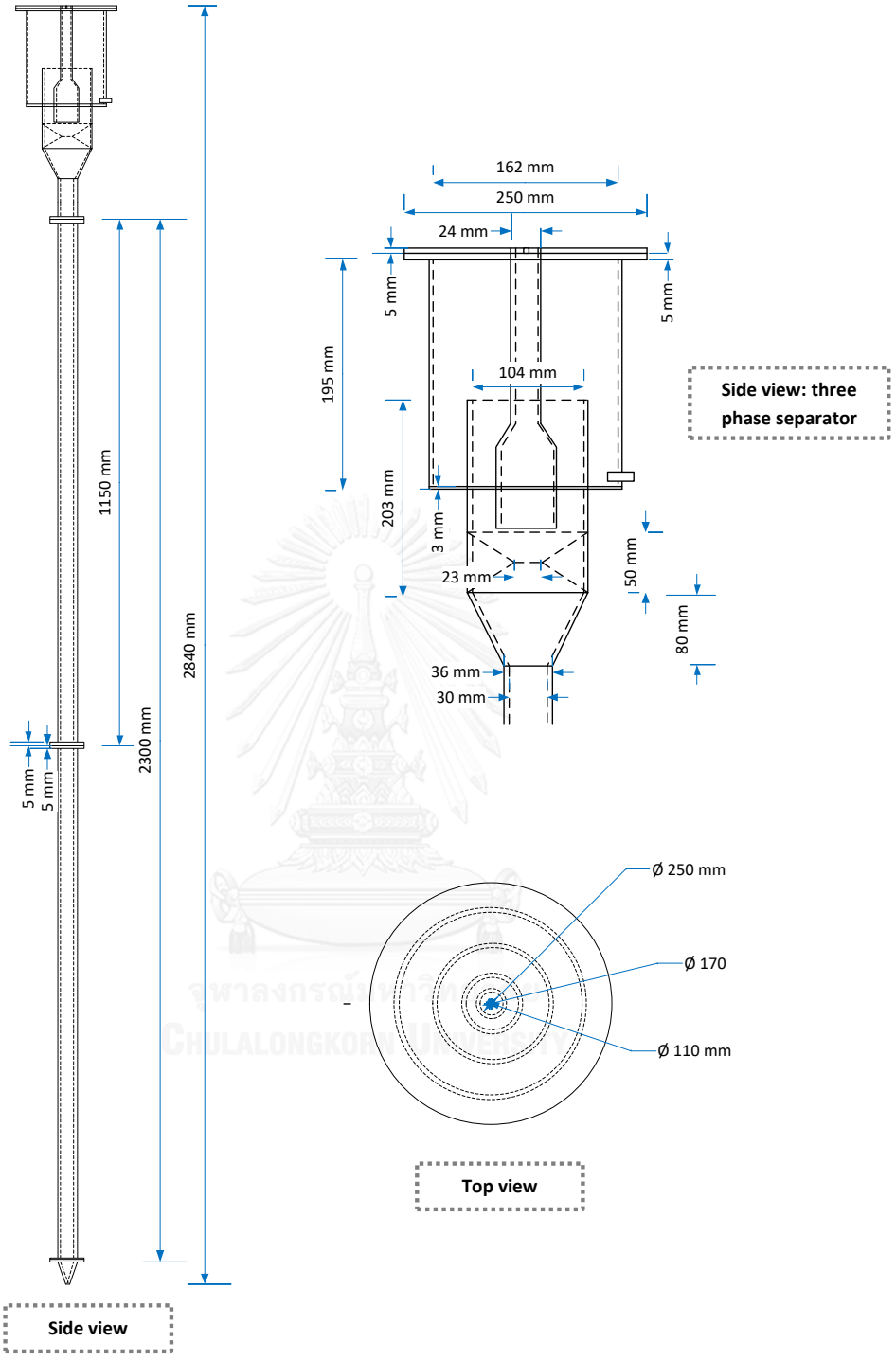

Figure 4.2 Side view and top view of a novel configuration anaerobic FBR used in this study.

During start-up, 250 ml of seed sludge from an anaerobic filter reactor and around 1000 ml of granular rubber were added to the FBR. The seed sludge was collected from an anaerobic filter reactor at a wastewater treatment reactor at the Faculty of Engineering, Chulalongkorn University. Total solids (TS) concentration of the seed sludge was 8,443 ± 588 mg/L. The schematic diagram of the FBR is illustrated in Figure 4.3.

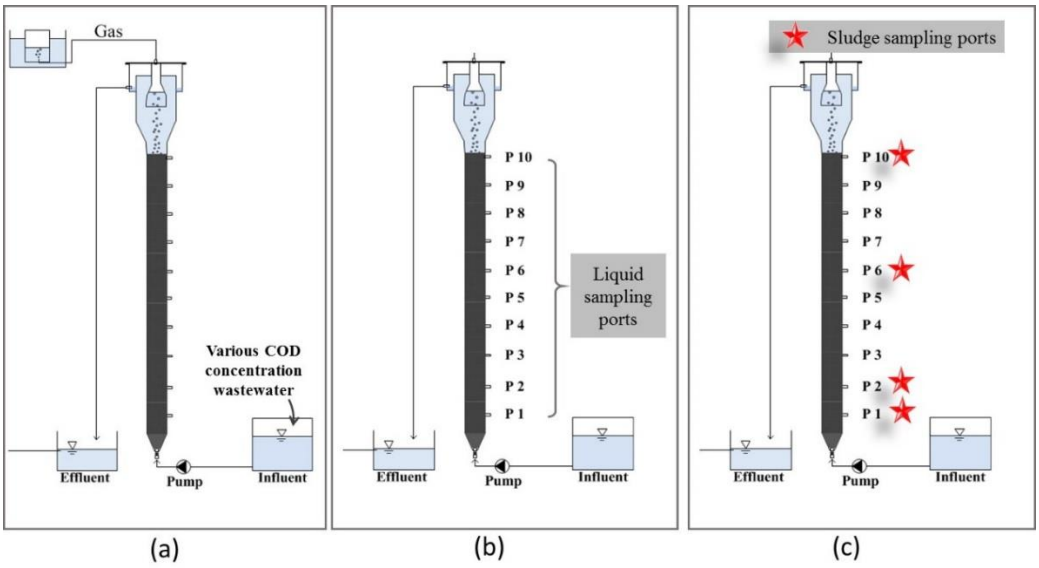

Figure 4.3 Schematic diagram of a novel FBR for low strength anaerobic wastewater treatment, (a) performance of the reactor study, (b) profiling of substrate removed study and (c) distribution of microbial community study.

For COD and substrate profiling study, the liquid samples were taken from the sampling ports. There were 10 sampling ports installed along the reactor height. The sampling port P1 was located at 30 cm from the bottom of the reactor and the distance between each port was 22 cm (as shown in Figure 4.3b).

4.5.1 Synthetic wastewater preparation and operational conditions

Synthetic wastewater was prepared from tap water using glucose as a carbon source with different COD concentrations at 150, 250 and 500 mg/L. Synthetic

wastewater contained sufficient alkalinity and trace elements as presented in Table 4.2.

Table 4.2 The compositions of synthetic wastewater in denitrification and anaerobic treatment.

Synthetic wastewater compositions	Low-strength anaerobic wastewater		
	COD 150 mg/L	COD 250 mg/L	COD 500 mg/L
Glucose (g/L)	0.15	0.25	0.50
$NaHCO_3$ (g/L)	0.10	0.15	0.20
K_2HPO_4 (g/L)	0.011	0.028	0.056
$MgSO_4.7H_2O$ (µg/L)	400	400	400
$FeCl_2.4H_2O$ (µg/L)	4	4	4
$CoCl_2.6H_2O$ (µg/L)	1	1	1
EDTA (µg/L)	10	10	10
$NiCl_2.6H_2O$ (µg/L)	0.5	0.5	0.5
$MnCl_2.4H_2O$ (µg/L)	0.5	0.5	0.5
$ZnCl_2$ (µg/L)	0.5	0.5	0.5
$CaCl_2$ (µg/L)	0.5	0.5	0.5
$CuCl_2.2H_2O$ (µg/L)	0.5	0.5	0.5
$(NH_4)_6Mo_7O_4.4H_2O$ (µg/L)	0.5	0.5	0.5

Modified from Speece (1996) and Xie *et al.* (2012)

4.5.2 Process parameters

Before chemical analysis, influent and effluent were filtered through glass micro-fiber filter (GF/CTM, WATCHMANTM, UK). COD and total solid were measured according to the standard method for the examination of water and wastewater (APHA *et al.*, 2012). pH and conductivity were monitored by pH meter (SevenGo Duo pro, METTLER TOLEDO, Switzerland). The biogas volume was collected from the effluent

gas tube that was located on top of the reactor. The composition of biogas was measured by Gas Chromatography (GC-2010, Shimadzu, Japan) with thermal conductivity detector (TCD) and PQS column. The parameter analyzed and frequency are shown in Table 4.3.

Table 4.3 Analytical methods and sensors or meters used.

Parameters	**Methods[1]**	**Frequency**
Water sample		
COD	Close reflux	Twice a week
pH	Electrode	Every day
ORP	Electrode	Every day
Volatile fatty acid	Titration	Every two days
Alkalinity	Titration	Every two days
Sludge sample		
Suspended solid	At 103 °C	Once a week
Microbial distribution	FISH technique	One time after steady state
Gas sample		
Biological gas composition	Gas chromatographic	One time after steady state

Noted: [1] Standard method for examination of water and wastewater (American Public Health Association, 2001).

4.5.3 Microbial community analysis

- DNA extraction and polymerase chain reaction (PCR) amplification

Approximately 0.5 g of the sludge samples were extracted using a FastDNA SPIN KIT for soil (MP Biochemicals, Santa Ana, California, USA) as described in the manufacturer's protocol (Appendix A). The extracted DNA was used as the template

for PCR amplification. The 16S rRNA gene fragment was amplified using the universal primer pair Univ515F (5′GTGCCAGCMGCCGCGGTAA3′) and Univ806R (5′GGACTACHVGGGTWTCTAAT3′) (Caporaso *et al.*, 2012). The modified primer pair, Univ515F/Univ806R, targeted on the V3 - V4 region of the archaeal and bacterial 16s rRNA gene (252 bp).

The PCR amplification was performed using Premix Ex Taq™ Hot Start Version (TaKaRa, Bio, Otsu, Japan) and 20 ng of template DNA in a 20 µL reaction volume and a Veriti 200 thermal cycler (Applied Biosystems, USA). The amplification program showed in Appendix A.

The PCR products were purified using a QIAquick PCR Purification KIT (QIAGEN, Germany) according to the manufacturer's instruction. DNA sequencing was conducted on the Miseq Illumina platform with a Miseq reagent Kit V2 (Illumina, USA). The experimental step of PCR product preparing before MiSeq Illumina sequencing illustrates in Figure 4.4.

Sequencing data was analyzed using QIIME software (version 1.8.0) (Caporaso *et al.*, 2012). Operational taxonomic units (OTUs) were selected at the 97% identity level using UCLUST (Edgar, 2010) according to Kuroda *et al.* (2015). The relationship between the predominant OTUs and various genera was confirmed using BLAST searches (http:blast.ncbi.nlm.nih.gov/Blast.cgi). Representative OTUs were selected on the basis of having an over 2% abundance rate in each sludge sample. Correspondence analysis was performed to determine the appropriate type of model for direct gradient analysis, redundancy analysis (RDA) was performed with CANOCO software (Šmilauer and Lepš, 2014; Sooria *et al.*, 2015).

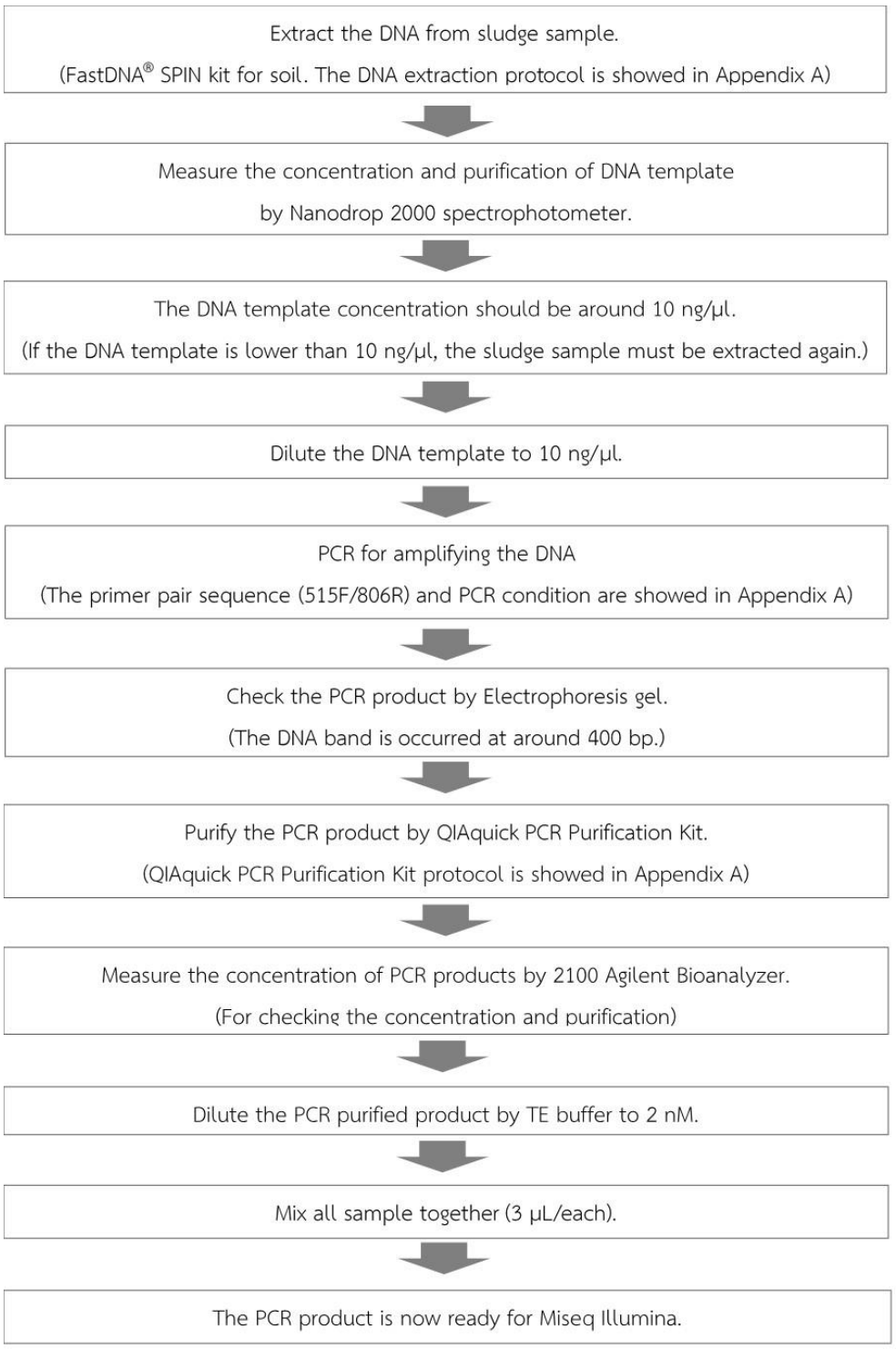

Figure 4.4 Steps of DNA extraction and PCR analysis for sludge samples from low-strength anaerobic wastewater treatment

4.6 Results and discussions

4.6.1 Start-up period for biofilm formation

During the start-up period, 250 mL of seed sludge from an anaerobic filter reactor (located at the Faculty of Engineering, Chulalongkorn University) with a total solids content of 8,443 ± 588 mg/L was mixed with 1,000 mL of granular rubber and were added to the reactor. The reactor was operated under anaerobic condition at room temperature. The synthetic wastewater was fed at an average flow rate of 60 L/d and HRT was controlled at 50 min.

During biofilm preparation periods, the novel FBR was operated for 30 days. The average influent COD concentration was 528 ± 26 mg/L and average effluent COD concentration was 326 ± 49 mg/L.

4.6.2 Performance of a novel FBR for low-strength anaerobic wastewater treatment

4.6.2.1 COD removal efficiency

A novel FBR was started-up to promote biofilm attached on the fluidized media. Then, wastewater with various COD concentrations was fed to the reactor to study its performance. Influent and effluent COD and operation time in each experiment are illustrated in Figure 4.5. It can be observed that COD removal efficiency increased when COD influent decreased. The highest COD removal efficiency was found at the OLR of 5.6 g COD/L-d. This is equal to the COD concentration of 147 ± 19 mg/d.

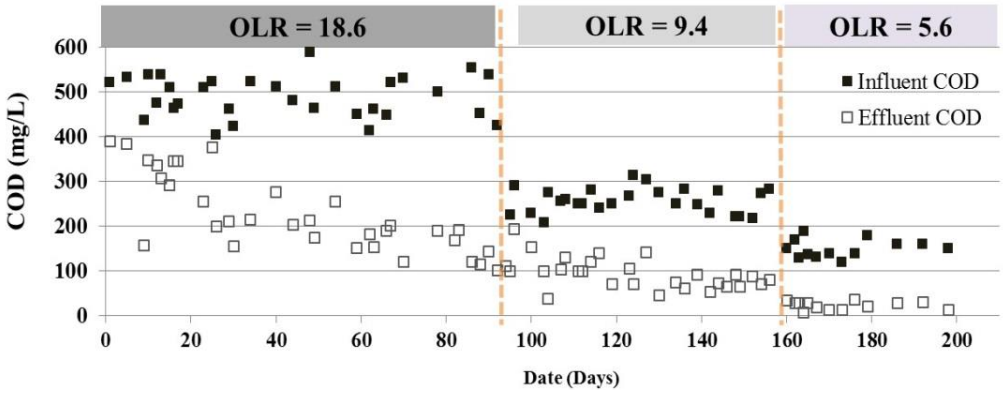

Figure 4.5 Influent and effluent COD at OLR of 18.6, 9.4, and 5.6 g COD/L-d.

After reaching steady state, the results showed that COD concentration in the effluent were 21 ± 9, 68 ± 18 and 191 ± 40 mg/L, at the OLR of 5.6, 9.4 and 18.6 g COD/L-d respectively (as shown in Table 4.4). At the OLR of 5.6 g COD/L-d, COD removal efficiency was 86 ± 6%. The increase in influent COD concentration resulted in the decrease of COD removal efficiency. The result revealed 60 ± 7% of COD removal efficiency at the OLR of 18.6 g COD/L-d. The value was lower than what found in the previous research, which reported that the COD loading of 10 - 20 g COD/L-d were appropriate for FBR, resulting in the COD removal efficiency greater than 90% (Metcalf and Eddy, 2003). However, HRT in this research was drastically lower than the previous research. Low-strength anaerobic wastewater treatment should be operated at HRT higher than 3 h (Huang *et al.*, 2011; Krishna *et al.*, 2009; Singh *et al.*, 1996).

Table 4.4 The reactor performance of a novel configuration anaerobic FBR for treating low strength wastewater.

Parameters	OLR (g COD L/d)		
	5.6	**9.4**	**18.6**
Operation time (d)	38	64	94
Influent COD (mg/L)	147 ± 19	252 ± 39	481 ± 48
Effluent COD (mg/L)	21 ± 9	68 ± 18	191 ± 40
COD removal efficiency (%)	86 ± 6	71 ± 8	60 ± 7
Total suspended solid (mg/L)	10 ± 4	28 ± 2	58 ± 28
CH_4 content in biogas (%)	15.11	28.60	45.99

4.6.2.2 Methane gas production

Overall results demonstrated that the FBR achieved high performance for COD removal at the OLR of 5.6 g COD/L-d. At the OLR of 18.6 g COD/L-d, the result showed the lowest COD removal efficiency. As shown in Table 4.4, methane content in biogas increased when the OLRs increased. Although the highest COD removal can be achieved at the OLR of 5.6 g COD/L-d, but only 15% of methane content was found. At the OLR of 9.4 g COD/L-d, the methane content was 28.60%. At the highest OLR, 18.6 g COD/L-d, the result showed the highest methane content in the biogas, 45.99%.

It can be concluded that the increase in COD concentration in the influent related to the increase in methane content in the biogas. At OLR of 5.6 and 9.4 g COD/L-d, methane contents in anaerobic treatment related to the concentration of organic compounds (COD) and efficiency of the reactor or treatment. Generally, the percentage of methane in biogas is around 60% to 70% with a balance of 30% to 40% of carbon dioxide. The practical minimum limit of 1,000 mg/L in the influent is needed to obtain successful anaerobic treatment. According to Henry's law, however, the solubility of methane for such a biogas composition would result in 65 to 75 mg COD/L of dissolved methane at 30 °C in equilibrium. This leads to the loss of dissolved

methane from the reactor without being collected as biogas. The loss of methane gas would become small at the influent COD concentration higher than 750 mg/L (Takayuki, 1994).

4.6.2.3 ORP, pH, volatile fatty acid and total alkalinity

The summarized results of pH, volatile fatty acid (VFA) and total alkalinity are presented in Table 4.5. The quality of influent and effluent during the reactor operation period (200 days) is shown in Figure 4.6.

ORP dropped significantly after feeding influent into the reactor. The value of ORP depended on the OLRs operation. Higher OLR condition showed lower value of ORP. The lowest average ORP was found at the OLR of 18.6 g COD/L-d, -171± 31 mV. Methane production was performed by methane-forming bacteria and can occur over a large range of ORP values, from -175 to -400 mV, whereas, acid formation (fermentation) can be performed at ORP values of -100 to -225 mV.

The influent pH increased when the OLR in the reactor increased due to the alkalinity added to the wastewater. However, the effluent pH decreased when OLR in the reactor increased. This result related to the concentration of appeared VFA in the reactor. As the OLR increased, VFA concentration increased. However, the addition of alkalinity in the form of $NaHCO_3$ was appropriate for the VFA produced in this study. The results were described using the ratio of VFA to alkalinity, which remained lower than 0.4 during the reactor operation period (200 days). It can be observed that there was low concentration of VFA in the influent, because the influent was prepared daily.

Table 4.5 Average (±SD) of process parameter results from a novel FBR for treating low-strength wastewater under anaerobic treatment.

Process parameter	Organic loading rate (OLR)		
	5.6 g COD/L-d	9.4 g COD/L-d	18.6 g COD/L-d
Influent COD (mg/L)	147 ± 19	252 ± 39	481 ± 48
Effluent COD (mg/L)	21 ± 9	68 ± 18	191 ± 40
COD removal efficiency (%)	86 ± 6	71 ± 8	60 ± 7
Methane gas content (%)	15.11	28.60	45.99
Influent pH	7.33 ± 0.4	7.44 ± 0.6	7.48 ± 0.7
Effluent pH	7.70 ± 0.3	7.45 ± 0.3	7.27 ± 0.4
Influent ORP (mV)	-139 ± 27	-156 ± 40	-139 ± 27
Effluent ORP (mV)	-146 ± 23	-165 ± 28	-171± 31
Suspended solid (mg/L)	10 ± 4	28 ± 2	30 ± 5
Influent VFA (mg/L)	50 ± 22	64 ± 40	94 ± 53
Effluent VFA (mg/L)	40 ± 22	82 ± 46	118 ± 54
Influent Alkalinity (mg/L)	474 ± 32	626 ± 210	754 ± 193
Effluent Alkalinity (mg/L)	530 ± 68	706 ± 227	755 ± 267
Influent VFA/Alk ratio	0.10 ± 0.04	0.12 ± 0.06	0.13 ± 0.06
Effluent VFA/Alk ratio	0.08 ± 0.05	0.12 ± 0.04	0.16 ± 0.06

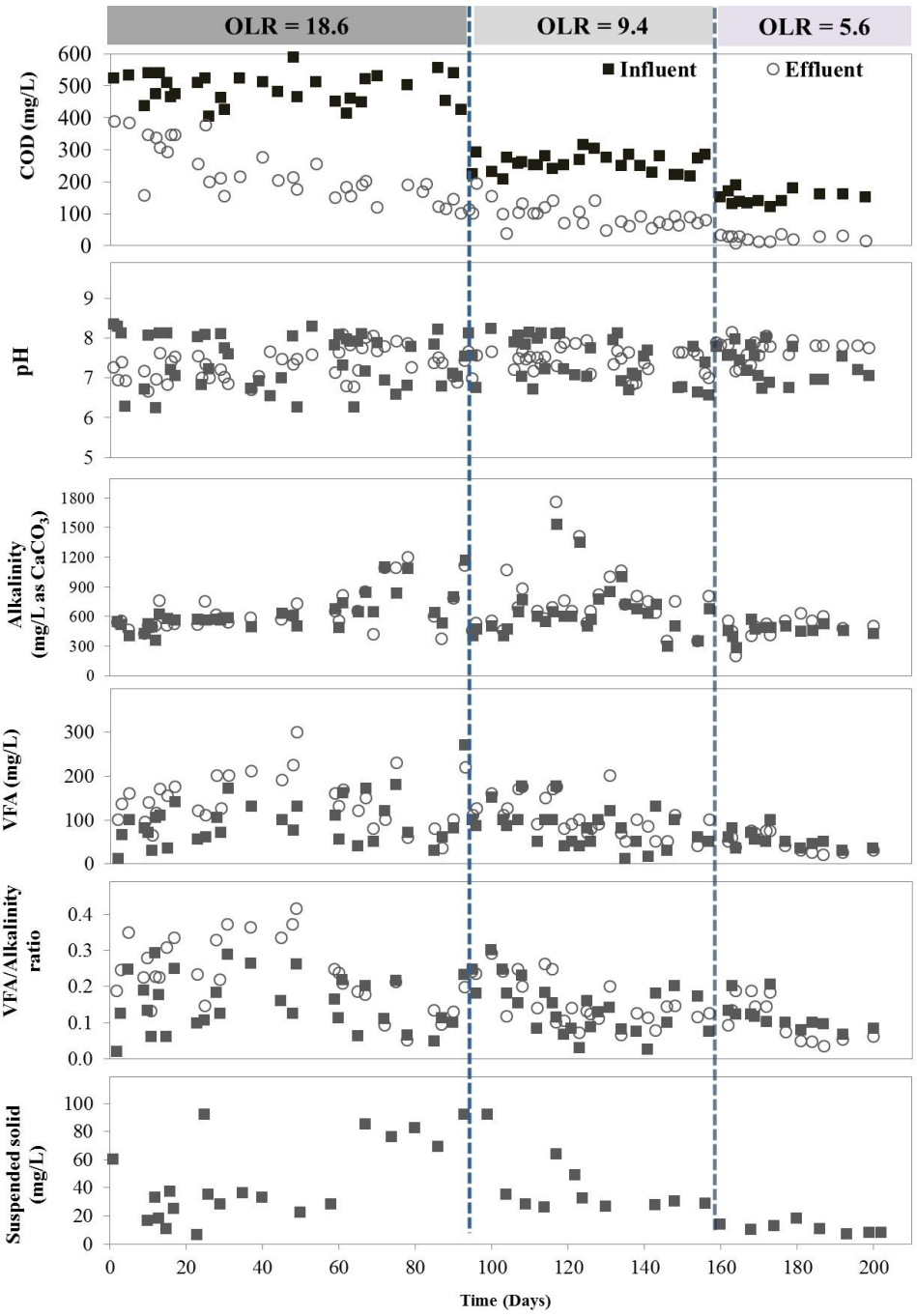

Figure 4.6 Influent and effluent quality with operation time at various OLR operation.

4.6.2.3 Suspended solid

Suspended solid is a parameter that was used for evaluating the performance of wastewater treatment. High quality effluent should contain low concentration of

suspended solid. In this experiment, the results showed that a total suspended solid was found at the OLR of 5.6 g COD/L-d and it slightly increased when OLR increased. However, at the OLRs of 5.6 and 9.4 g COD/L-d, suspended solids were lower than the standard quality of effluent (Board, 1994) which allowed suspended solids in the effluent from municipal and industrial wastewater treatment at lower than 30 and 50 mg/L, respectively. Therefore, the suspended solids in the effluent from this experiment could reach acceptable quality in the same level as the effluent from municipal wastewater treatment plant.

Yield of anaerobic microorganisms depends on acidifiers and methanogens presenting. Yield of acidifiers is 0.15 g VSS/g COD and methanogens is 0.03 g VSS/g COD. So, the overall microbial yield is 0.18 g VSS/g COD (van Lier *et al.*, 2008). The biomass yields at different OLRs are presented in Table 4.6.

Table 4.6 Biomass yields and effluent suspended solid at different OLRs

OLR (g COD/L-d)	**Bacterial yield (g VSS/d)**	**Suspended solid (g/d)**
5.6	1.36	0.62
9.4	1.99	1.67
18.6	3.87	3.49

The effluent suspended solids were lower than the bacterial growth yield for every OLR operation. This means that a novel FBR had an ability to keep biomass inside the reactor.

4.6.3 COD removal profiles and process parameters along the reactor height in the novel FBR for treating low-strength wastewater

In this part, the profiles of COD removal, pH and ORP in the novel FBR were investigated to study the substrate removal pattern. COD concentration, pH and ORP were measured in liquid sample which were taken from the sampling ports along the

reactor height. Sampling port P1 was located at the bottom of the reactor and sampling port P10 was located at the top of reactor column as shown in Figure 4.3b.

Profiles of COD concentration, pH and ORP at several levels along the reactor height were illustrated in Figure 4.7.

COD concentrations gradually decreased from the bottom of the reactor to the top part of the reactor. After port P2, the COD concentrations slightly decreased through the end of reactor, while OPR also gradually reduced from the bottom to the top of the reactor. The ORP in the effluent were higher than the influent ORP (as shown in Figure 4.7a). In contrast, the fluctuation of pH profile can be observed along the reactor height. The pH dropped occurred inside the reactor column and they increased gradually through the height of the reactor. At OLR condition of 9.4 and 18.6 g COD/L-d, pH dropped after feeding wastewater into the reactor. pH decreased continuously until sampling port P2. After port P2, the fluctuation of pH profiles was found. Finally, effluent pH was higher than that in the influent.

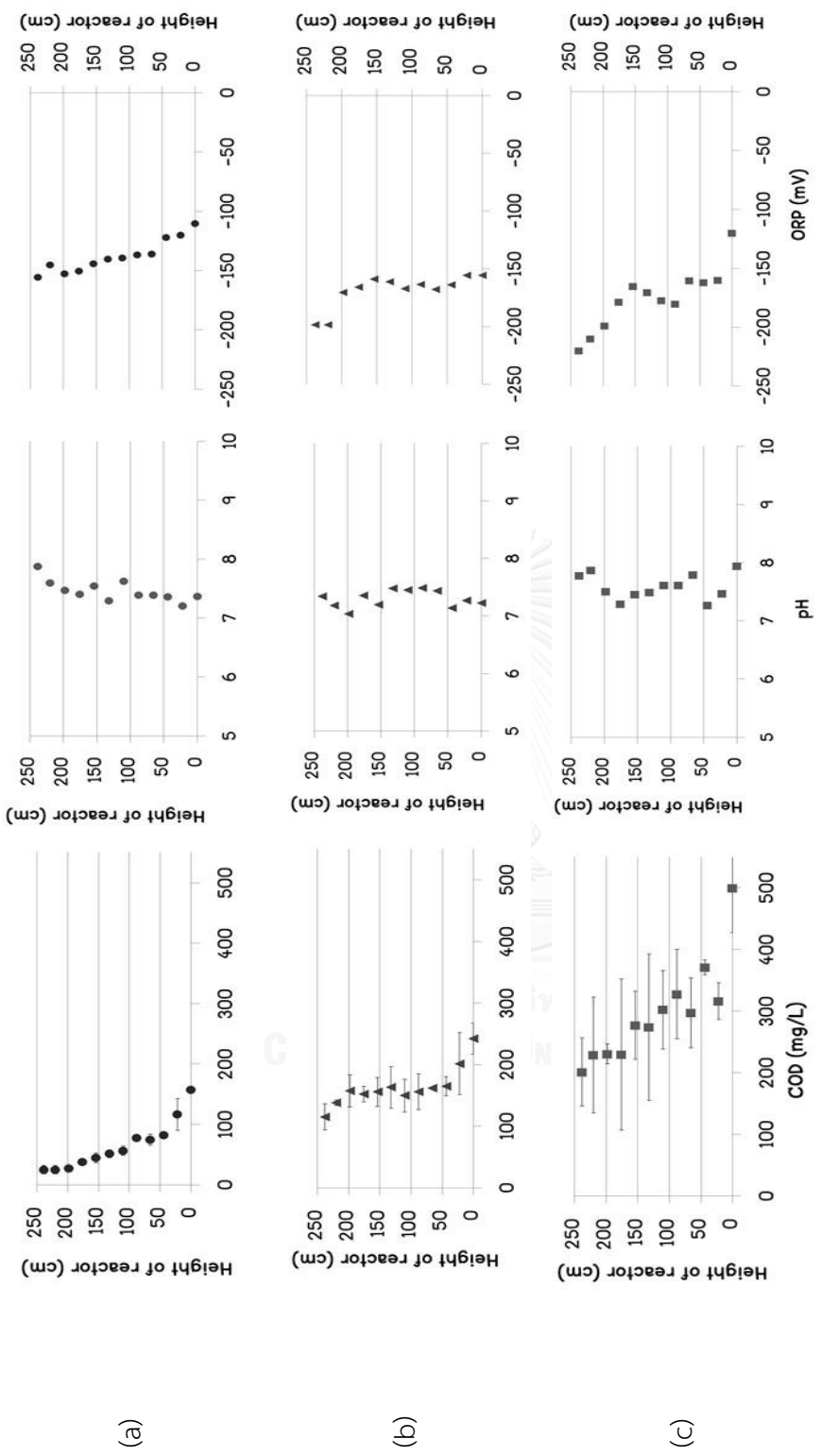

Figure 4.7 Profiling of COD concentration, pH and ORP at several levels along the reactor height, OLR 5.6 g COD/L-d (a), OLR 9.4 g COD/L-d (b), and OLR 18.6 g COD/L-d (c).

4.6.4 Microbial community distribution analyzed using MiSeq Illumina technique

After reaching steady state in each condition, the granular sludge samples were taken from the sampling ports located along the reactor column as shown in Figure 4.3c. The results of microbial community studied using MiSeq Illumina sequencing technique are shown in Figure 4.8a (phylum level) and Figure 4.8b (class level).

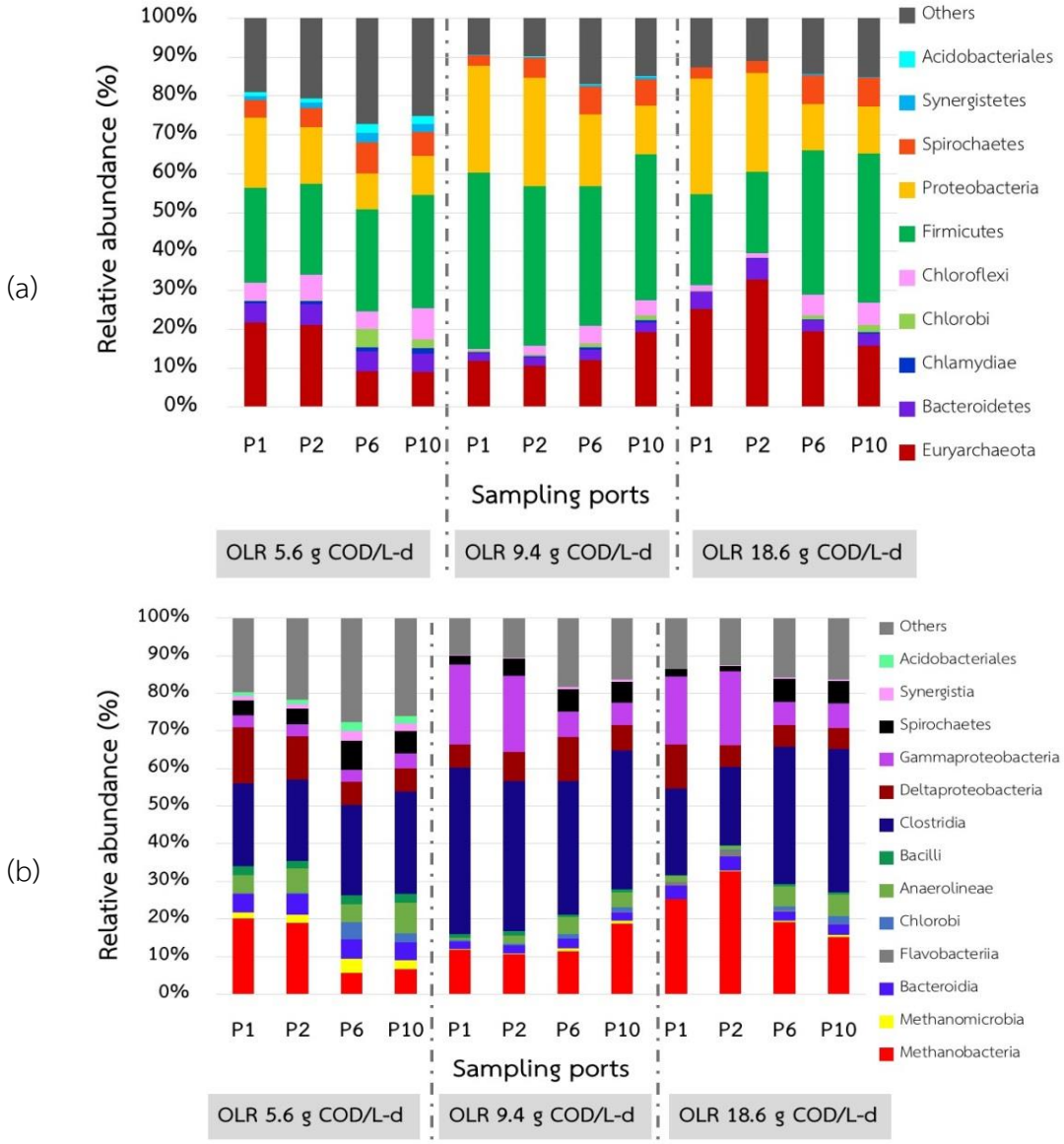

Figure 4.8 Microbial distribution in a novel FBR for treating low-strength wastewater at various OLRs, (a) Phylum level and (b) Class level.

As illustrated in Figure 4.8a, *Euryarchaeota*, *Firmicutes* and *Proteobacteria* were the predominant Phylum in this study. Additionally, Bacteroidetes, Chloroflexi, and Spirochaetes were presented in every level along the reactor height and for every OLR operation.

As shown in Figure 4.8a, 21.6%, 12.0% and 25.3% of *Euryarchaeota* were showed for different OLR operations of 5.6, 9.4 and 18.6 g COD/L-d. The highest abundance was showed at the OLR of 18.6 g COD/L-d. Most of *Euryachaeota* consisted of *Methanobacteria* and *Methanomicrobia* (the class level is shown in Figure 4.8b). *Methanobacteria* became a major microorganism when OLR increased and 32.7% relative abundance was found at the bottom (port P2) of the reactor for an OLR of 18.6 g COD/L-d, whereas the abundance of *Methanomicrobia* decreased when the OLR increased. They were found at every level along the reactor height for an OLR of 5.6 g COD/L-d and showed lower than 1% of abundance in every level of the reactor for OLRs of 9.4 and 18.6 g COD/L-d. This means that *Methanomicrobia* can survive in the low OLR system.

Firmicutes were a dominant phylum in each OLR operation, especially for the OLR of 9.4 g COD/L-d. The percentages of relative abundance found at the bottom and the top of the reactor were 45.3 and 37.5%, respectively. They can be found in every level along the reactor height under different OLR operations with relative abundance higher than 20%. There are two major microbial groups (in the class level) from Firmicutes family: Clostridia and Bacilli. As shown in Figure 4.8b, Clostridia were a dominate microbe, especially for an OLR of 9.4 g COD/L-d. In contrast, around 2% of Bacilli were presented for an OLR of 5.6 g COD/L-d. Their relative abundance decreased when the OLRs increased.

Moreover, the abundance of *Proteobacteria* was found to be related to the levels of the reactor. At the bottom of the reactor, *Proteobacteria* had relative abundance of 18.0, 27.4 and 29.7% for the OLRs of 5.6, 9.4 and 18.6 g COD/L-d. Whereas their relative abundances were shown to be 10.0, 12.6 and 12.1% in the top part of the reactor for the OLRs of 5.6, 9.4 and 18.6 g COD/L-d. *Gamma* – and *Deltaproteobacteria* classes belong to the *Proteobacteria* phylum, and they were

dominant microorganisms in this study. *Gammaproteobacteria* became a major group during the highest OLR, 18.6 g COD/L-d. For various OLRs, *Deltaproteobacteria* were found with high relative abundance at the bottom part of the reactor.

In this experiment, the predominant microorganisms in the genus level were also analyzed. Figure 4.9 illustrates dominant microorganisms and their distribution along the reactor height at different influent COD concentrations (different OLRs).

Methanobrevibacter (OTU 8885) were found in every samples. They presented in high abundance at the bottom of the reactor (sampling port P1 and P2). Their relative abundant related to the COD concentration in the reactor. At the bottom of the reactor where it contained high concentration of COD, this created favorable condition for *Methanobrevibacter*. *Methanosaeta* (OTU 3210) and *Methanosarcina* (OTU 9048) were also found in this study, but they were found at an OLR of 5.6 g COD/L-d.

From the results, it can be concluded that *Methanobrevibacter* were presented with the highest abundance among the members of phylum *Euryarchaeota*. They played an important role in anaerobic treatment process. The genus *Methanobrevibacter* consists of eight well characterized species, namely *Methanobrevibacter ruminantium*, *Methanobrevibacter smithii*, *Methanobrevibacter arboriphilicus*, *Methanobrevibacter oralis* (Ferrari *et al.*, 1994), *Methanobrevibacter curvatus*, *Methanobrevibacter cuticularis* (Leadbetter and Breznak, 1996), *Methanobrevibacter filiformis* and *Methanobrevibacter acididurans* (Savant *et al.*, 2002). It has been reported that the genus *Methanobrevibacter* was found in anaerobic digester. They can survive under pH 5-7.5 and the optimum pH is 6.0 (Savant *et al.*, 2002).

Clostridium (OTU 6969) was found to be the dominant microbe for every sample of the novel FBR. The highest relative abundance was found at an OLR of 5.6 g COD/L-d. Additionally, the members of the order *Clostridiales* (OTU 11390) were also presented with high relative abundance. *Clostridium* belongs to the family of *Clostridium* and *Firmicutes* phylum. It may be concluded that the FBR operation with

the OLR of 5.6 g COD/L-d was favorable for *Clostridium*. *Clostridium* group is the main anaerobic bacteria in hydrolysis, which played important role in degrading cellulose in the waste (Palmisano and Morton, 1996).

The genus population in the phylum *Proteobacteria* consisted of *Desulfobulbus* (OTU 6967), *Desulfovibrio* (OTU 11911 and 751), *Aeromonas* (OTU 7595) and *Enterobacter* (OTU 4894). Around 10% of *Desulfovibrio* and *Aeromonas* gerera were found for every OLR operation, whereas *Enterobacter* were dominant for the OLRs of 9.4 and 18.6 g COD/L-d. They showed low abundance when the OLR decreased to 5.6 g COD/L-d.

In addition, the abundance of *Treponema* (OTU 1991 and 4848) can be observed in every sludge sample at 1% to 5%. They showed similar abundance for every level along the reactor height for different OLRs operation. *Treponema* belongs to *Spirochaetaceae* family and *Spirochaetes* phylum.

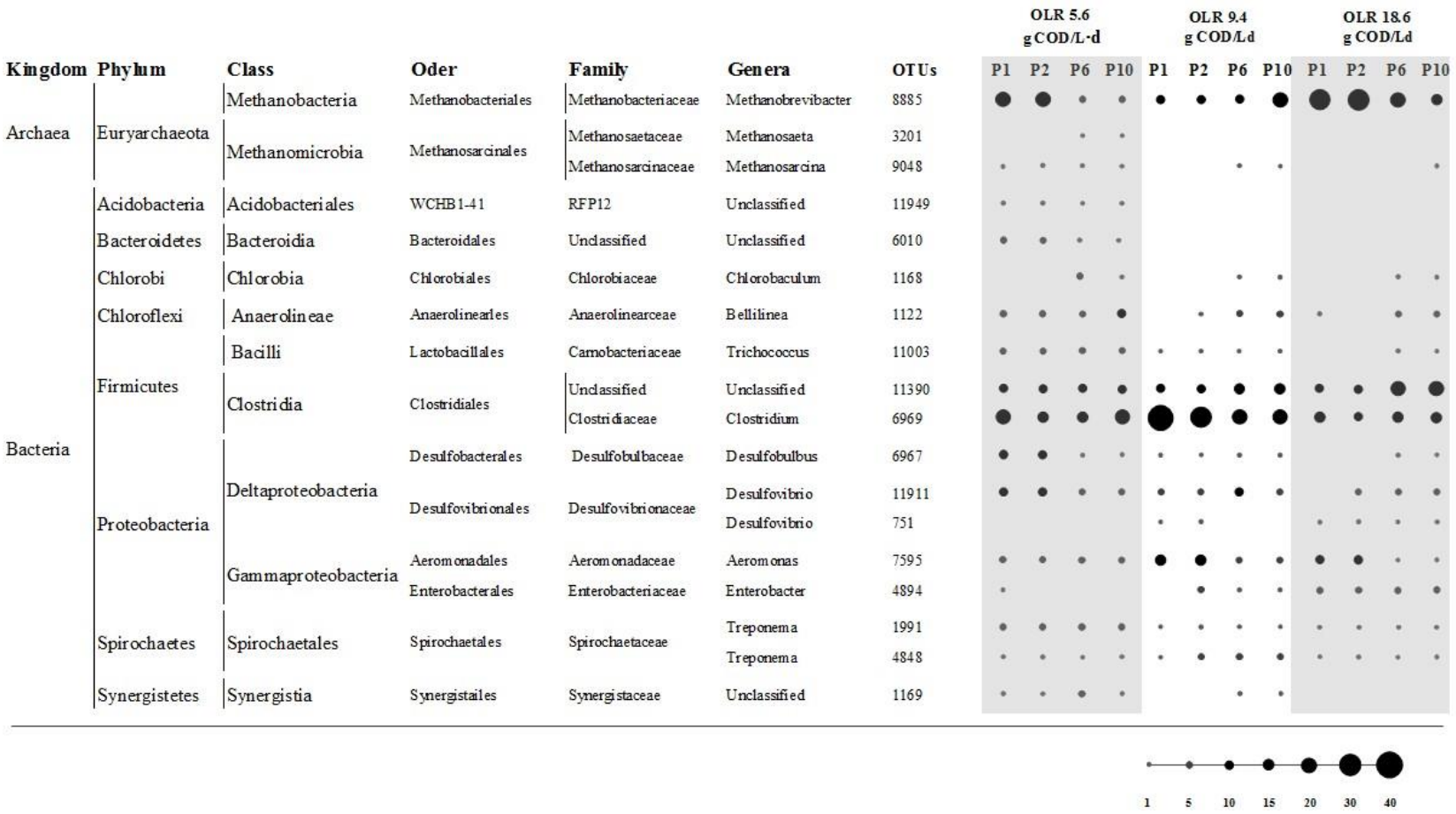

Figure 4.9 Microbial diversity and distribution in a novel FBR at different OLRs. Circle sizes relate to abundance rate, as shown in the bottom of the figure.

In this experiment, the relationship between the environmental parameters and the dominant microbial genera were investigated. At different levels along the reactor height (sampling port P1, P2, P6 and P10) and in various OLR operations, COD concentration, pH and ORP data were collected. The relative abundance of microorganisms in the genus levels were represented by OTUs.

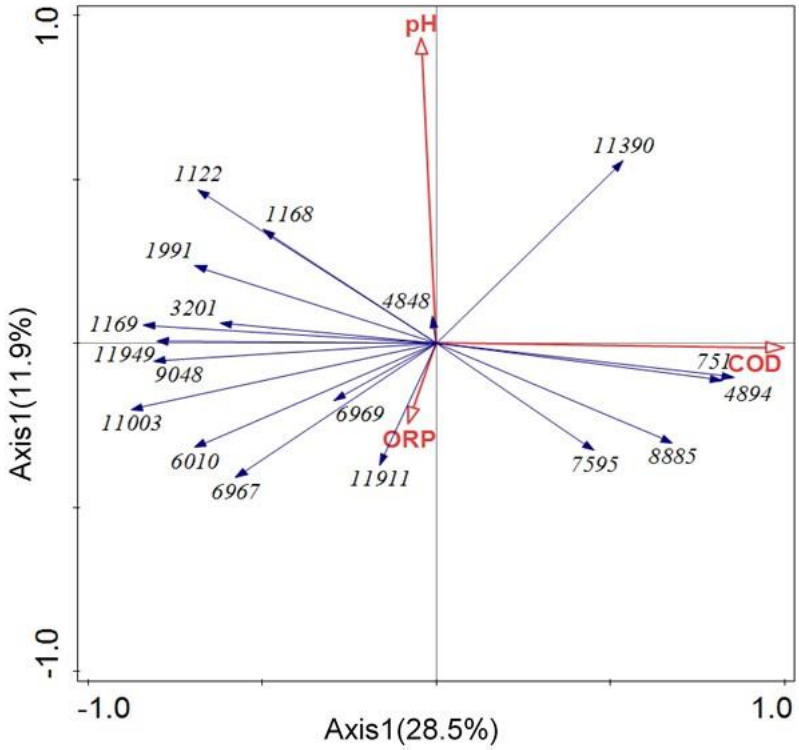

Figure 4.10 Redundancy analysis of microbial community and environmental analysis in sludge sample at different COD:NO_3^- -N ratios.
(VFA/Alk = volatile fatty acid to alkalinity ratio)

As illustrated in Figure 4.10, COD concentration strongly affected the occurrence of *Desulfovibrio* (OTU 751) and *Enterobacter* (OTU 4894). Their percentages of relative abundance were high when COD concentration was high. *Methanobrevibacter* (OTU 8885) and *Aeromonas* (OTU 7595) were influenced by the increase in COD concentration. They were dominant microbes for the high COD concentration. Only OTU 11390 was affected by both pH and COD concentration. It

means that the abundance of this microbe will increase when COD concentration and pH increase. *Treponema* (OTU 4848) increased slightly with the increase in pH. Moreover, most of the microbial communities had strong negative relationship with COD concentration in the reactor. The increase in COD concentration caused the decrease in their abundance and distribution.

4.7 Conclusions

The performance of the novel configuration anaerobic FBR was studied at different OLRs. The reactor was operated for 200 d under anaerobic condition and with very low HRT at 50 min. The novel configuration anaerobic FBR performed excellent COD removal efficiency at the OLR of 5.6 g COD/L-d (equal to 147 ± 19 mg/L of influent COD). The results showed that the effluent contained 21 ± 9 mg COD/L. The increase in OLR in the reactor decreased the reactor performance. The lowest COD removal efficiency was found at the OLR of 18.6 g COD/L-d (equal to 481 ± 48 mg/L of influent COD). Methane content in the biogas was also related to the OLR operation when the OLR increased the methane content increased. Moreover, MiSeq Illumina sequencing study revealed that the reactor operating under different OLRs affected microorganisms in the group of Methanobrevibacter, which belongs to the Archaea phylum, and was the dominant microorganisms in every OLR condition. They played an important role in methanogensis step, while Methanosaeta and Methanosarcina presented at low COD concentration with small relative abundance.

CHAPTER 5
A NOVEL FBR USING RUBBER GRANULE AS A MEDIA FOR DENITRIFICATION PROCESS AT DIFFERENT COD TO NITRATE RATIOS

5.1 Introduction

Wastewater containing high nitrogen compounds can cause serious problems to the environment. Ammonia-nitrogen is changed to nitrate during aerobic wastewater treatment. Consequently, the effluent has high nitrate and low COD concentration. Nitrate is easily diluted and can contaminate the water stream injuring human health. Nitrate contamination is a cause of eutrophication (algal bloom) in water streams. Furthermore, the US Environmental Protection Agency (US EPA) reports that the consumption of contaminated water with NO_3^--N concentration over 10 mg/L causes blue baby syndrome in children below six months of age. Therefore, nitrate reduction before wastewater discharge is necessary. Biological denitrification process is applied to convert nitrates to nitrite, nitrous oxide, and gaseous nitrogen, which can be conducted under anoxic condition to promote denitrifying bacteria. They use nitrate as electron acceptor and external carbon source as electron donor. However, addition of carbon source increases the total cost of wastewater treatment. Effective wastewater treatment system that can operate under low carbon input can serve as an alternative option for cost reduction. In wastewater treatment plant, methanol has been widely used as a carbon source (Addison *et al.*, 2011; Her and Huang, 1995; Wen *et al.*, 2003) probably due to the low cost and low sludge production. However, results showed limited bacterial population when methanol was used as a carbon source during denitrification (Ginige *et al.*, 2005; Labbe *et al.*, 2003; Osaka *et al.*, 2006). Akunna et al. (1993) reported that the use of methanol as the sole carbon source needed a long adaptation period and affected the diameter, size, distribution, and stability of the granular sludge. The granular sludge loosened and became large particles that moved to the top of reactor as colloidal matter (Jin *et al.*, 2012b). Akunna *et al.* (1992)

used glucose as the sole carbon source and found that only denitrification was observed at COD:NO_3^--N ratios less than 8.86 while both denitrification and methane production were achieved at COD:NO_3^--N ratios higher than 8.86 but lower than 53.

The fluidized bed reactor (FBR) is an attached growth wastewater treatment which has high potential for denitrification. It provides good mass transfer for substrate to biofilm covering on the carrier particle. It maintains high biomass concentration and short HRT due to the high up-flow rate. Several studies have focused on improving the performance of FBR (Calderon *et al.*, 1996; Kida *et al.*, 1990a). Horkam (2011) found that FBRs using granular rubber as media achieved high nitrate removal efficiency at COD:NO_3^--N ratio of 2:1 with sucrose as a carbon source. Sirinukulwattana *et al.* (2013) studied the performance of an FBR for anaerobic treatment operated without internal recirculation and used granular rubber as a media. Rubber was used because of its low density, suitable surface area, and non-toxicity allowing microbial growth (Park *et al.*, 2006). Their reactor was small, required low energy, and differed from the classical FBRs in terms of configuration, height, and diameter ratio.

In this research, a novel FBR (operated without internal recirculation and using granular rubber as the media) was operated at a low hydraulic retention time (HRT) of 50 min. It has been utilized for denitrification. To the best of our knowledge, no research has focused on the performance of FBR under low HRT without internal recirculation for denitrification. Additionally, our research highlighted information regarding the profiles of substrate removal and microorganisms in the novel FBR.

The objective was to study the FBR in terms of COD and nitrate removal efficiencies under different COD:NO_3^--N ratios of 1:1, 2:1, 3:1, 5;1 and 10:1. Glucose was used as the carbon source to evaluate the effect of the carbon source on denitrification capacity. Utilization of the carbon source and nitrate reduction were investigated and compared for different COD:NO_3^--N ratios. Moreover, the study of microbial communities using MiSeq Illumina sequencing improved understanding on denitrifying bacteria that played an important role in the FBR.

5.2 Research objectives

- To evaluate the performance of a novel configuration anaerobic FBR in terms of COD and nitrate removal efficiency for wastewater with different COD:NO_3^--N ratios.
- To evaluate the profiles of COD and nitrate removal at several levels of the novel configuration anaerobic FBR for wastewater with different COD:NO_3^--N ratios.
- To examine the distribution of microbial community at several levels of the novel configuration anaerobic FBR under different COD concentrations.

5.3 Research approaches

In this part, there are three main approaches as indicated in Figure 5.1

(1) The performance of a novel configuration anaerobic FBR under low COD concentration.

(2) The profiles of COD and nitrate removal of a novel configuration anaerobic FBR under different COD/NO_3^- - N ratios.

(3) The microbial community distribution in a novel configuration anaerobic FBR using MiSeq Illumina sequencing technique.

5.4 Experimental scope

A novel configuration FBR and its equipment were set-up at the 1st floor of the Department of Environmental Engineering building, Faculty of Engineering, Chulalongkorn University. There were experimental scopes as follows,

1) Synthetic wastewater was prepared from tap water using glucose as carbon source and sodium nitrate as nitrate-nitrogen source and sufficient trace elements were added. The different COD to nitrate ratio as 1:1, 2:1, 3:1, 5:1 and 10:1 were fed to evaluate the performance of the reactor, and to make

profiles of substrate removal and microorganism community distribution as shown in Figure 5.1.

2) The anaerobic FBR was made from transmitted plastic tube with 0.03 m of diameter and 3.0 m height. The active volume was 1.6 L.
3) Rubber granule was used as a media for the novel FBR with effective size of 0.43 mm and density of 1.2 g/cm^3.
4) The hydraulic retention time of 50 minutes was used in every condition.
5) Inoculum was prepared from the seed sludge of anaerobic filter reactor that located in Faculty of Engineering, Chulalongkorn University.

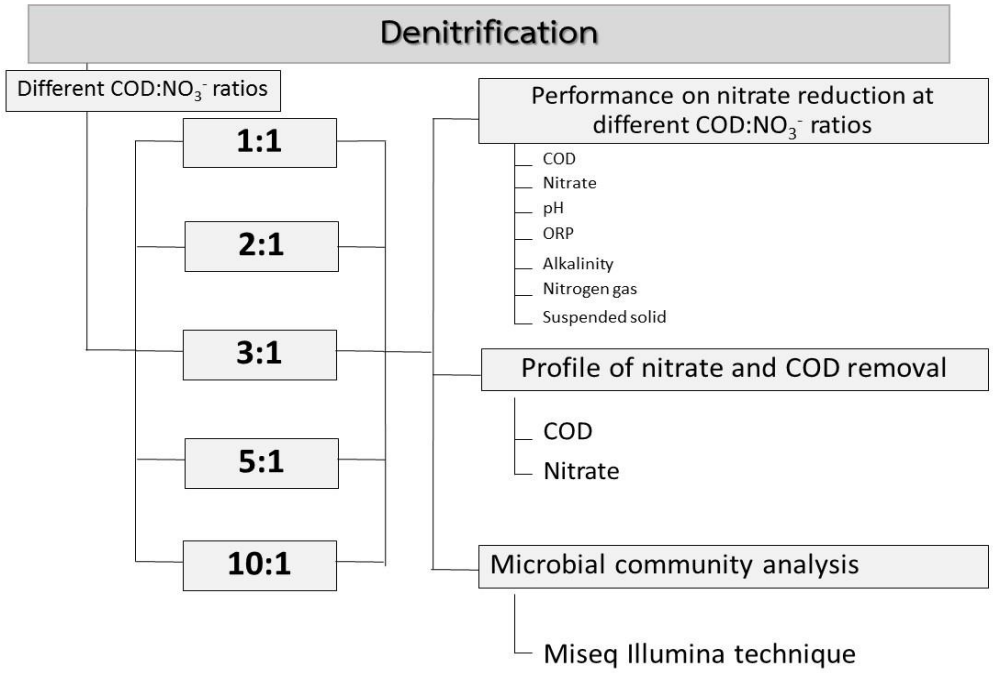

Figure 5.1 Framework of denitrification process at different COD:NO_3^- - N ratios.

5.5 Material and Methods

5.5.1 Reactor configuration and operation

The schematic diagram of the fluidized bed reactor is shown in Figure 5.2. The reactor column was made from transparent plastic, with 0.03 m inner diameter and 2.30 m bed height. It was covered with a released cap, which was a three phase separator with 10-cm inner diameter and 37.5 cm height. The main function of three

phase separator design was to facilitate the bio-particle return without external energy and control device. Moreover, it provides enough gas-water interfaces inside the gas dome and sufficient settling area outside the dome to control surface overflow rate and to allow proper return of solid back to the reactor.

The feeding flow rate was calculated from minimum fluidization velocity and terminal fluidization velocity using Eq. (2.6). The parameter values are shown in Table 5.1. The minimum fluidization velocity (V_{0m}) was 1.16 m/h and the terminal fluidization velocity (V_0) was 7.19 m/h. It can be seen that the fluidization state of rubber granule can be controlled by low up-flow velocity.

Table 5.1 The parameters values for calculating minimum and terminal fluidizing velocity.

Parameter	Value
D_p	0.43 cm
ρ	1 g/cm^3
ρ_p	1.2 g/cm^3
φ	1
ε_m	0.40
μ	0.008 cm^3/s
L	1.5 cm
L_m	1.0 cm
G	981 cm/s^2

As illustrate in Figure 5.3, feeding medium stored in the influent tank was pumped into the inlet port of the reactor by peristaltic pump with average flow rate of 60 L/d. The biological gas was measured by gas volume counter. The effluent flowed

out from the effluent port. This reactor needed only a pump for feeding and controlling fluidization state in the reactor.

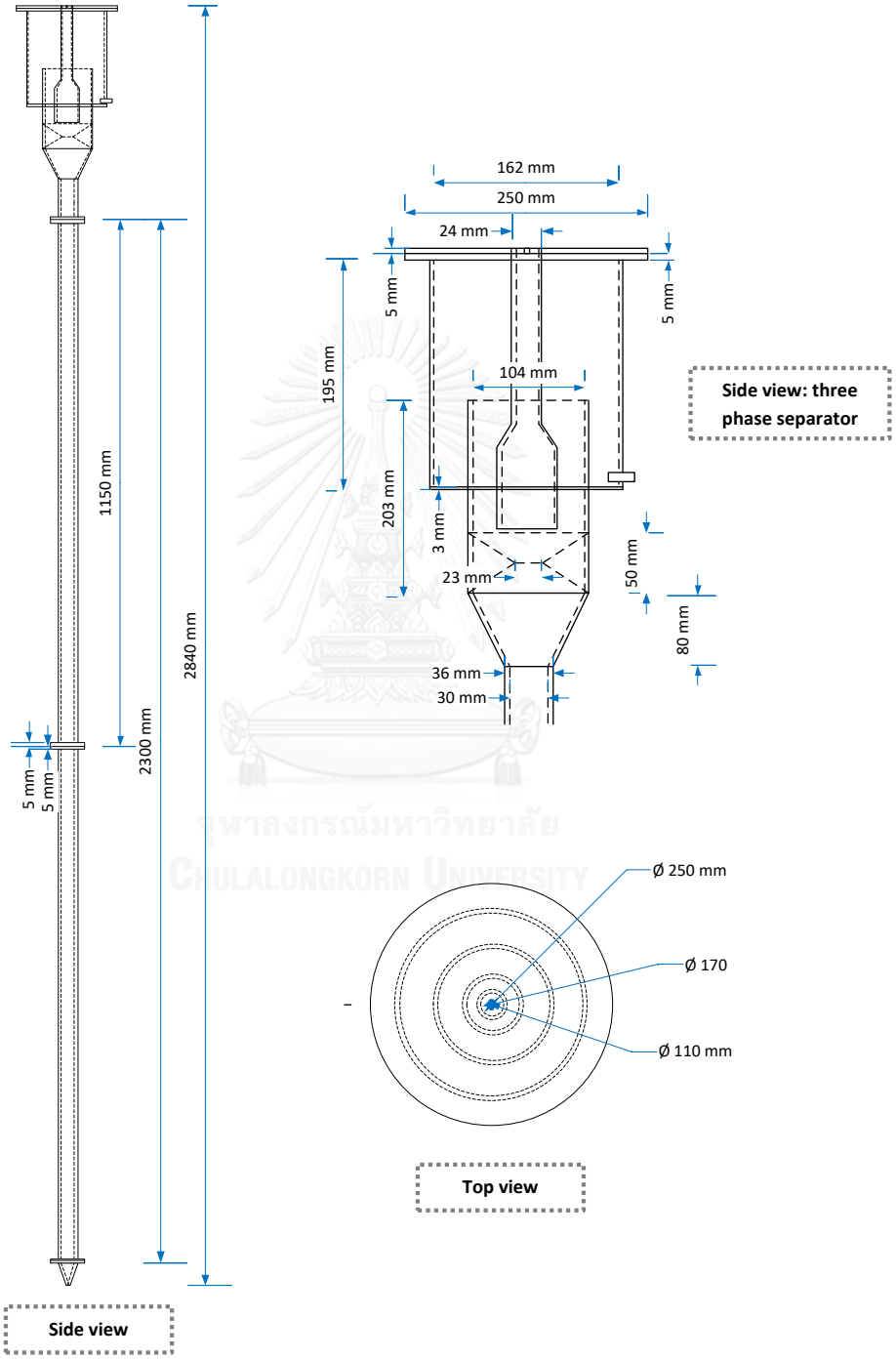

Figure 5.2 Side view and top view of a novel anaerobic FBR used in this study.

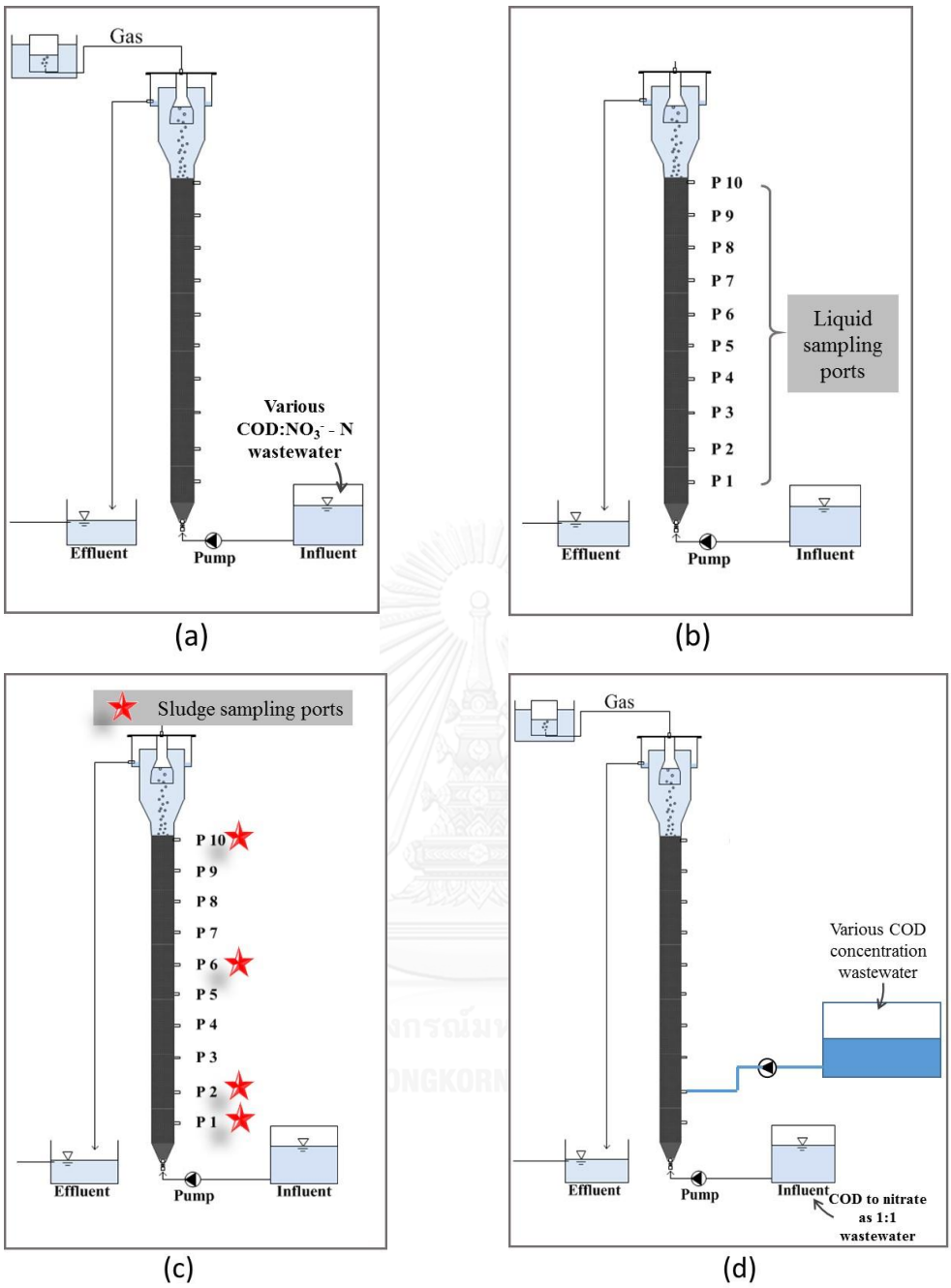

Figure 5.3 Schematic diagram of a novel FBR for denitrification process, (a) performance of the reactor study, (b) profiling of substrate removed study and (c) microbial community distribution study.

During start-up, 250 ml of seed sludge from an anaerobic filter reactor and around 1000 ml of granular rubber were added to the FBR. The seed sludge was collected from an anaerobic filter reactor at a wastewater treatment reactor at the

Faculty of Engineering, Chulalongkorn University. The total solid (TS) concentration of the seed sludge was 8,443±588 mg/L.

5.5.2 Supporting media

Crumb rubber granule is a low density material. The properties of crumb rubber granules used in this research are presented in Table 5.2 and its picture is illustrated in Figure 5.4.

Table 5.2 Properties of crumb rubber granule used in this study.

Properties	Value
Effective size	0.43 mm
Density	1.2 g/cm^3
Specific surface area	0.025 m^2/g
Uniformity coefficient	1.53

(a) real photo b) under microscope 10X

Figure 5.4 Picture of crumb rubber granule used as media in the new configuration fluidized bed reactor.

5.5.3 Operational conditions

The FBR was operated under anoxic conditions at room temperature (29±2 °C) and was fed with synthetic wastewater at a flow rate of 60 L/d. The HRT was controlled at 50 min. There are two experimental parts in this study.

1) In the first part, the FBR was initiated at the COD:NO_3^--N ratio of 5:1, which is recommended for nitrate removal via biological denitrification processes. The ratio of carbon to nitrogen around 5:1 has been used for complete denitrification process (Metcalf *et al.*, 2003). Using glucose as a carbon source, the theoretical stoichiometry of carbon to nitrogen ratio was 4.9 (Chen *et al.*, 2015; Franco *et al.*, 2006). Glucose was added at varying concentrations to the synthetic wastewater to achieve COD concentrations of 150 mg/L, 250 mg/L, 300 mg/L, 500 mg/L, and 1000 mg/L. Thus, the novel FBR was fed with wastewater that contained the COD:NO_3^--N ratios of 1:1, 2:1, 3:1, 5:1, and 10:1, respectively. The composition of synthetic wastewater was shown in Table 5.3. After reaching steady state in each operating condition, liquid and solid sludge sample were taken from several sampling ports along the reactor height as shown in Figure 5.3b and Figure 5.3c, respectively.

2) The second part is a carbon source step feed experiment, the FBR was started-up by feeding the wastewater containing COD:NO_3^--N ratios of 5:1. After the reactor achieved steady state, the FBR was fed by wastewater containing low carbon source (COD:NO_3^--N ratio of 1:1). Then, liquid and solid sludge samples were taken from several sampling ports along the reactor height as shown in Figure 5.3b and Figure 5.3c, respectively.

Wastewater with various COD concentration was fed to find the optimum value that provided the highest efficiency for COD and nitrate removal under the lowest amount of carbon source. After the optimum condition was reached, liquid and solid sludge sample were taken from several sampling ports along the reactor height as shown in Figure 5.3b and Figure 5.3c, respectively.

5.5.4 Synthetic wastewater preparation

Synthetic wastewater was prepared from tap water using glucose as the sole carbon source. The feeding solution contained different COD concentrations but NO_3^-

-N concentration was maintained at 100 mg/L. The synthetic wastewater composition is showed in Table 5.3.

Table 5.3 The composition of synthetic nitrate-rich wastewater

Components	unit	COD concentration (mg/L)				
		100	200	300	500	1,000
Glucose	g	0.130	0.23	0.40	0.57	1.15
$NaNO_3$	g	0.61	0.61	0.61	0.61	0.61
K_2HPO_4	g	0.006	0.011	0.020	0.028	0.056
$MgSO_4.7H_2O$	mg	0.4	0.4	0.4	0.4	0.4
$NaHCO_3$	mg	0.50	0.10	0.13	0.15	0.20
$FeCl_2.4H_2O$	mg	0.04	0.04	0.04	0.04	0.04
$CoCl_2.6H_2O$	mg	0.01	0.01	0.01	0.01	0.01
EDTA	µg	10.0	10.0	10.0	10.0	10.0
$NiCl_2.6H_2O$	µg	0.5	0.5	0.5	0.5	0.5
$MnCl_2.4H_2O$	µg	0.5	0.5	0.5	0.5	0.5
$ZnCl_2$	µg	0.5	0.5	0.5	0.5	0.5
$CuCl_2.2H_2O$	µg	0.5	0.5	0.5	0.5	0.5
$(NH_4)_6Mo_7O_4.4H_2O$	µg	0.5	0.5	0.5	0.5	0.5

(Speece, 1996; Xie *et al.*, 2012).

5.5.5 Liquid samples

Liquid samples were taken from the sampling ports P1, P2, P6, and P10 along the height of the reactor and filtered through a 0.45-µm glass micro-fiber filter (GF/C™, WATCHMAN™, UK) before chemical analysis. COD, total volatile fatty acid (VFA), and total alkalinity were measured using titration method as described by the Standard Method for the Examination of Water and Wastewater (APHA *et al.*, 2012). pH and ORP were monitored using a pH meter (SevenGo Duo pro, METTLER TOLEDO, Switzerland) and ORP meter (Orion 4 star, Thermo Scientific, Singapore), respectively. Nitrate concentration was analyzed using an Ion Selective Electrode (SevenCompact™ pH/Ion

S220, METTLER TOLEDO, Switzerland). Total suspended solids were measured at least once a week until the reactor reached steady state. Analytical methods and sensors or meters used are shown in Table 5.4.

Table 5.4 Analytical methods and sensors or meters used.

Parameters	**Methods**[1]	**Frequency**
Water sample		
COD	Close reflux	Twice a week
NO_3^- - N	Nitrate electrode	Twice a week
NO_2^- - N	Colorimetric	Twice a week
NH_3^- - N	Colorimetric/titrimetric	Twice a week
pH	Electrode	Every day
ORP	Electrode	Every day
Volatile fatty acid	Titration	Every two days
Alkalinity	Titration	Every two days
Sludge sample		
Suspended solid	At 103 ℃	Once a week
Microbial community	MiSeq Illumina	One time after steady state

Note: [1] Standard Methods for the Examination of Water and Wastewater (American Public Health Association, 2001).

5.5.6 Granular sludge samples

After reaching steady state, the sludge samples were extracted from the sampling ports of the FBRs. There were four samples from each COD: NO_3^--N ratio. Granular sludge samples were collected from port P1 (30 cm from the bottom of reactor), P2 (52 cm), P6 (140 cm) and P10 (228 cm) as shown in 5.3 (c). A total of 20 samples were collected. The sludge samples were gently washed and stored at -20 ℃ until DNA extraction.

5.5.7 Microbial community analysis

Approximately 0.5 g of the sludge samples were extracted using a FastDNA SPIN KIT for soil (MP Biochemicals, Santa Ana, California, USA) as described by the manufacturer's protocol (Appendix A). The extracted DNA was used as the template for PCR amplification. The 16S rRNA gene fragment was amplified using the universal primer pair Univ515F (5′GTGCCAGCMGCCGCGGTAA- 3′) and Univ806R (5′-GGACTACHVGGGTWTCTAAT- 3′) (Caporaso *et al.*, 2012). The modified primer pair, Univ515F/Univ806R, targeted V3-V4 region of the archaeal and bacterial 16S rRNA gene, giving 252-bp PCR product.

The PCR amplification was performed using Premix Ex Taq™ Hot Start Version (TaKaRa, Bio, Otsu, Japan) and 20 ng of template DNA in a 20 µL reaction volume and a Veriti 200 thermal cycler (Applied Biosystems, USA). The amplification program was as shown in Appendix A.

The PCR products were purified using a QIAquick PCR Purification KIT (QIAGEN, Germany) according to the manufacturer's instruction. DNA sequencing was conducted on the Miseq Illumina platform with a Miseq reagent Kit V2 (Illumina, USA). The experimental steps of PCR product preparing before MiSeq Illumina sequencing were as illustrated in Figure 5.6.

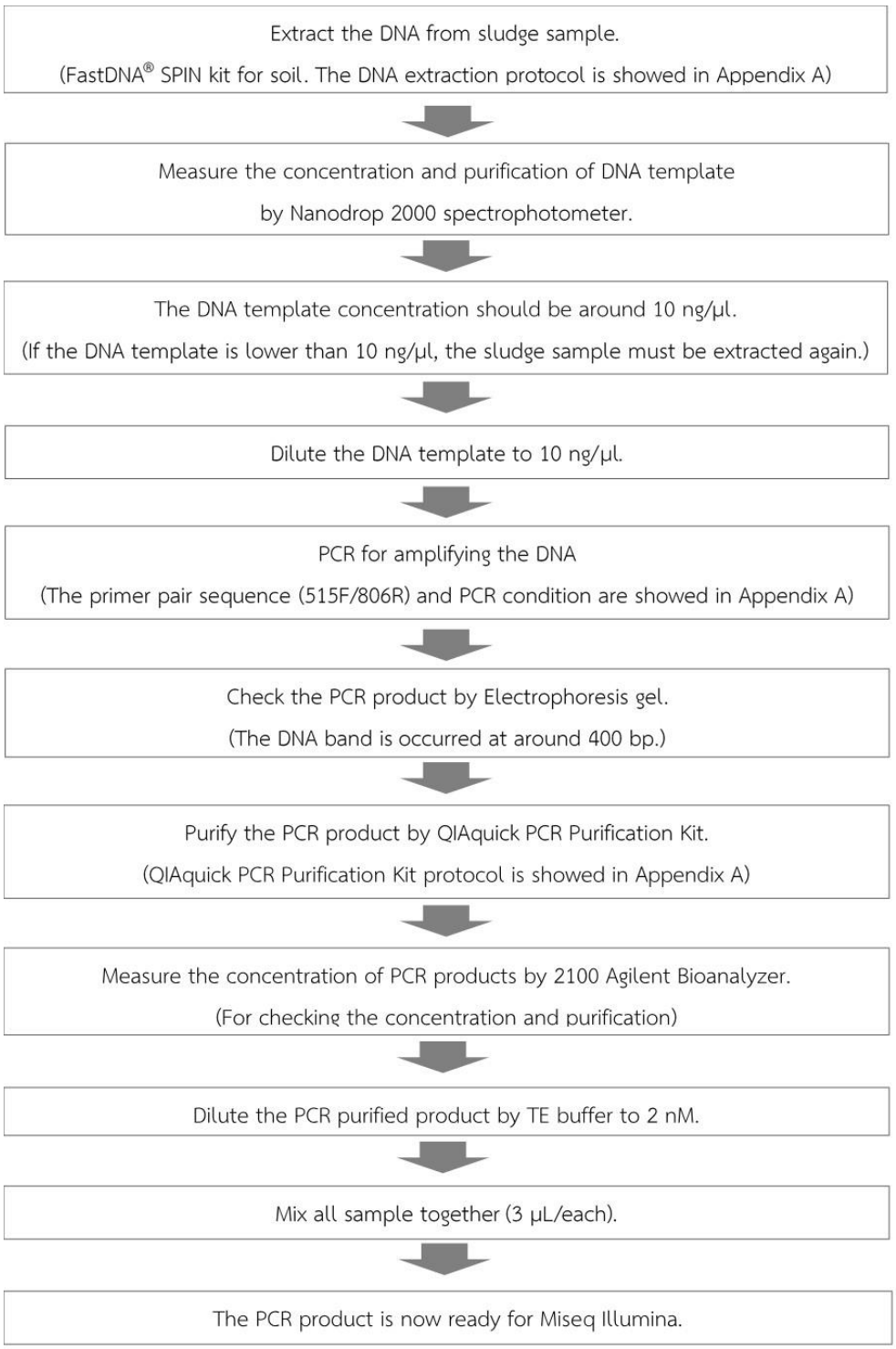

Figure 5.5 Steps of DNA extraction and PCR analysis for sludge samples from low-strength anaerobic wastewater treatment.

- Data Analysis

The PCR products were purified using a QIAquick PCR Purification KIT (QIAGEN, Germany) according to the manufacturer's instruction (Appendix A). DNA sequencing was conducted on the Miseq Illumina platform with a Miseq reagent Kit V2 (Illumina, USA) according to the manufacturer's protocol (Appendix A). Sequencing data was analyzed using QIIME software (version 1.8.0) (Caporaso *et al.*, 2012). Operational taxonomic units (OTUs) were selected at the 97% identity level using UCLUST (Edgar, 2010) according to Kuroda *et al.* (2015). The relationship between the predominant OTUs and various genera was confirmed using BLAST searches (http:blast.ncbi.nlm.nih.gov/Blast.cgi). Representative OTUs were selected on the basis of having an over 3% maximum abundance rate in each sludge sample. Based on linear models, the relationship between abundance and environmental parameter analysis was determined through redundancy analysis using Canoco 4.5.

5.6 Results and Discussion

The FBR was initially operated with a COD:NO_3^--N of 5:1 for biofilm formation. After 60 d, the reactor reached steady state and the nitrate removal efficiency was 99 ± 1% and the COD removal efficiency was 89 ± 5%. Subsequently, different COD:NO_3^--N ratios were fed into the reactor. The operation time for COD:NO_3^--N ratios of 1:1, 2:1, 3:1, and 10:1 were 52 days, 54 days, 71 days, and 75 days, respectively.

Figure 5.6 illustrates the granular rubber as media (without biofilm) and the media bed after the start-up period.

Granular rubber bed

Granular rubber and biofilm after start-up period

Figure 5.6 Granular rubber bed (without biofilm) and biofilm formation after start-up period.

5.6.1 Performance of a novel FBR for denitrification at different COD:NO_3^--N ratios

5.6.1.1 Nitrate and COD removal efficiency

Wastewater with different COD:NO_3^- - N ratios were fed into the FBR. In this experiment, the performance of nitrate and COD removal were investigated under a low HRT of 50 minutes. Moreover, effluent pH and suspended solid were also investigated.

Nitrate nitrogen source was prepared from $NaNO_3$ with fixed nitrate concentration of 100 mg/L. Glucose with varied COD concentrations (150, 250, 300, 500, and 1000 mg/L) was added to the synthetic wastewater corresponding to COD: NO_3^- -N ratio of 1:1, 2:1, 3:1, 5:1 and 10:1. The novel FBR was started-up with the COD:NO_3^- - N ratio of 5:1. After 60 days, the reactor reached steady state. Nitrate and COD removal efficiency were 99 ± 1% and 89 ± 5%, respectively. After reaching steady state, the different COD:NO_3^--N ratios were fed to the reactor at 1:1, 2:1, 3:1 and 10:1, as illustrate in Figure 5.7 and Figure 5.8.

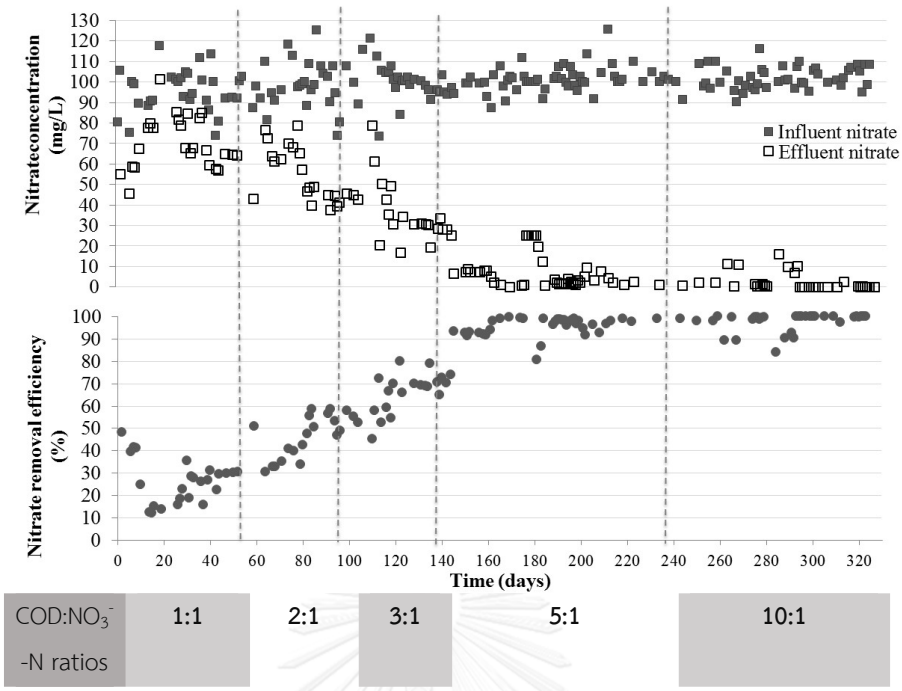

Figure 5.7 Influent and effluent nitrate concentration and nitrate removal efficiencies at different COD:NO_3^- - N ratios.

There was different time period required for reaching steady state for each COD:NO_3^--N ratio. Low COD to nitrate ratio required start-up period longer than the high COD to nitrate ratio. Due to insufficient carbon source at the low ratios of COD:NO_3^- - N, which were the ratios of 1:1 and 2:1, the results revealed low nitrate removal efficiency of 28 ± 3 % and 54 ± 4 % and COD removal efficiencies of 87 ± 5 % and 90 ± 5 %, respectively. It means that most COD was used for denitrification process but it was insufficient to remove nitrate from the wastewater. This result was in accordance with the stoichiometry from previous research which showed the ratio of COD:NO_3^--N around 5:1 (Franco *et al.*, 2006). However, at the ratio of 3:1, the results indicated that almost all nitrate and COD were reduced. The nitrate and COD removal efficiencies were 99 ± 1 % and 94 ± 3 %, respectively. It can be concluded that, at the COD:NO_3^--N ratio of 3:1, the effluent contained both low nitrate and COD concentrations.

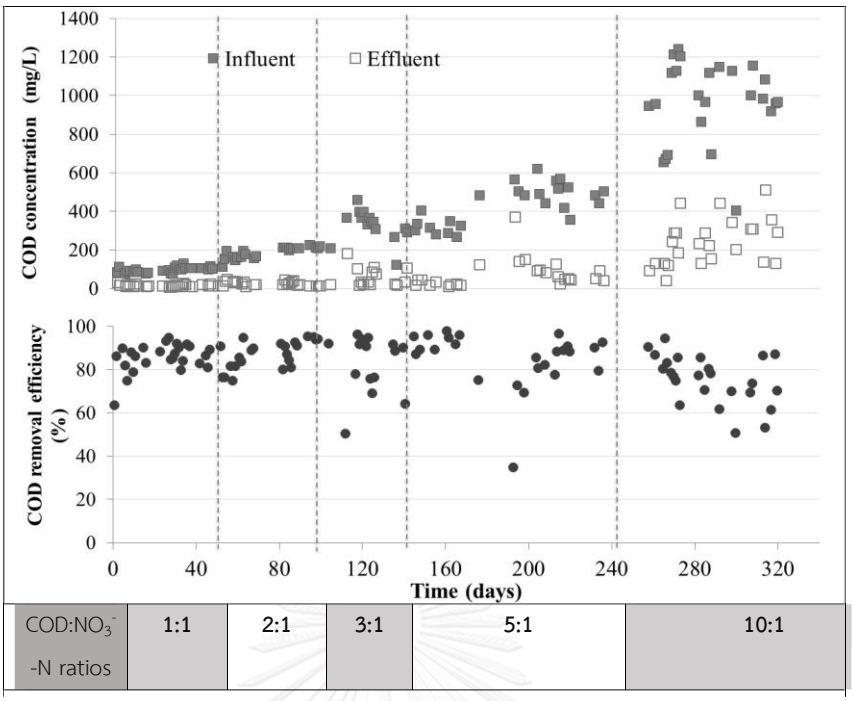

Figure 5.8 Influent and effluent COD concentration and COD removal efficiencies at different COD:NO_3^- - N ratios.

Average values of substrate concentrations and the removal efficiencies were presented in Table 5.5.

Table 5.5 Average values of substrate concentrations and removal efficiencies at different COD:NO_3^--N ratios.

COD:NO_3^--N ratios	Nitrate (mg/L, %)			COD (mg/L, %)		
	Influent	Effluent	Efficiency	Influent	Effluent	Efficiency
1:1	94±11	62±4	28±3	106±15	14±8	87±5
2:1	99±12	43±3	54±4	208±7	21±11	90±5
3:1	101±6	1.0±2	99±1	301±29	18±8	94±3
5:1	104±6	1.3±1	99±1	476±63	50±22	89±5
10:1	104±6	1±1	99±1	1,006±82	290±132	71±12

The performance of the novel FBR was compared to the conventional FBR (FBR with internal recirculation). As presented in Table 5.6, the conventional FBR was performed at 8-h HRT for treating fixed nitrate concentration of 100 mg/L with different COD:NO_3^--N ratios of 2:1, 5:1, 10:1 and 15:1 (Horkam, 2011).

Under lower HRT, the novel FBR achieved high performance as well as the conventional FBR.

Table 5.6 The performance of the novel FBR and the conventional FBR (with recirculation) using crumb rubber granule as a media.

COD:NO_3^--N ratios	**The novel FBR that operated 0.8 h of HRT. (In this study)**		**A conventional FBR (with internal recirculation) that operated 8 h of HRT. (Horkam, 2011)**	
	COD removal efficiencies	**Nitrate removal efficiencies**	**COD removal efficiencies**	**Nitrate removal efficiencies**
1:1	87±5	28±3	-	-
2:1	90±5	54±4	78	95
3:1	94±3	99±1	-	-
5:1	89±5	99±1	78	96
10:1	71±12	99±1	72	96
15:1	-	-	74	96

According to the stoichiometry, 1 mole of nitrate is reduced by 5 moles of carbon source. From the experimental results, it can be observed that the novel FBR performed high efficiencies for nitrate and COD removal at COD:NO3--N ratio of 3:1. It has been found that denitrifying bacteria in biofilm could achieve better nitrate reduction activity than suspended denitrifying bacteria (van Loosdrecht *et al.*, 1990).

From the experimental analysis, COD removal was investigated at different COD:NO_3^--N ratios as illustrated in the Figure 5.9. The amount of organic carbon for removing nitrate in wastewater by denitrification is also presented. After reaching steady states in each condition, nitrate removal increased when COD:NO_3^--N ratio increased. It can be seen that nitrate removal showed the lowest value at the ratio of 1:1 and it was slightly increased from the COD:NO_3^--N ratio of 1:1 to 3:1. At COD:NO3--N ratios of 3:1, 5:1 and 10:1, the nitrate removal was similar. It means that the amount of organic carbon was sufficient for complete denitrification when the COD:NO_3^--N ratio was higher than 3:1. However, it can be observed that COD was reduced after denitrification. At COD:NO_3^--N ratio of 10: 1, removed COD was higher than that of the COD:NO_3^--N ratios of 3:1 and 5:1 (as shown in Figure 5.9). At COD:NO_3^--N ratio of 10:1, an average removed COD of 300 mg/L was obtained, comparing to the ratio of 5:1. It might be concluded that the co-occurrence of denitrification and anaerobic condition had taken place, which is called simultaneous denitrification and anaerobic digestion. The process can be found at high concentrations of carbon source.

However, at a COD: NO_3^--N ratio of 10:1, the remaining COD was still found at high concentration. Low quality of the effluent can be found and post wastewater treatment system was required to enhance the quality of the effluent. So, the recommended COD: NO_3^--N ratio in a novel FBR was 3:1 for treating 100 mg/L of nitrate in wastewater.

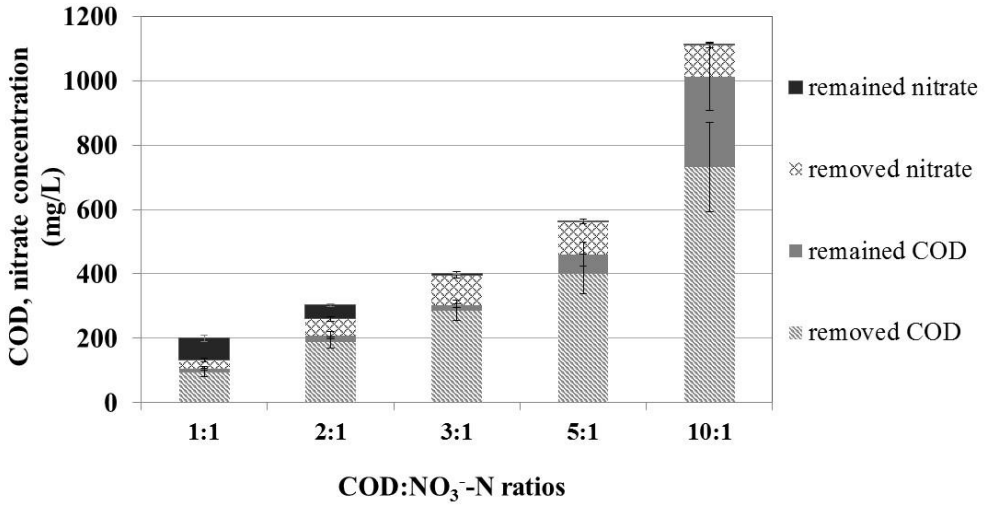

Figure 5.9 Removed and remained substrate concentration at different COD to nitrate ratios. Data are shown as the mean ± 1SD.

5.6.1.2 pH, volatile fatty acid and total alkalinity

pH, volatile fatty acid (VFA) and total alkalinity results were illustrated in Table 5.7. Influent pH was in the range of 7.7 to 8.2 while pH of the effluent was found in the range of 7.7 to 8.1. pH values in the effluent from this study were the recommended values for denitrification process.

VFA values related to the increase in COD:NO_3^--N ratio. The lowest VFA appeared at the COD:NO_3^--N ratios of 1:1 and 2:1, which were 18 ± 4 and 18 ± 10 mg/L respectively. The highest of VFA occurred at COD:NO_3^--N ratio of 10:1. However, total alkalinity in the effluent was higher than in the influent. For complete denitrification process, 3.57 g of alkalinity is produced for 1 g of nitrogen converted to nitrogen gas. Therefore, alkalinity is one of the process parameters used for confirming denitrification process. Using glucose as carbon source, nitrate reduction can be described by Eq. (5.1). It can be seen that alkalinity is produced during denitrification process.

$$24NO_3^- + 5C_6H_{12}O_6 \rightarrow 12N_2 + 24HCO_3^- + 6CO_2 + 18H_2O \qquad (5.1)$$

Table 5.7 pH, Total alkalinity and Total VFA in a novel FBR for treating various COD to nitrate ratios wastewater

Parameters	COD to Nitrate ratios									
	1:1		2:1		3:1		5:1		10:1	
	Inf.	Eff.	Inf.	Eff.	Inf.	Eff.	Inf.	Eff.	Inf.	Eff.
pH	7.94±0.4	8.07±0.3	7.72±0.4	8.12±0.5	8.12±0.5	8.12±0.2	7.76±0.42	7.69±0.53	8.20±0.4	7.72±0.4
Total VFA (mg/L)	19±4	18±4	19±6	18±10	31±13	38±27	82±53	122±36	67±26	175±47
Total Alkalinity (mg/L)	249±57	315±60	371±53	484±30	580±136	828±139	624±277	750±218	878±135	1,189±151
VFA/Alkalinity	0.08	0.06	0.05	0.05	0.06	0.05	0.17	0.17	0.08	0.15

5.6.1.3 Total suspended solid

Suspended solid is one of the parameters that can indicate the performance of wastewater treatment system. As shown in Figure 5.10, suspended solid concentration is related to COD:NO_3^--N ratio.

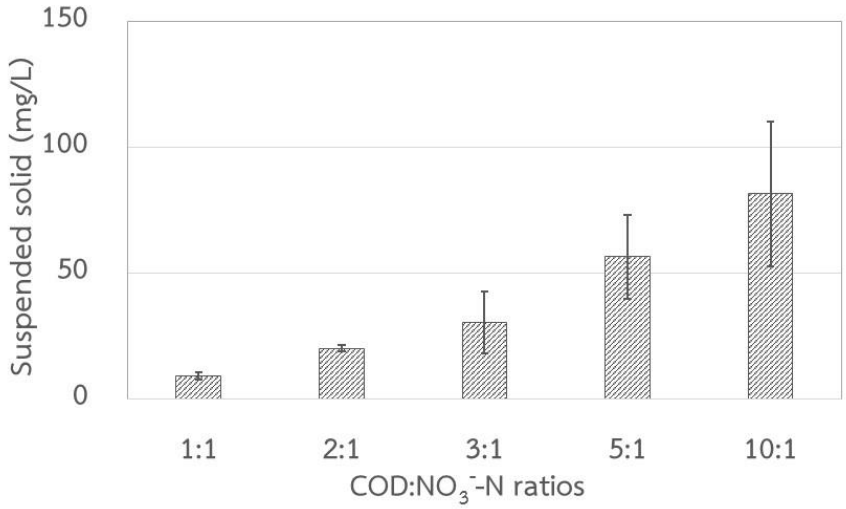

Figure 5.10 Effluent suspended solid from different COD:NO_3^- - N ratios.

Suspended solid is one of the process parameters used for evaluating the performance of the system. High quality effluent should contain low concentration of suspended solid. In this study, the lowest total suspended solid was found at COD:NO_3^- - N ratio of 1:1 condition, 9.2 ± 1.33 mg/L. The increase in suspended solid in the effluent related to the increase in COD:NO_3^- - N ratio. The results revealed that suspended solid contained in the effluent were 20.1 ± 1.35, 30.3 ± 12.23, 56.6 ± 16.61 and 81.5 ± 28.81 mg/l, at the COD:NO_3^- - N ratios of 2:1, 3:1, 5:1 and 10:1, respectively. The amount of carbon source affected the amount of suspended solid directly. In case of low ratio of COD to nitrate, carbon source posed limitation to the biofilm grow on the supporting media. It means that the biomass yield was low. In contrast, reactor operating under rich-carbon source condition promoted the amount of biomass inside the reactor. Finally, dead cells and miscellaneous substrates were washed out from the system, provided high amount of suspended solid in the effluent.

Growth yield of heterotrophic denitrifying bacteria is around 0.4 g VSS/g COD removed (Metcalf & Eddy, 2003). Therefore, yield of biomass in the reactor for different COD:NO_3^- - N ratios are presented in Table 5.8.

Table 5.8 Yield and suspended solid at different COD : NO_3^- - N ratios.

COD : NO_3^- - N ratios	Yield (g/d)	Suspended solid (g/d)
1:1	2.3	0.6
2:1	4.5	1.2
3:1	6.9	1.8
5:1	9.6	3.4
10:1	17.6	4.9

It can be observed that the biomass production inside the reactor was higher than the suspended solids in the effluent for every COD:NO_3^- - N ratio. Even when the reactor was operated under very low COD:NO_3^- - N ratios of 1:1 and 2:1, the biomass was keep both in the form of attached growth and suspended growth inside the reactor. The result showed a very low suspended solid loading in the effluent, 0.6 and 1.2 g/d, respectively. Whereas the highest biomass accumulation occurred at COD:NO_3^- - N ratio of 10:1.

5.6.1.4 Nitrite and ammonia accumulation

Nitrite is one of the nitrogen species. It has been known as a bacterial inhibitor. In this experiment, nitrite was examined at different COD:NO_3^--N operations. Influent and effluent nitrite is as shown in Table 5.9. The results showed that 0.33, 0.86, 0.19 and 0.15 mg/L of nitrite was found in the effluent at COD:NO_3^--N ratios of 1:1, 2:1, 3:1 and 5:1, whereas, at the ratio of 10:1, nitrite was not detected. At COD:NO_3^--N ratio of 1:1, an average nitrite of 0.49 mg/L was found. At COD:NO_3^--N ratios of 5:1 and 10:1, the results showed the average nitrite concentration of 0.8 mg/L.

Table 5.9 Nitrite and ammonia concentration at COD : NO_3^--N ratios of 1:1, 2:1, 3:1, 5:1 and 10:1.

COD : NO_3^--N ratios	Ammonia-nitrogen (mg/L)		Nitrite nitrogen (mg/L)	
	Influent	Effluent	Influent	Effluent
1:1	0.11	0.16	0	0.33
2:1	0.17	0.33	0	0.86
3:1	0.17	0.29	0	0.19
5:1	1.64	0.70	0	0.15
10:1	0.25	0.31	0	0

In this experiment, ammonia can be found in the effluent from every COD:NO_3^--N ratios. However, it can be seen that the concentration of ammonia was lower than 1 mg/L as shown in Table 5.9.

5.6.1.5 Profiles of nitrate and COD removal at several levels along the reactor height at different COD:NO_3^--N ratios

After steady state, liquid samples were collected from top to bottom of the reactors to reduce disturbance. The profiles of nitrate and COD removal are presented in Figure 5.11.

In this part, nitrate and COD concentrations were measured at different levels along the reactor height. To investigate nitrate reduction and COD degradation profiles along reactor height, liquid samples from 10 sampling ports were collected. Data of each COD to nitrate ratio and reactor levels are shown in Figure 5.11. Nitrate and COD concentrations decreased continuously as it passed though the fluidized bed. At low COD:NO_3^- - N ratios of 1:1 and 2:1, nitrate and COD concentrations were gradually reduced from the bottom of the reactor to sampling port P2, as shown in Figure 10b. After sampling port P3, nitrate and COD concentrations reached steady state. Therefore, the effluent contained high nitrate with low COD concentration. An average

soluble COD of 18.7 ± 6.2 mg/L and average nitrate of 6.0 ± 2.5 mg/L were observed. However, at high COD:NO_3^--N ratios of 5:1 and 10:1, most nitrate was removed at the bottom of the reactor with high residual COD presenting after port P2 particularly at the ratio 10:1. Therefore, the COD:NO_3^--N ratio of 3:1 was appropriate for the treatment of both COD and nitrate which completely removed at the bottom of the reactor.

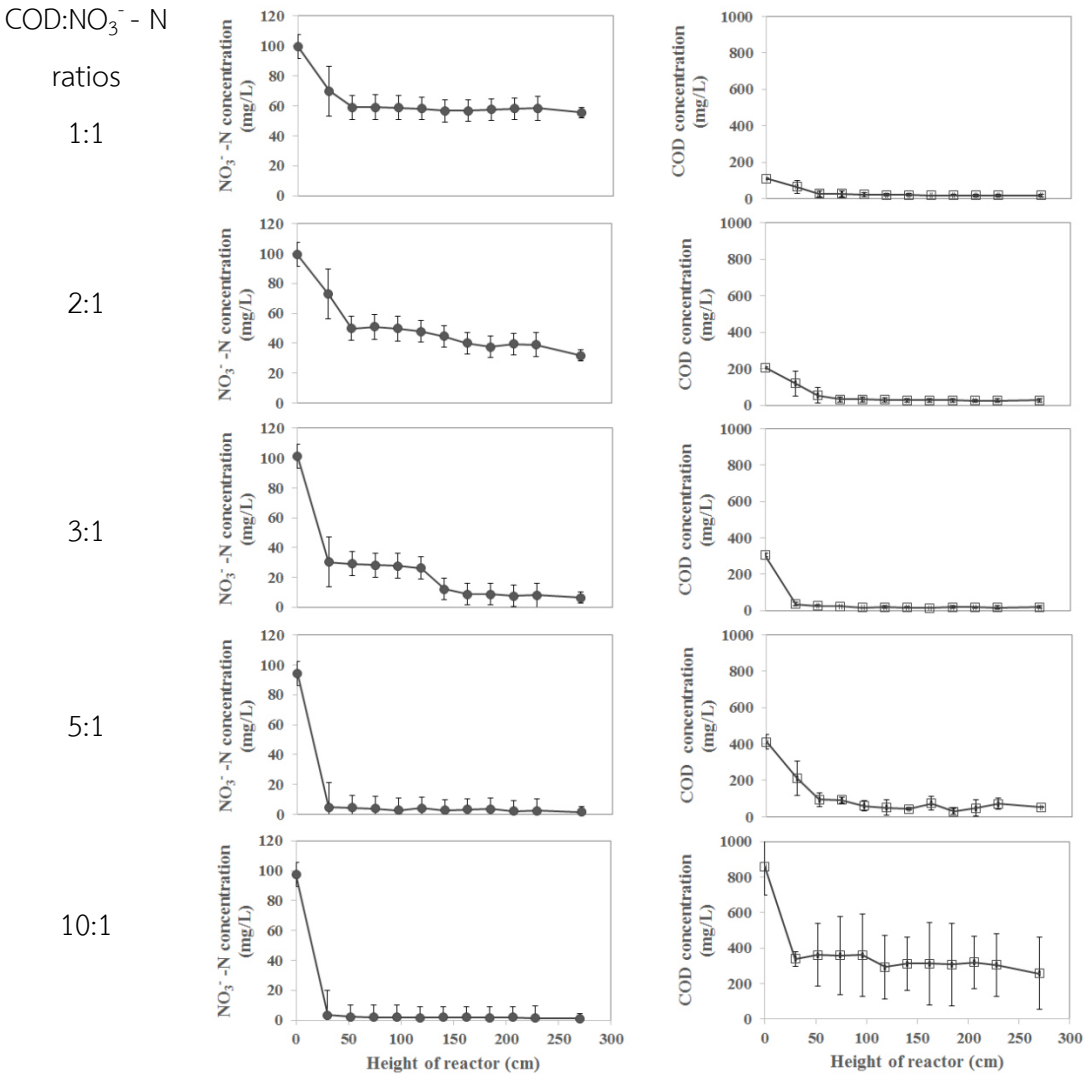

Figure 5.11 The profiles of nitrate and COD concentrations at different levels along the reactor height.

From the overall experiment, it could be seen that COD and nitrate were mostly removed at the bottom of the reactor. This phenomenon depended on the COD:NO_3^--N ratio of the wastewater. Most COD was removed at low COD:NO_3^--N ratio while most nitrate was removed at high COD:NO_3^--N ratio.

5.6.1.6 Relationship between environmental parameters and microbial community distribution along the reactor height at different COD:NO_3^--N ratios.

As illustrated in Figure 5.12a, nitrate decreased from the bottom of the reactor and decreased rapidly from P1 to P2 at the ratios 1:1, 2:1, and 3:1. At the ratios of 5:1 and 10: 1, most nitrate was reduced at the bottom of the reactor at P1. At the ratios 1:1, 2:1, 3:1, and 5:1, the COD concentrations rapidly deceased from port P1 to P2 and reached a steady state after port P2 (Figure 5.12b). However, the COD concentration at ratio 10:1 was steady at port P1 and showed very small decrease after port P2. This may be explained by the excess of carbon source at this ratio. In Figure 5.12c and Figure 5.12d, the results indicated that the pH and ORP at different sampling ports were similar to that of anoxic condition, which was appropriate for denitrifying bacteria. In general, denitrifying bacteria can grow at pH 7–9 and temperature about 20℃ – 30 ℃ (Grady *et al.*, 1999). Denitrification can occur at ORP between -100 mV to +100 mV. In this study, the results showed that the wastewater had low ORP of less than -130 mV for all ratios, as shown in Figure 5.12d. Glucose is easily biodegradable substrate, anaerobic fermentation can thus be responsible for the production of VFA, H_2 and CO_2 (Grady *et al.*, 2011).

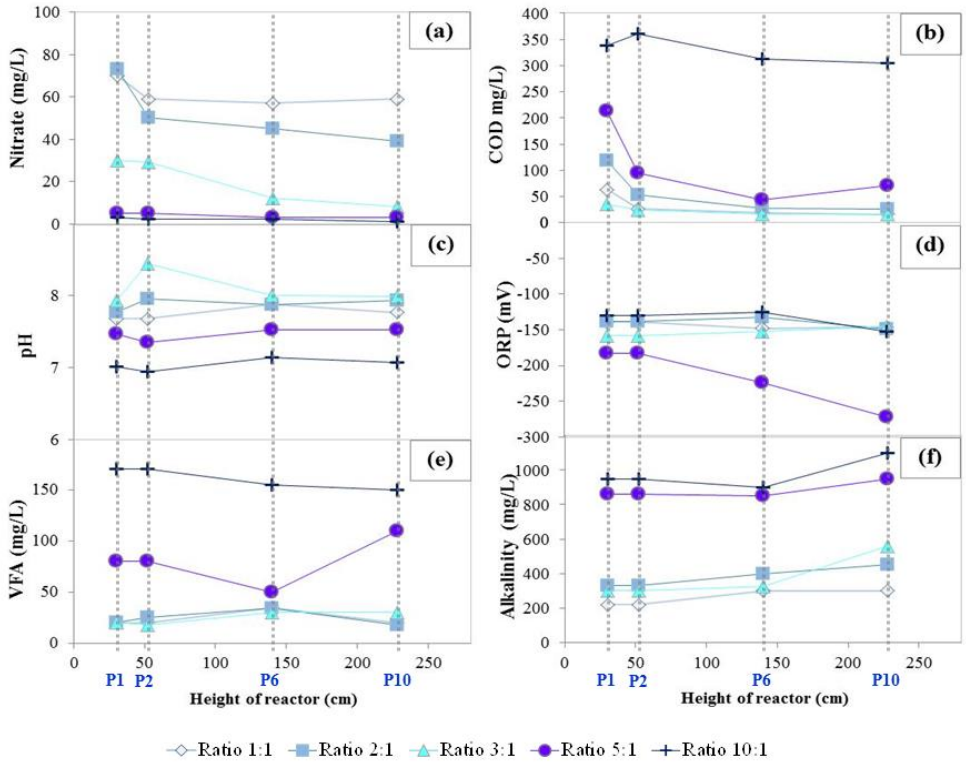

Figure 5.12 Profiles of (a) nitrate removal, (b) COD removal, (c) pH, (d) ORP, (e) total VFA and, (f) alkalinity from sampling ports P1, P2, P6, and P10 at different COD:NO_3^--N ratios.

Figure 5.12e illustrates the total VFA levels, which were related to the COD concentration at the ratios 1:1, 2:1, and 3:1. At the ratio of 5:1, the VFA slightly decreased from P2 to P6 and increased from P6 to P10, indicating that microorganisms utilized glucose and converted it to VFA. However, the result of the ratio 10:1 indicated that the VFA slightly decreased after port P2. The VFA was about 150 mg/L while the COD concentration was higher than 300 mg/L. This is probably because a small part of glucose was degraded and converted to VFA. However, in this research, $NaHCO_3$ was added with the influent for maintaining alkalinity and as a buffer to neutralize VFA. As illustrated in Figure 5.12f, alkalinity in the wastewater slightly increased after port P2 for various COD:NO_3^--N ratios.

After steady state in each COD:NO_3^--N ratio, the granular sludge was collected from top to bottom of the reactor column to reduce disturbance in the reactor. Figure 5.11 presents the results of bacterial community in phylum level (Figure 5.13a) and class level (Figure 5.13b). Most of the microorganisms in all COD:NO_3^--N ratios belonged to the phyla *Proteobacteria*, followed by *Bacteriodes*, *Chloroflexi*, *Firmicutes*, *Spirochaetes*, *Chlorobi*, *Actinobacteria,* and *Euryarchaeota*. *Proteobacteria* was the most dominant followed by *Bacteroides*. *Firmicutes* was dominant at the ratio of 5:1. *Spirochaetes* increased when the COD: NO_3^- - N ratio increased and showed highest abundance at the ratio of 10: 1. However, *Chlorobi* were found at low COD: NO_3^- - N ratios, especially at the ratios of 1: 1 and 2: 1. *Anaerolinieae* was the second major microbe at the ratio 2:1.

As shown in Figure 5.13b, at ratios of 3: 1 and 5: 1 *Alphaproteobacteria* was relatively abundant compared to other ratios. The results agreed with previous research by (Lee *et al.*, 2008). They found that *Beta-* and *Gammaproteobacteria* were important denitrifying bacteria under low COD. However, small communities of *Gamma* - and *Deltaproteobacteria* were found in all ratios.

Principal component analysis plots clearly showed that the community composition varied according to the COD: NO_3^- - N ratio (Figure 5.15). Community compositions at the ratios of 5:1 and 10:1 were distinct compared to other conditions.

Dominant microbial genera, with over 3% abundance in each sludge sample, are highlighted with different OTUs as shown in Figure 5.14. Sequencing results confirmed that the genus *Acidovorax* (OTU 14365), which belongs to the family *Comamonadaceae* in the class *Betaproteobacteria*, was the most dominant microorganism at the low COD: NO_3^- - N ratio of 1: 1, with nearly 51. 1% detected at P1 and 50. 9% detected at P2. The abundance of *Acidovorax* changed with the height of the reactor. At the top of the reactor, *Acidovorax* was around 14. 7% (P6) and it was slightly increased at the top part of the reactor, detected around 19.7% (P10).

The VFA concentration was quite low at COD:NO_3^--N ratios of 1:1 and 2:1, while it was higher at the ratios of 5: 1 and 10: 1 (Figure 5.12). This result is related to the

appearance of *Acidovorax*, which degrades VFA and aromatic compounds (Lu *et al.*, 2014) and was dominant at low VFA concentration. This indicates that the low COD: NO_3^--N ratio promotes the abundance of *Acidovorax*. *Comamonadaceae* are gram-negative bacteria, which oxidize organic compounds using nitrate as an electron acceptor under mesophilic condition. They had been found in denitrifying reactors with acetate as a carbon source (Ginige *et al.*, 2005; Osaka *et al.*, 2008). Moreover, Khan *et al.* (2002) reported that they were found as the main species during poly 3-hydroxybutyrate-co-3-hydroxyvalerate (PHBV) degradation. Furthermore, *Bacillus* (OTU 12807) and *Trichococcus* (OTU 11003) were predominant in the middle (P6) part of the reactor with 13.0% and 13.5% abundance, respectively.

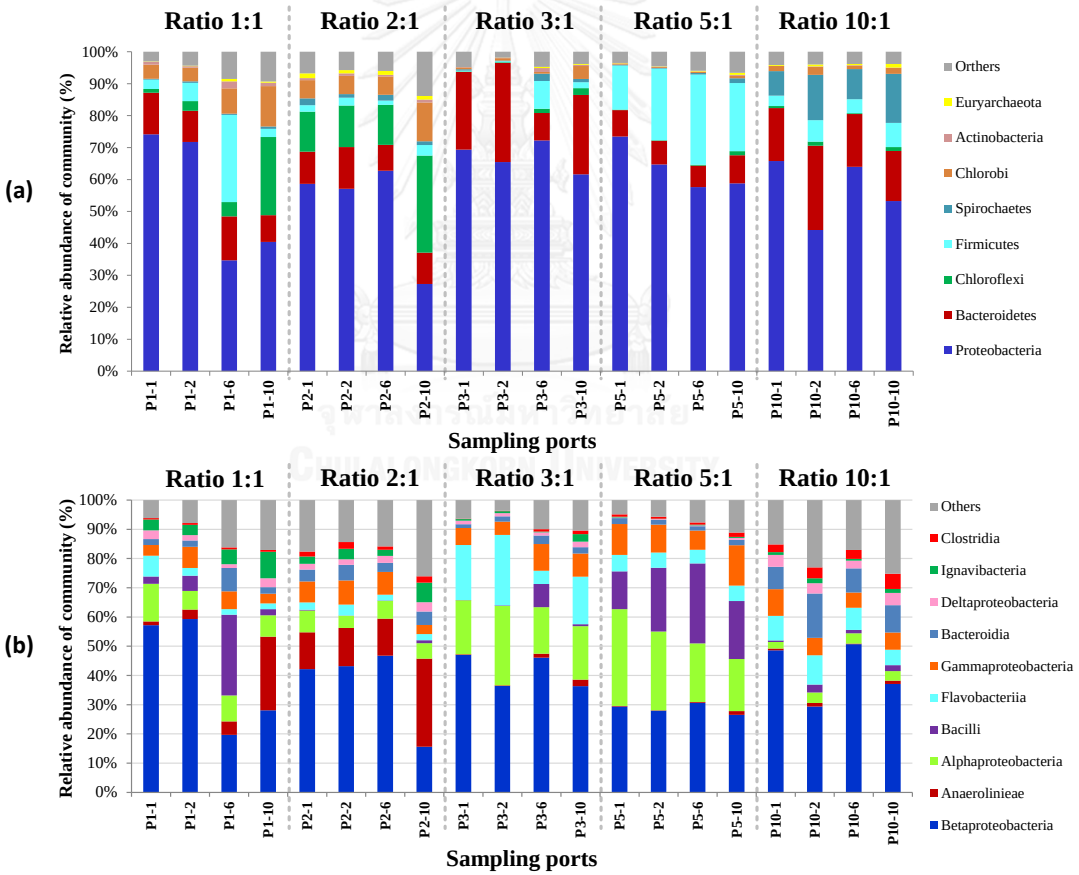

Figure 5.13 Relative abundance of (a) predominant phyla and (b) microorganism classes at different COD:NO_3^--N ratios.

At the COD: NO_3^--N ratio of 2: 1, *Acidovorax* abundance was 16. 5%, 31. 8%, 22.4%, and 9.6% at sampling ports P1, P2, P6, and P10, respectively. *Thauera* (OTUs 11289 and 13648) and *Uliginosibacterium* (OTU 12733) from the COD: NO_3^--N ratio of 2: 1 were more abundant compared to the ratio of 1: 1. Thomson *et al.* (2007) found that *Thauera* was active and utilized oxygen and nitrate as electron accepters. Their research supported the presence of *Thauera* under COD: NO_3^--N ratios of 1:1 and 2:1. At these ratios, *Longilinea* (OUT 4334) and *Thermomarinilinea* (OTU 1122) belonging to the class *Anaerolineae* were the dominant genera. At the COD: NO_3^--N ratio of 3:1, both *Acidovorax* (20% –25%) and *Rhizobium* (OTU 11351) (10%) were found in abundance. *Dechloromonas* (OTU 4478) (16. 3%) and *Cloacibacterium* (OTU 9022) (14.2%) were observed at the bottom of the reactor. *Cloacibacterium* and *Rhizobium* increased to 18.8% and 19.4%, respectively at port P2.

Around 10% of *Acidovorax* and *Dechloromonas* were found at the COD: NO_3^--N ratio of 5: 1 and the dominant community changed from *Betaproteobacteria* to *Alphaproteobacteria* and *Bacilli* classes as shown in Figure 5.14. A high amount of *Rhizobium* (31.8%) was observed at the bottom of the reactor, which decreased slightly from the bottom to the top of the reactor. *Trichococcus* became the major microbe at COD: NO_3^-- N ratio of 5:1, with 27.4% in the middle part (P6) of the reactor.

At the COD: NO_3^--N ratio of 10: 1, *Zoogloea* (OTU 6318) and *Dechloromonas* were abundant. *Zoogloea* presented as the dominant genus with 36.5% and 35.7% at the bottom (P1) and in the middle (P6) of the reactor, respectively. *Zoogloea* belongs to the family *Rhodocyclaceae* in the class *Betaproteobacteria,* and were found in aerobic granular sludge process with high organic loading rate operation (Adav *et al.*, 2009) and in the reactor fed with glucose (Li *et al.*, 2008). Huang et al. (2015) have found that *Zoogloea* associated with high nitrate removal system operating under high COD to nitrate ratio. However, *Zoogloea* can produce viscous biofilm during wastewater treatment (Gerardi, 2006), leading to packed bioparticle bed. Moreover, *Treponema* (OTU 4848) and *Bacteroides* (OTU 4113) were found in abundance in this ratio. In contrast, they were observed in small amounts at low COD: NO_3^- - N ratios.

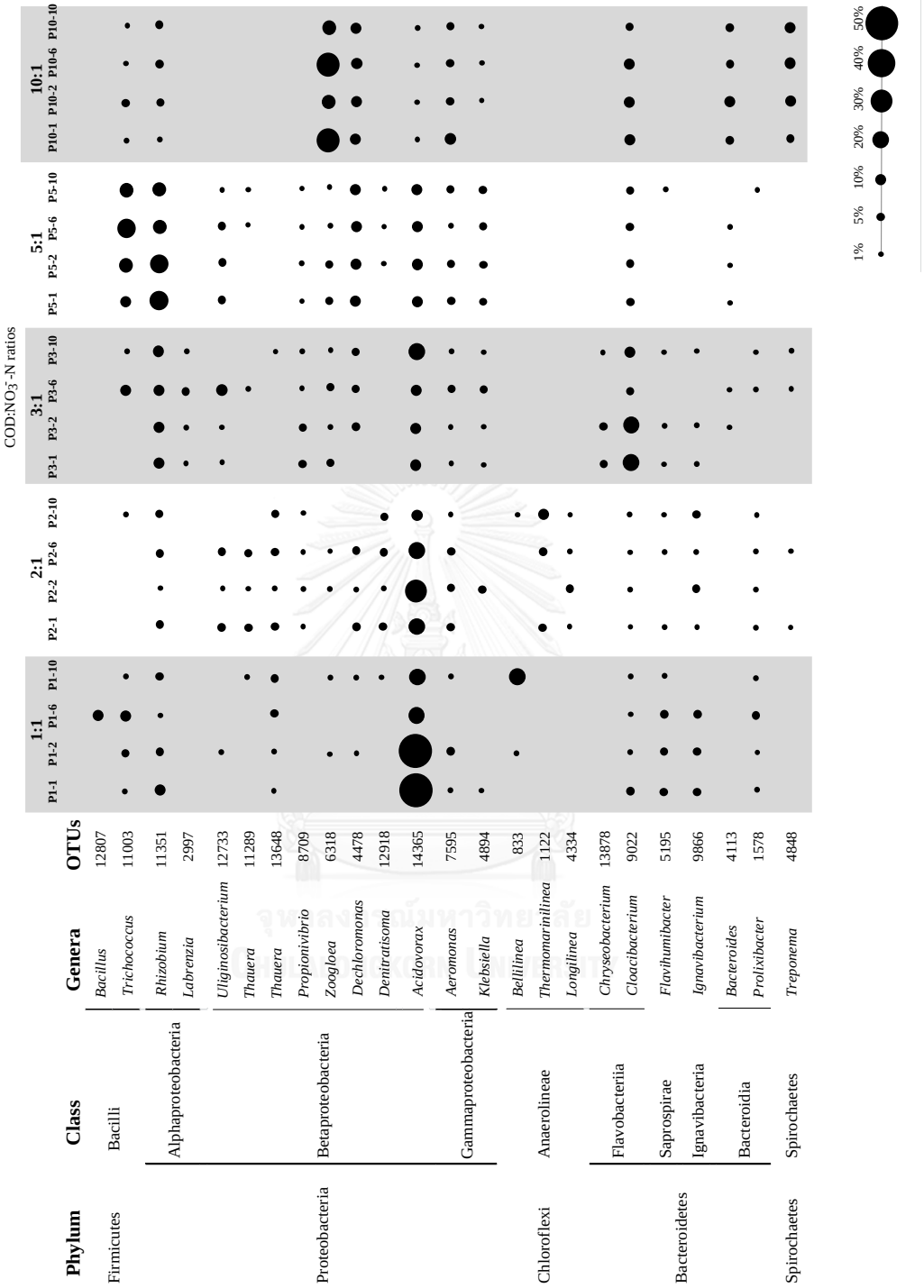

Figure 5.14 Microbial diversity and distribution in the novel FBR at different COD:NO_3^--N ratios. Circle sizes relate to abundance rate.

Principal component analysis plots clearly showed that the community composition varied according to the COD:NO_3^--N ratios (Figure 5.15). Microbial community compositions at the ratios of 5:1 and 10:1 were distinct compared to other conditions.

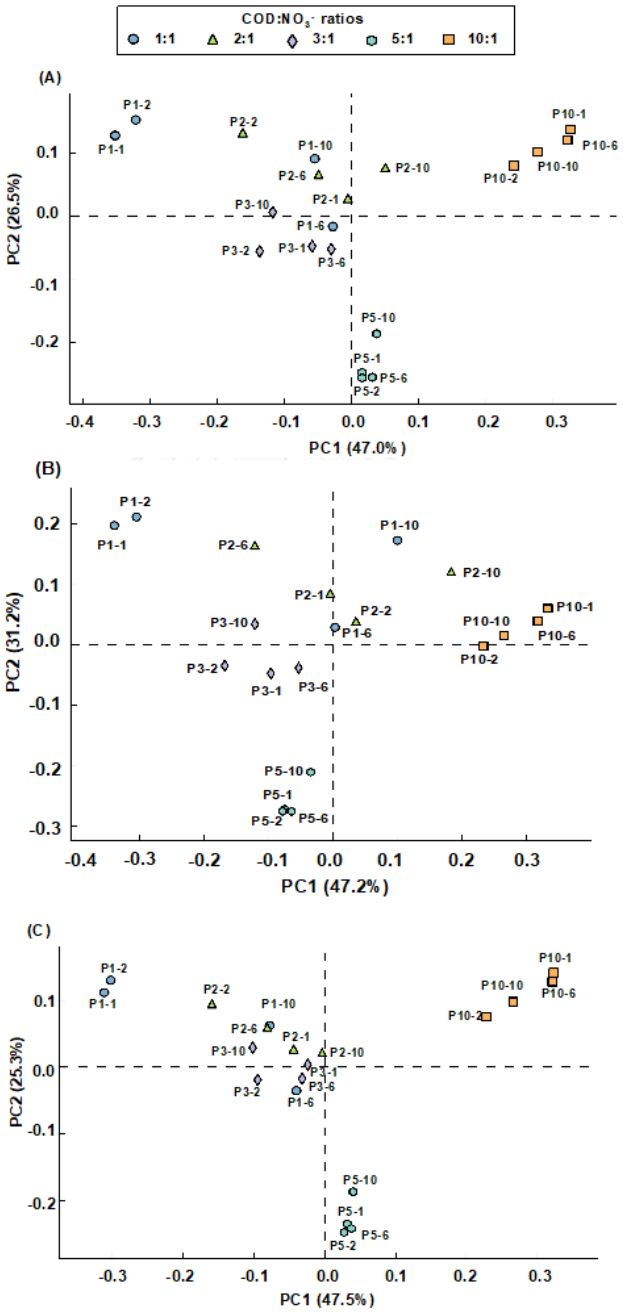

Figure 5.15 Principal component analysis plots of microbial community in the (A) Order level, (B) Family level, and (C) OTU level.

The RDA diagram is shown in Figure 5.16. The dominant microbes were identified using OTU numbers and can be explained by multivariate analysis. Based on linear modeling, RDA was used to explain the relationship between OTUs numbers and environmental parameters. The results focused on 24 OTUs of microbes and environmental parameters such as nitrate, COD, pH, ORP, VFA, alkalinity, and VFA to alkalinity ratio.

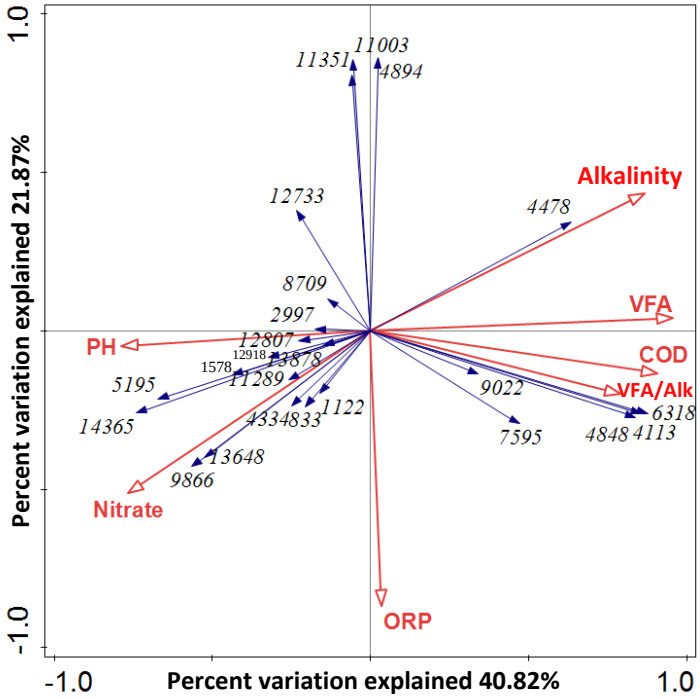

Figure 5.16 Redundancy analysis of microbial community and environmental analysis in sludge sample at different COD:NO3- - N ratios.
(VFA/Alk = volatile fatty acid to alkalinity ratio).

The results demonstrated that the increase in COD concentration and VFA to alkalinity ratio strongly influenced *Zoogloea*, *Bacteroides*, *Treponema*, and *Aeromonas* (OTU 7595) levels, but had little influence on *Cloacidobacter*, *Ignavibacterium* (OTU 9866), and *Thauera*, which were affected by the increase in nitrate concentration in the reactor. Both nitrate and pH showed positive correlation to *Acidovorax* and *Flavihumibacter* (OTU 5195). These results supported the finding of *Zoogloea* at high

COD:NO_3^--N ratios such as 10:1, whereas the *Thauera* vanished at this ratio. However, *Acidovorax,* previously found at low COD concentration and high nitrate concentration, was detected. (Maintinguer *et al.*, 2013) found that complete nitrate reduction to N_2 was achieved by *Acidovorax* species. High COD concentration was detected at the top of the reactor (as shown in Figure 5.12)

Rhizobium, *Thicococcus* (OTU 11003), and *Klebsiella* did not exhibit any relationship with the nitrate concentration in the reactor. However, they had negative relationship with the ORP, when the ORP increased they were decreased. Only *Dechloromonas* was strongly related to the increase in alkalinity. Two stains of *Dechloromonas* was reported to completely degrade mono- aromatic compounds including benzene to CO_2 and biodegradable polymer using nitrate as electron accepter in the absent of O_2 (Coates *et al.*, 2001; Shen *et al.*, 2013).

5.6.2 Performance of a novel FBR under a carbon step feeding concept

In this experiment, a novel FBR was modified by installing a step feeding pump. The concept of carbon step feeding was created to conserve carbon source in denitrification process. The study approach in this part can be divided to four experiments. The first experiment, a novel FBR was set-up and inoculated to promote microbial growth on supporting media inside the reactor. In the second experiment, the FBR was fed with wastewater at the COD:NO_3^--N of 1:1 to study its performance under low carbon source operation. The third experiment, the FBR was perform at various COD:NO_3^--N ratios in the range of 1.5:1 to 5:1. The various COD concentrations were fed to the reactor port by step feeding pump. The experimental objective was to evaluate the optimum COD concentration that provided the best performance in term of nitrate and COD removal efficiencies. The last experiment, the distribution of microbial community was studied. The profiles of microbial community before (operated at the COD:NO_3^--N ratio of 1:1) and after carbon step feed (operated at the COD:NO_3^--N ratio of 3.6:1) were compared.

5.6.2.1 The performance of a novel FBR in initial state

The novel FBR was initiated by feeding with wastewater at COD:NO_3^--N ratio of 5:1 until it reached steady state. Process parameter results are illustrated in Figure 3.16 and the average values are shown in Table 5.10.

Nitrate concentration in the influent was 102 ± 7 mg/L. After reaching steady state, nitrate contained in the effluent was lower than 1 mg/L. COD removal efficiency was 86 ± 9%. Average pH was in the optimum range for denitrifying growth, which was 8.03 ± 0.25 and 8.18 ± 0.10 in the influent and effluent, respectively. This result related to the high value of total alkalinity. The total alkalinity in the effluent was higher than that in the influent due to the alkalinity production in nitrate reduction process.

Table 5.10 Process parameter values at initial state

Parameters	**COD/NO_3^--N as 5:1**		**Removal efficiency (%)**
	Influent	**Effluent**	
Nitrate concentration (mg/L)	102±7	0.09±0.1	98±8.3
COD concentration (mg/L)	495±28	73±46	86±9
pH	8.03±0.25	8.18±0.1	-
Total alkalinity (mg/L as $CaCO_3$)	447±29	913±93	-
Volatile fatty acid (mg/L as $CaCO_3$)	20.83±8.61	22.0±15.65	-
VFA/Alkalinity	0.05±0.02	0.04±0.04	-
ORP (mV)	-121±3	-147±18	-
Total suspended solid (mg/L)	-	112±8.5	-

The interesting process parameter in this experiment was the suspended solid. After steady state, the effluent contained 112 ± 9 mg/L of the total suspended solid.

5.6.2.3 Effect of low carbon source on the performance of a novel FBR

The previous experiment showed performance of the novel FBR under insufficient carbon source. At COD:NO_3^--N ratios of 1:1 and 2:1, it was found that the FBR performed with the lowest nitrate removal efficiency and most of the carbon source added was used. Due to this low carbon source, the effluent contained high nitrate concentration and additional carbon source was necessary. Therefore, to investigate the performance during drastically low carbon source condition, the FBR was fed by wastewater containing COD:NO_3^--N ratio of 1:1. The process parameters and operation period is illustrated in Figure 5.17.

The average process parameter results are presented in Table 5.11. It can be observed that most COD was reduced and the effluent contained low COD concentration with 79 ± 8% COD removal efficiency. Average nitrate removal efficiency was 26 ± 10%. There was no different in pH value between the influent and the effluent. The accumulation of nitrite and ammonia were less than 5 mg/L. After 45 days, nitrite and ammonia was observed in the effluent. Effluent VFA concentration was related to the COD concentration. After the treatment, VFA concentration in the effluent was very low while the total alkalinity increased due to the production from denitrification process. It is interesting that the influent contained high value of dissolved oxygen (DO), 5 to 6 mg/L, whereas the effluent DO was lower than 1 mg/L along the reactor operation period. Consequently, nitrate and carbon source were removed under this anoxic condition.

It can be concluded that the novel FBR exhibited low performance in nitrate reduction when carbon source was insufficient. Although the effluent contained low COD concentration but nitrate was quite high in value. Therefore, the external carbon source was necessary to complete denitrification process.

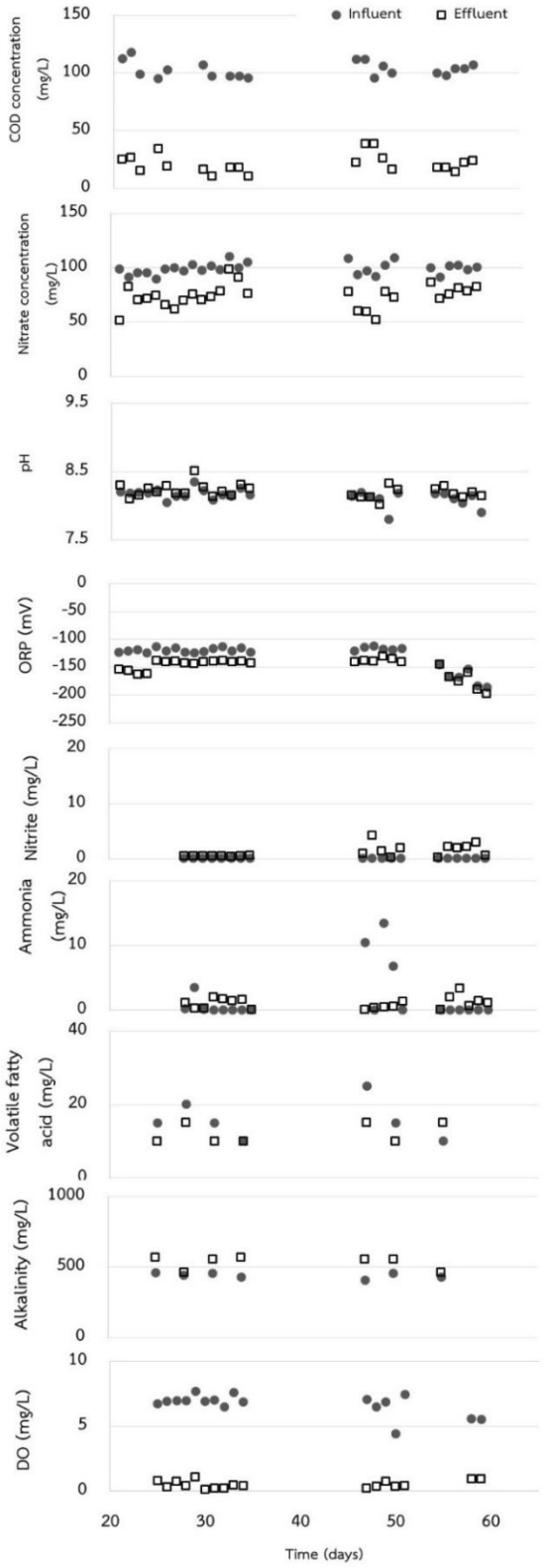

Figure 5.17 process parameter results at COD:NO_3^--N as 1:1

Table 5.11 Average value of process parameter results at COD/NO_3^- -N as 1:1

Parameters	COD/NO_3^- -N as 1:1		Removal efficiency (%)
	Influent	Effluent	
Nitrate concentration (mg/L)	99±5	73±10	26±10
COD concentration (mg/L)	103±7	21±8	79±8
pH	8.14±0.11	8.21±0.1	-
Total alkalinity (mg/L as $CaCO_3$)	436±18	529±47	-
Volatile fatty acid (mg/L as $CaCO_3$)	16±5	12±3	-
VFA/Alkalinity	0.06±0.03	0.03±0.01	-
ORP (mV)	-130±22	-151±17	-
Nitrite (mg/L)	0.01±0.00	1.15±1.19	-
Ammonia (mg/L)	0.01±0.02	1.01±0.87	
Dissolved oxygen (mg/L)	6.66±0.82	0.49±0.32	
Total suspended solid (mg/L)	-	25±4	-

5.6.2.4 Performance of the novel FBR in carbon source step feeding

In the previous experimental part, performance of the novel FBR was investigated for treating low COD/NO_3^- -N ratio, 1:1. The results showed that most COD was removed and effluent was still contained high nitrate concentration. To develop this system, a concept of carbon step feeding was applied. A step feeding pump was installed at a sampling port P2 (as shown in Figure 5.3d). Wastewater with various COD concentrations was fed to the reactor to monitor the best performance for both nitrate and COD removal efficiencies. The FBR with carbon step feeding concept was operated for more than 180 days. The relationship between nitrate and COD containing in the influent and the effluent at various COD:NO_3^- -N ratios was illustrate in Figure 5.18.

(a)

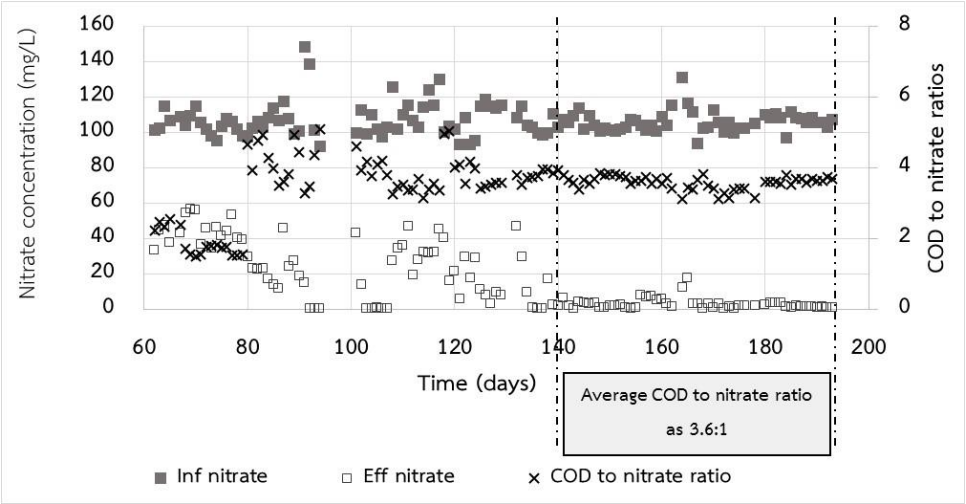

(b)

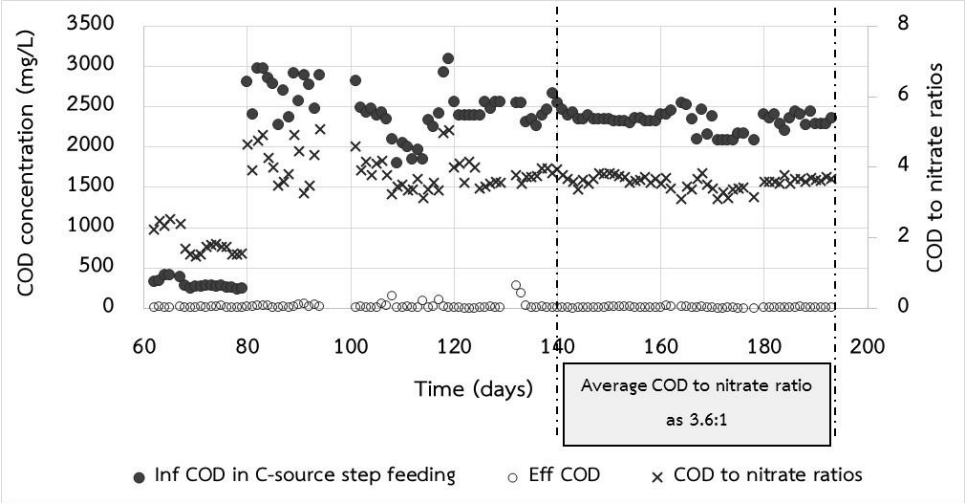

Figure 5.18 The novel FBR with carbon step feeding concept for treating different COD/NO_3^- -N ratios (a) influent and effluent nitrate and (b) influent and effluent COD.

As illustrated in Figure 5.18, COD concentrations were varied to provide the COD:NO_3^- -N ratios in the range of 1.5:1 to 5:1. At the average COD:NO_3^- -N ratio of 3.6, the results showed that most nitrate was removed (as illustrated in Figure 5.18a). Average nitrate contained in the effluent was 3 ± 4 mg/L, as shown in Table 5.12. The reactor performance achieved 97 ± 3% nitrate removal efficiency.

Similar to nitrate removal, the highest COD removal efficiency was occurred when the reactor was operated at COD:NO_3^- -N of 3.6:1, as presented in Figure 5.19b. 96±1% average COD removal efficiency was observed.

Table 5.12 Average parameter results at different COD:NO_3^- -N as 3.6:1

Parameters	COD/NO_3^- -N ratio as 3.6:1		Removal efficiency (%)
	Influent	Effluent	
Nitrate concentration (mg/L)	106±6	3±4	97±3
COD concentration (mg/L)	103±6 2,325±120	14±7	99±0.3
pH	7.8±0.16	8.0±0.07	-
Total alkalinity (mg/L as $CaCO_3$)	357±34	727±17	-
Volatile fatty acid (mg/L as $CaCO_3$)	22±20	8±8	-
ORP (mV)	-139±13	-143±14	-
Nitrite (mg/L)	0.01±0.00	1.58±1.18	-
Ammonia (mg/L)	0.13±0.19	0.83±0.73	
Dissolved oxygen (mg/L)	5.27±1.73	0.18±0.29	
Total suspended solid (mg/L)	-	13±2	-

There are similar results between the reactor operation at low COD:NO_3^- -N as 1:1 and 3.6:1. Effluent VFA was still low concentration that related to low COD

concentration in the effluent. Nitrite and ammonia were occurred with low concentration. However, DO in the effluent was 0.18 ± 0.29 mg/L. It was lower than that at the COD:NO_3^- -N as 1:1. The increase of influent COD concentration promoted anoxic condition for denitrification process. Moreover, effluent suspended solid was 12 ± 2 mg/L, which was lower than that at COD:NO_3^- -N as 1:1.

5.6.2.5 Effect of carbon step feeding on the performance of the novel FBR

The results in the previous experiment showed that the carbon step feeding to the novel FBR could successfully treat drastically low carbon wastewater. In this part, the results from the carbon step feeding and the different COD:NO_3^- -N ratio experiments were compared for their nitrate removal efficiency, COD removal efficiency and total suspended solid contained in the effluent.

- Nitrate and COD removal efficiencies

The results show the performance of the novel FBR for treating wastewater that contained different COD:NO_3^- -N ratios and operating under the carbon step feeding. Similar COD and nitrate removal efficiency was found for both experiments. Among various COD:NO_3^- -N ratios, the ratios of 3:1 and 3.6:1 provided the highest performance. More than 94% and 97% of COD and nitrate were removed (as shown in Figure 5.19). Although the results from both conditions were not different, the long-term operation cost differed. The novel FBR has advantage in term of the low cost operation because it can be operated using only one pump (for feeding and controlling the fluidization state inside the reactor), whereas the carbon step feeding FBR needed two pumps. The first pump was required for a reason similar to the novel FBR and the second pump was for the carbon step feeding.

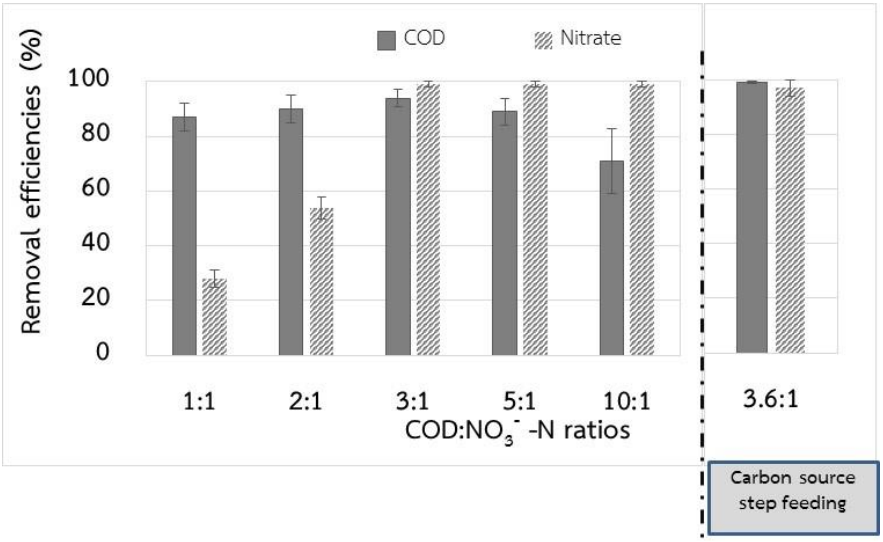

Figure 5.19 COD and nitrate removal efficiencies for treating different COD:NO_3^- -N ratios and for the carbon step feeding to the novel FBR.

- Suspended solid contained in effluent

Effluent suspended solid is one of the parameters that can be used to indicate the reactor performance. Low suspended solid means high quality effluent. In Figure 5.20, total suspended solids in the effluent were presented. At different COD:NO_3^--N ratios, the increase in COD:NO_3^--N ratio caused the effluent suspended solid to increase. In contrast, at the COD:NO3- -N ratio of 3.6:1, the effluent suspended solid was similar to that at the COD:NO3- -N ratio of 1:1.

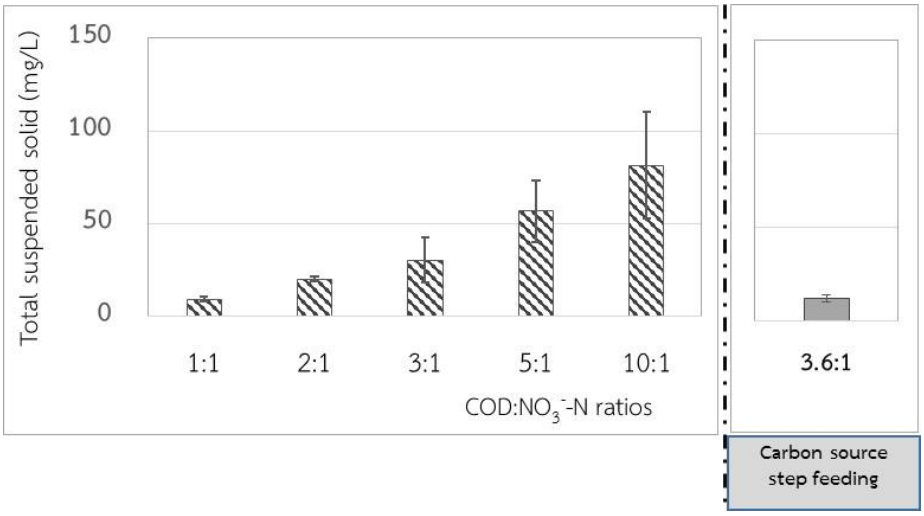

Figure 5.20 Total suspended solid in the novel FBR for treating different COD:NO_3^--N ratios and for the carbon feeding concept.

5.6.2.6 Profiles of substrate concentration and process parameters at several levels along the reactor height: a comparison between before and after carbon step feeding condition

As described above, the novel FBR modified the reactor configuration and operation. For deeper understanding on the wastewater treatment inside the reactor for both before and after the operation had been modified, profiles of substrate concentration and process parameters was used to explain the phenomena inside the reactor.

Figure 5.21 presents the profiles of substrate concentration at several levels along the reactor height. There were two operational conditions, at COD:NO_3^- - N ratios of 1:1 (Figure 5.21a) and 3.6:1 (Figure 5.21b).

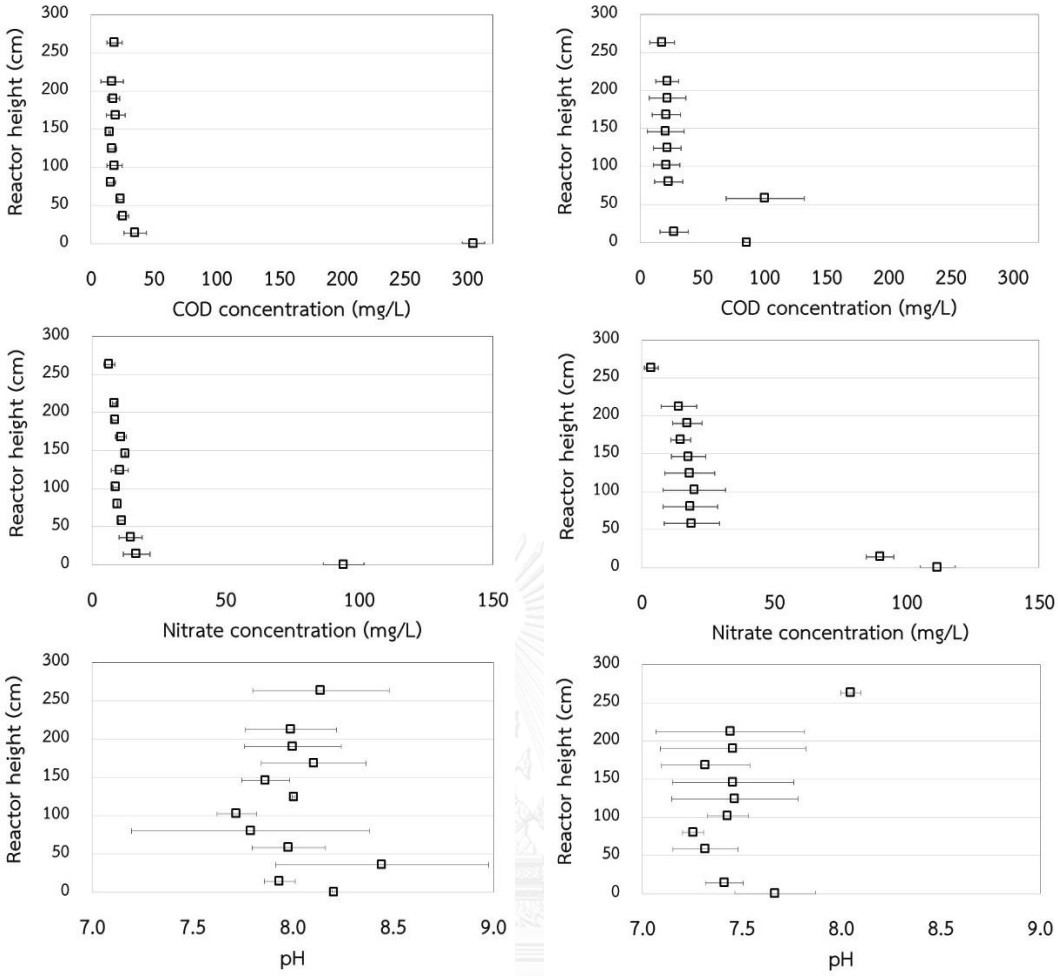

Figure 5.21 Profiles of substrate concentration at several levels along the reactor height at (a) COD:NO_3^--N of 3:1 and (b) COD:NO_3^--N of 3.6:1 (carbon step feeding condition).

The liquid samples were taken from ten sampling ports which located along the reactor height. Y axis is the reactor height and X axis is the substrate concentration and process parameters.

At COD:NO_3^- - N ratio of 3:1, most nitrate and COD were removed at the bottom of the reactor. After sampling port P2, COD and nitrate concentrations reached steady concentration. At COD:NO_3^- - N ratio of 3.6:1, high concentration of carbon was fed into the reactor by step feeding at sampling port P2. Therefore, the COD concentration

fluctuated at the bottom part of the reactor, and about 70 to 140 mg COD/L was observed. After sampling port P4, COD concentration reached steady concentration.

It can be observed that both COD and nitrate were removed at the bottom of the reactor, both at the COD:NO_3^- - N ratios of 3:1 and 3.6:1. The results from both conditions presented similar values of COD and nitrate concentration profiles along the reactor height. Moreover, the fluctuation of pH value can be observed at the COD:NO_3^- - N ratios of 3:1 and 3.6:1.

The substrate profile study confirmed that the novel FBR operating at COD:NO_3^- - N ratio of 3.6:1 (by carbon step feeding concept) could provide COD and nitrate removal efficiencies as high as the novel FBR at COD:NO_3^- - N ratio of 3:1. However, the disadvantage of the carbon step feeding was the additional pump installation and long-term operation cost. Consequently, the novel FBR is still proved as an alternative reactor which provides high performance in denitrification process, low cost in long-term operation, and can function without a requirement of an optional system.

5.6.2.7 The Distribution of microbial community in a novel FRB with carbon step feed concept

In this experimental part, the microbial distribution was studied. Granular sludge samples were taken from sampling ports along the reactor height at the bottom part (P1 and P2), middle part (P6) and top part (P10). The sequencing data from MiSeq Illumina analysis are illustrated in Figure 5.22.

(a)

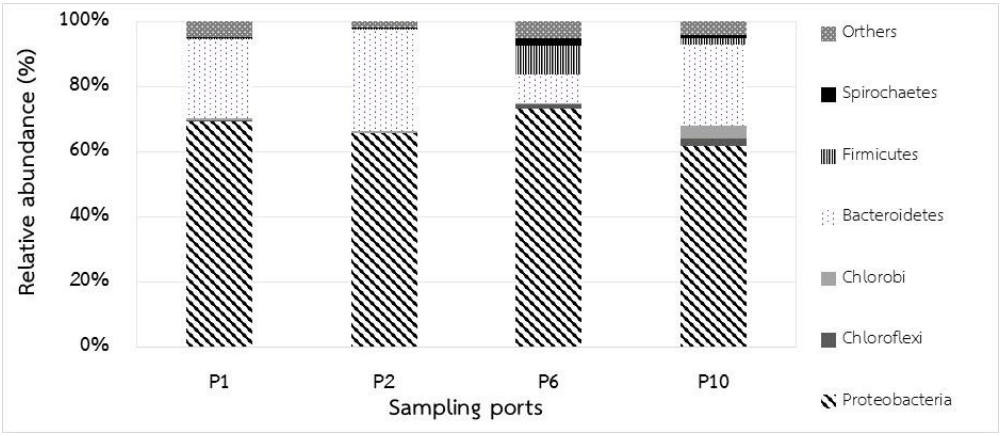

(b)

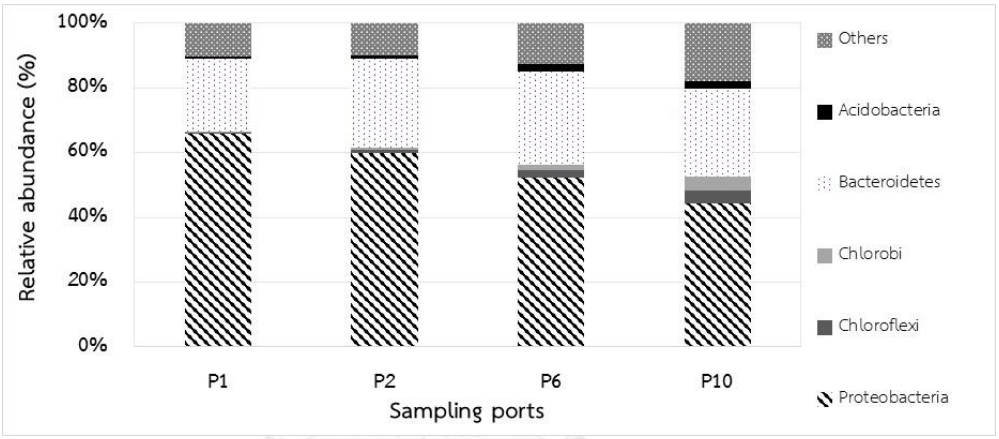

Figure 5.22 Microbial distribution in phylum level from different operational conditions (a) COD:NO_3^- - N ratio of 3:1 and (b) carbon step feeding.

From MiSeq Illumina analysis showed that most of the bacteria in the novel FBR belonged to the phylum *Proteobacteria* and *Bacteroidestes*. They ware dominant microorganisms when the novel FBR was operated at COD:NO_3^- - N ratio of 3:1 (Figure 5.22a) and during carbon step feeding (Figure 5.22b). *Proteobacteria* presented in every sample with higher than 60% relative abundance at COD:NO_3^- - N ratio of 3:1, while higher than 40% was found in the carbon step feeding reactor. The phylum *Bacteroidestes* showed the abundance of about 20%.

The phylum *Chloroflexi* and *Chlorobi* were also presented with 5% relative abundance at the top of the reactor.

Generally, *Proteobacteria* (59%), *Bacteroidestes* (16%), *Chlorobi* (3%), and *Chloroflexi* (4%) are dominant microorganisms in denitrification process. The abundance of microbial population depend on the influent characteristics, treatment configurations and operating conditions (DeSantis *et al.*, 2006a; Lu *et al.*, 2014) and (Letunic and Bork, 2011b).

In Figure 5.23, the microbial distributions were illustrated in class level. The microbial distribution in class level from the COD:NO_3^- - N ratio of 3:1 are presented in Figure 5.23a and the carbon step feeding samples are presented in Figure 5.23b.

(a)

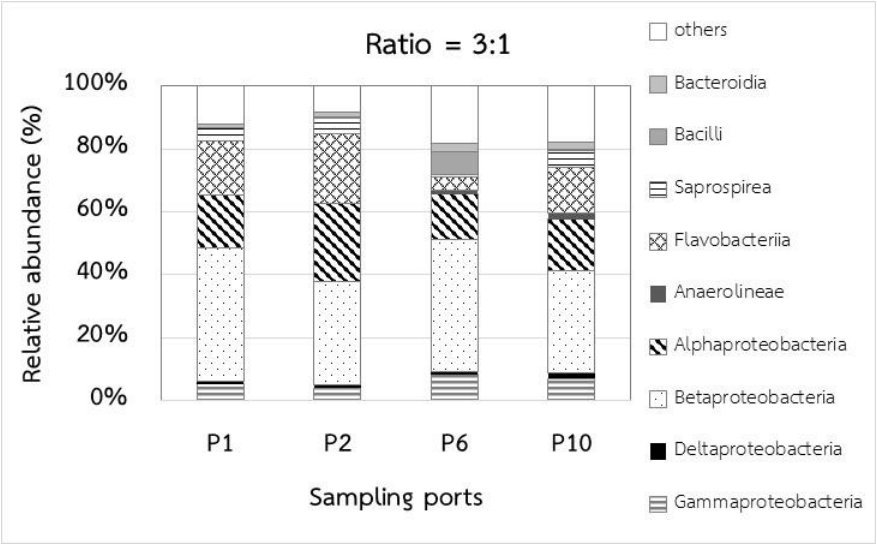

(b)

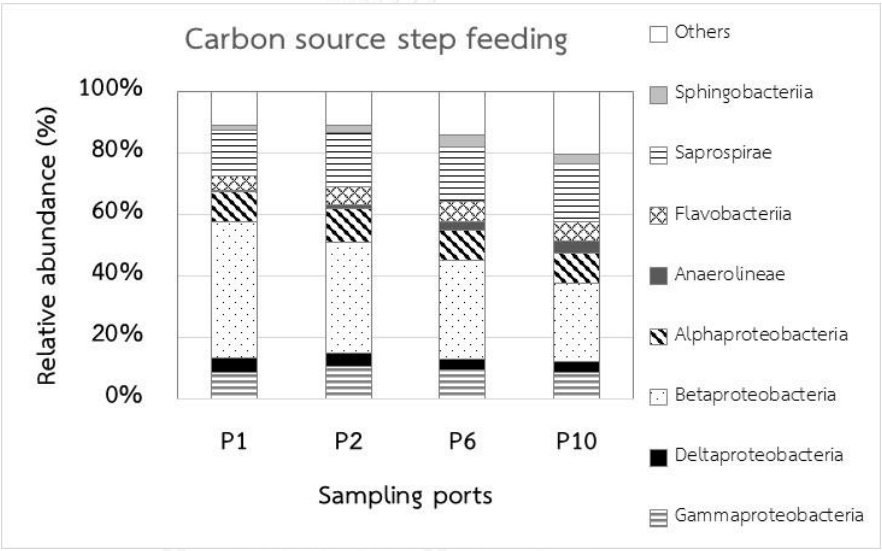

Figure 5.23 Microbial distribution in class level from different operational conditions (a) COD:NO_3^- - N ratio of 3:1 and (b) carbon step feeding.

For the reactor operating with COD:NO_3^- - N ratio of 3:1 and with carbon step feeding concept, *Betaproteobacteria* were the major microbe in both conditions, 23% to 45% of relative abundance were observed, as illustrated in Figure 5.23. At COD:NO_3^- - N ratio of 3:1, the abundance of *Alphaproteobacteria* were higher than that of the carbon step feeding concept, whereas *Delta-* and *Gammaproteobacteia* presented in similar abundance. In wastewater treatment, the phylum *Proteobacteria*, *Alpha-*, *Beta-*, *Gamma-* and *Sigmaproteobacteria* appear in higher amounts than the *Epsilonproteobacteria* (Zheng *et al.*, 2012).

For genus level, *Bradyrhizobium, Aquitalea, Flavobacterium, Treponema, Pseudoxanthomonas, Zoogloea, Aquimonas, Thermomonas, Thauera* and *Solitalea* were presented in this study. They belong to the class *Betaproteobacteria*. Some of them, for example, *Zoogloea* have been reported as complete denitrifiers.

Candidatus Solibacter, Anaerolinea, Bosea and *Ignavibacterium* were found as the genera in the class Alphaproteobacteria. Moreover, *Flavobacterium, Desulfovibrio* and *Stenotrophomonas* were dominate genera in the class *Gammaproteobacteria*.

The class *Flavobacteriia* were observed as dominant microbe at COD:NO_3^- - N ratio of 3:1. The highest value was found at the bottom part of the reactor. For the carbon step feeding, about 5% abundance was found and *Saprospirae* became the dominant group with 15 to 18% relative abundance. Moreover, *Anaerolineae*, *Sphingobacteriia*, *Bacilli* and *Bacteroidia* were observed with small abundances.

The class *Flavobacteriia* belong to the phylum *Bacteroidetes.* In this study, the class *Flavobacteriia* consisted of the genera *Rhodocyclus*, *Dechloromonas*, *Aeromonas* and *Dokdonella*. The class *Saprospirae* also belong to the phylum *Bacteroidetes.* Their population consisted of the genera *Diaphorobacter* and *Rhizobium*.

From the microbial analysis in both COD:NO_3^--N ratio of 3:1 operation and the carbon step feeding condition, the results showed similar dominant microbial groups for both conditions.

5.7 Conclusions

The performance of the novel configuration anaerobic FBR was studied at different COD: NO_3^--N ratios and with carbon step feeding concept under a very low HRT operation. The novel configuration anaerobic FBR achieved high performance for nitrate and COD removal efficiencies at COD:NO_3^--N ratio of 3:1. Overall results in this study demonstrated that the novel FBR without internal recirculation, using rubber granules as the biofilm carrier media, can achieve adequate performance for biological denitrification at a low HRT of 50 min. The result from the carbon step feeding study proved that the novel FBR can operate without additional treatment system.

The sequencing results showed that COD: NO_3^--N ratios affects the distribution of microbial community. Dominant microorganisms belonging to *Beta-* and *Gammaproteobacteria* played important roles in nitrate reduction. *Acidovorax* was the most abundant at low COD:NO_3^--N ratios while *Rhizobium* and *Zoogloea* were the dominant microbes at high COD: NO_3^- N ratios. The results revealed that different COD: NO_3^--N ratios affected the dominant microbial community. Thus, the study provides a better understanding of the reactor performance for nitrate reduction under low HRT.

Chapter 6
CONCLUSIONS AND RECOMMENDATIONS

6.1 Conclusions

This research consists of three experimental parts with different research approaches. In the first part, hydrodynamic behavior was studied to described the phenomenon and liquid flow pattern inside the reactor. The hydrodynamic behavior study via RTD experiment revealed that the liquid flow pattern in the FBR was closed to plug flow reactor (22 – 30 tanks of CSTR connected in series). This result provided adequate information of flow pattern and phenomenon of the FBR that can be used to modify the reactor for further wastewater treatment applications. In the second and the last parts, a novel configuration anaerobic FBR was employed for various wastewater treatment applications. Overall results of this study demonstrated that the novel FBR, which contained rubber granules as biofilm supporting media, achieved adequate performance for low strength and nitrate-rich wastewater treatment under low HRT of 50 min. Moreover, MiSeq Illumina sequencing results revealed more understanding the relationship between substrate removal phenomenon and dominant microorganism. And, the results showed that different COD to nitrate ratios and OLRs operation affected the dominant microbial community distribution.

The novel FBR has been proved as high performance in low strength anaerobic wastewater treatment and nitrate reduction by denitrification process. The novel FBR is an interesting alternative wastewater treatment for municipal and industrial wastewater treatment applications due to energy conservation for the reactor operation, small reactor size (small footprint) and high quality effluent.

6.2 Recommendations

From the experimental results, a novel configuration anaerobic FBR has been proved as an alternative system for various applications in wastewater treatment as follows,

1) Low-strength anaerobic wastewater treatment

At OLR 5.6 g COD/L-d, the effluent contained low COD concentration while the effluent could reach the standard quality control. The FBR has been recommended for domestic and industrial wastewater treatment. The recommendation for further studies are as follows,

1.1) Domestic wastewater treatment applications

- In case of high ammonia-nitrogen containing in wastewater, it may result in low quality effluent due to high nitrogen contains in the effluent.
- High suspended solid concentration in influent may disturb reactor operation, due to the accumulation of suspended solid in form of inert solid in fluidized bed.

1.2) Industrial wastewater treatment applications

- It is recommended to use in low-strength wastewater. The effluent quality is in accordance with the effluent controlling standard.
- In case of high-strength wastewater treatment, laboratory scale study is necessary before using in pilot plant and real system.

2) Nitrate reduction by denitrification process

Various external carbon sources should be investigated to specify the optimum carbon source that provides high performance with low cost in long term operation. The novel FBR is recommended for domestic and industrial wastewater treatment for nitrate reduction. The applications of The novel FBR for nitrate reduction are as follows,

2.1) Domestic wastewater treatment applications

- It is an alternative system for removing nitrate in the effluent after aerobic aeration process such as activated sludge (AS). The effluent released from the novel configuration anaerobic FBR contained low nitrate and low COD concentration.

2.2) Industrial wastewater treatment applications

- It is possible to operate without post treatment system for nitrate-containing wastewater from industries such as food industry and fertilizer industry.

In this research, glucose was used a sole substrate in all experimental studies, resulting in the high performance of wastewater treatment. Besides, the type of reactors, substrate also affect the performance of wastewater treatment. Therefore, in real wastewater treatment, the performance of a novel configuration anaerobic FBR should be investigated in laboratory scale.

REFERENCES

Abeling, U.and Seyfried, C.F. 1992. Anaerobic-Aerobic Treatment of High-Strength Ammonium Wastewater - Nitrogen Removal via Nitrite. *Water Science and Technology*, 26(5-6), 1007-1015.

Adav, S.S., Lee, D.J.and Lai, J.Y. 2009. Functional consortium from aerobic granules under high organic loading rates. *Bioresour Technol*, 100, 3465-3470.

Addison, S., Slade, A.and Dennis, M. 2011. Effect of substrate composition on the structure of microbial communities in wastewater using fluorescence in situ hybridisation. *Syst Appl Microbiol*, 34, 337-343.

Akunna, J.C., Bizeau, C.and Moletta, R. 1992. Denitrification in anaerobic digesters: Possibilities and influence of wastewater COD/N-NOx ratio. *Environ Technol*, 13, 825-836.

Akunna, J.C., Bizeau, C.and Moletta, R. 1993. Nitrate and nitrite reductions with anaerobic sludge using various carbon sources: glucose, glycerol, acetic acid, lactic acid and methanol. *Water Res*, 27, 1303-1312.

American Public Health Association, A.W.W.A., Water Environment Federation. 2001. Standard Methods for the Examination of Water and Wastewater 20th ed. *American Public Health Association*, Washington D.C.

Andalib, M., Elbeshbishy, E., Mustafa, N., Hafez, H., Nakhla, G.and Zhu, J. 2014. Performance of an anaerobic fluidized bed bioreactor (AnFBR) for digestion of primary municipal wastewater treatment biosolids and bioethanol thin stillage. *Renewable Energy*, 71, 276-285.

Angelidaki, I., Karakashev, D., Batstone, D.J., Plugge, C.M.and Stams, A.J.M. 2011. Biomethanation and its potential. in: *Methods in Enzymology*, Vol. 494, pp. 327-351.

APHA, AWWAand AEF. 2012. Standard Methods for the Examination of Water and Wastewater. 20th ed. Washington DC, USA.

Baumann, B., van der Meer, J.R., Snozzi, M.and Zehnder, A.J.B. 1997. Inhibition of denitrification activity but not of mRNA induction in Paracoccus denitrificans by nitrite at a suboptimal pH. *Antonie van Leeuwenhoek*, 72(3), 183-189.

Board, N.o.t.N.E. 1994. issued under the Enhancement and Conservation of National Environmental Quality Act B.E.2535 (1992), (Ed.) p.i.t.R.G. Gazette, Vol. 111.

Borja, R., Banks, C.J.and Wang, Z. 1995. Effect of organic loading rate on anaerobic treatment of laughterhouse wastewater in a fluidised-bed reactor. *Bioresour Technol*, 52, 157-162.

Burghate, S.P.and Ingole, N.W. 2013. Biodenitrification by fluidized bed biofilm reactor. *International Research Journal of Environment Sciences*, 2(12), 42-51.

Calderon, D., Buffiere, P., Moletta, R.and Elmaleh, S. 1996. Comparison of three granular support materials for anaerobic fluidized bed system. *Biotechnol Lett*, 18, 731-736.

Caporaso, J.G., Lauber, C.L., Walters, W.A., Berg-Lyons, D., Huntley, J., Fierer, N., Owens, S.M., Betley, J., Fraser, L., Bauer, M., Gormley, N., Gilbert, J.A., Smith, G.and Knight, R. 2012. Ultra-high-throughput microbial community analysis on the Illumina HiSeq and MiSeq platforms. *ISME J*, 6(8), 1621-1624.

Chen, H., He, L., Liu, A., Guo, Q., Zhang, Z.and Jin, R. 2015. Start-up of granule-based denitrifying reactors with multiple magnesium supplementation strategies. *J Environ Manage*, 155, 204-211.

Chen, Y., Zhou, W., Li, Y., Zhang, J., Zeng, G., Huang, A.and Huang, J. 2014. Nitrite reductase genes as functional markers to investigate diversity of denitrifying bacteria during agricultural waste composting. *Appl Microbiol Biotechnol* 98, 4233-4243.

Cloete, T.E.and Muyima, N.Y.O. 1997. Microbial community analysis: the key to the design of biological wastewater treatment systems. *IAWQ scientific and technical report*, 5, London.

Coates, J.D., Chakraborty, R., Lack, J.G., O'Connor, S.M., Cole, K.A., Bender, K.S.and Achenbach, L.A. 2001. Anaerobic benzene oxidation coupled to nitrate reduction in pure culture by two strains of Dechloromonas. *Nature*, 1039–1043.

Cydzik-Kwiatkowska, A., Zielinska, M.and Wojnowska-Baryla, I. 2012. Impact of operational parameters on bacterial community in a full-scale municipal wastewater treatment plant. *Pol J Microbiol*, 61(1), 41-9.

de Almeida, A., Nikel, P.I., Giordano, A.M.and Pettinari, M.J. 2007. Effects of granule-associated protein PhaP on glycerol-dependent growth and polymer

production in poly(3-hydroxybutyrate)-producing Escherichia coli. *Appl Environ Microbiol*, 73(24), 7912-6.

DeSantis, T.Z., Hugenholtz, P., Keller, K., Brodie, E.L., Larsen, N., Piceno, Y.M., Phan, R.and Andersen, G.L. 2006a. NAST: a multiple sequence alignment server for comparative analysis of 16S rRNA genes. *Nucleic Acids Research*, 34(Web Server issue), W394-W399.

DeSantis, T.Z., Hugenholtz, P., Keller, K., Brodie, E.L., Larsen, N., Piceno, Y.M., Phan, R.and Andersen, G.L. 2006b. NAST: A multiple sequence alignment server for comparative analysis of 16S rRNA genes. *Nucleic Acids Research*, 34(WEB. SERV. ISS.), W394-W399.

Dhaouadi, H., Poncin, S., Hornut, J.M., Wild, G., Oinas, P.and Korpijarvi, J. 1997. Mass transfer in an external-loop airlift reactor: experiments and modeling. *Chemical Engineering Science*, 52(21), 3909-3917.

Edgar, R.C. 2010. Search and clustering orders of magnitude faster than BLAST. *Bioinformatics*, 26(19), 2460-2461

Essadki, A.H., Gourich, B., Vial, C.and Delmas, H. 2011. Residence time distribution measurements in an external-loop airlift reactor: Study of the hydrodynamics of the liquid circulation induced by the hydrogen bubbles. *Chemical Engineering Science*, 66(14), 3125-3132.

Ferrari, A., Brusa, T., Rutili, A., Canzi, E.and Biavati, B. 1994. Isolation and characterization ofMethanobrevibacter oralis sp. nov. *Current Microbiology*, 29(1), 7-12.

Ford, M.and Tellam, J.H. 1994. Source, type and extent of inorganic contamination within the Birmingham urban aquifer system, United Kingdom. *J Hydrol* 156, 101-135.

Franco, A., Roca, E.and Lema, J.M. 2006. Granulation in high-load denitrifying upflow sludge bed (USB) pulsed reactors. *Water Res*, 40, 871-880.

Gavrilescu, M.and Tudose, R.Z. 1999. Residence time distribution of the liquid phase in a concentric-tube airlift reactor. *Chemical Engineering and Processing: Process Intensification*, 38(3), 225-238.

Gerardi, M.H. 2006. *Wastewater bacteria*, Wiley, Hoboken, New Jersey.

Ginige, M.P., Keller, J.and Blackall, L.L. 2005. Investigation of an acetate-fed denitrifying microbial community by stable isotope probing, full-cycle rRNA analysis, and fluorescents in situ hybridization-microautoradiography. *Appl Environ Microbiol*, 71(72), 8683-8691.

Grady, C.L., Daigger, G.T.and Lim, H.C. 1999. *Biological wastewater treatment*. Marcel Dekker, New York.

Grady, C.L., Daigger, G.T., Love, N.G.and Filipe, C.D. 2011. *Biological wastewater treatment*. CRC press.

Her, J.J.and Huang, J.S. 1995. Influence of carbon source C/N ratio on nitrate/nitrite denitrification and carbon breakthrough. *Bioresour Technol*, 54, 45-51.

Horkam, W. 2011. Nitrate removal by denitrification process in fluidized bed reactor using rubber granule as a media. Master thesis, Engineering. *Master thesis, Engineering*, Chulalongkorn University.

Hu, M., Wang, X., Wen, X.and Xia, Y. 2012. Microbial community structures in different wastewater treatment plants as revealed by 454-pyrosequencing analysis. *Bioresource Technology*, 117, 72-79.

Huang, Z., Ong, S.L.and Ng, H.Y. 2011. Submerged anaerobic membrane bioreactor for low-strength wastewater treatment: effect of HRT and SRT on treatment performance and membrane fouling. *Water Resource*, 45, 705-713.

Jin, X., Wang, F., Liu, G.and Yan, N. 2012a. A key cultivation technology for denitrifying granular sludge. *Process Biochemistry*, 47, 1122-1128.

Jin, X., Wang, F., Liu, G.and Yan, N. 2012b. A key cultivation technology for denitrifying granular sludge. *Process Biochem*, 47, 1122-1128.

Jones, D.S., Albrecht, H.L., Dawson, K.S., Schaperdoth, I., Freeman, K.H., Pi, Y., Pearson, A.and MacAlady, J.L. 2012. Community genomic analysis of an extremely acidophilic sulfur-oxidizing biofilm. *ISME Journal*, 6(1), 158-170.

Khan, S.T., Horiba, Y., Yamamoto, M.and Hiraishi, A. 2002. Members of the family Comamonadaceae as primary poly (3-Hydroxybutyrate-co-Hydroxyvalerate)-degrading denitrifiers in activated sludge as revealed by a polyphasic approach. *Appl Environ Microbiol*, 68(7), 3206-3214.

Kida, K., Morimura, S., Sonoda, Y., Obe, M.and Kondo, T. 1990a. Support media for microbial adhesion in an anaerobic fluidized-bed reactor. *J Ferment Bioeng*, 69(6), 354-359.

Kida, K., Morimura, S., Sonoda, Y., Obe, M.and Kondo, T. 1990b. Support media for microbial adhesion in an anaerobic fluidized-bed reactor. *J Biosci Bioeng*, 69(6), 354-359.

Knowles, R. 1982. Denitrification. *Microbiol Rev* 46, 43-70.

Kostov, G., Angelov, M., Mihailov, I.and Stoeva, D. 2011. Development of combined models to describe the residence time distribution in fluidized-bed bioreactor with light beads. *Procedia Food Science*, 1, 770-775.

Krishna, G.V.T.G., Kumar, P.and Kumar, P. 2009. Treatment of low-strength soluble wastewater using an anaerobic baffled reactor (ABR). *Journal of Environmental Management*, 90, 166-176.

Kuroda, K., Chosei, T., Nakahara, N., Hatamoto, M., Wakabayashi, T., Kawai, T., Araki, N., Syutsubo, K.and Yamagushi, T. 2015. High organic loading treatment for industrial molasses wastewater and microbial community shifts corresponding to system development. *Bioresour Technol*, 196, 225-234.

Labbe, N., Juteau, P., Parent, S.and Villemur, R. 2003. Bacterial diversity in a marine methanol-fed denitrification reactor at the Montreal Biodome, Canada. *Microbial Ecol*, 46(1), 12-21.

Leadbetter, J.R.and Breznak, J.A. 1996. Physiological ecology of Methanobrevibacter cuticularis sp. nov. and Methanobrevibacter curvatus sp. nov., isolated from the hindgut of the termite Reticulitermes flavipes. . *Appl Environ Microbiol*, 62(10), 3620-3631.

Lee, H.W., Park, Y.K., Choi, E.and Lee, J.W. 2008. Bacterial community and biological nitrate removal: comparisons of autotrophic and heterotrophic reactor for denitrification with raw sewage. *J Microbiol Biotechnol*, 18(11), 1826-1835.

Lee, N.M.and Welander, T. 1996. The effect of different carbon source on respiratory denitrification in biological wastewater treatment. *J Biosci Bioeng*, 82(3), 277-285.

Letunic, I.and Bork, P. 2011a. Interactive Tree of Life v2: Online annotation and display of phylogenetic trees made easy. *Nucleic Acids Research*, 39(SUPPL. 2), W475-W478.

Letunic, I.and Bork, P. 2011b. Interactive Tree Of Life v2: online annotation and display of phylogenetic trees made easy. *Nucleic Acids Res*, 39(Web Server issue), W475-8.

Levenspiel, O. 1999. *Chemical Reaction Engineering*. 3 *ed*. John Wiley & Son, New York.

Leyva-Diaz, J.C., Munio, M.M., Gonzalez- Lopez, J.and Poyatos, J.M. 2016. Anaerobic/anoxic/oxic configuration in hybrid moving bed biofilmreactor-membrane bioreactor for nutrient removal from municipal wastewater. *Ecological Engineering*, 91, 449-458.

Li, A.J., Yang, S.F., Li, X.Y.and Gu, J.D. 2008. Microbial population dynamics during aerobic sludge granulation at different organic loading rates. *Water Res*, 42, 3553-356.

Liu, Y.and Whitman, W.B. 2008. Metabolic, phylogenetic, and ecological diversity of the methanogenic archaea. in: *Annals of the New York Academy of Sciences*, Vol. 1125, pp. 171-189.

Lu, H., Chandran, K.and Stensel, D. 2014. Microbial ecology of denitrification in biological wastewater treatment. *Water Res*, 64, 237-254.

Lucena, R.M., Gavazza, S., Florencio, L., Kato, M.T.and Morias, M.A. 2011. Study of the microbial diversity in a full-scale UASB reactor treating domestic wastewater. *World J Microbiol Biotechnol*, 27, 2893-2902.

Ma, J., Wang, Z., Yang, Y., Mei, X.and Wu, Z. 2013. Correlating microbial community structure and composition with aeration intensity in submerged membrane bioreactors by 454 high-throughput pyrosequencing. *Water Res*, 47(2), 859-69.

Maintinguer, S.I., Sakamoto, I.K., Adorno, M.A.T.and Varesche, M.B.A. 2013. Evaluation of the microbial diversity of denitrifying bacteria in batch reactor. *Braz J Chem Eng*, 30(3), 457-465.

Manariotis, I.D.and Grigoropoulos, G. 2002. Low-strength water treatment using an anaerobic baffled reactor. *Water Environ Res*, 74(2), 170-176.

McCabe, W., Smith, j.and Harriott, P. 1993a. *UNIT OPERATIONS OF CHEMICAL ENGINEERING*. *fifth ed*. McGraw-Hill.

McCabe, W.L., Smith, J.C.and Harriott, P. 1993b. Unit Operation of Chemical Engineering. 5th edition. *New York: McGraw-Hill*.

McIlroy, S.J., Saunders, A.M., Albertsen, M., Nierychlo, M., McIlroy, B., Hansen, A.A., Karst, S.M., Nielsen, J.L.and Nielsen, P.H. 2015. MiDAS: The field guide to the microbes of activated sludge. *Database*, 2015.

Méndez-Romero, D.C., López-López, A., Vallejo-Rodríguez, R.and León-Becerril, E. 2011. Hydrodynamic and kinetic assessment of an anaerobic fixed-bed reactor for slaughterhouse wastewater treatment. *Chemical Engineering and Processing: Process Intensification*, 50(3), 273-280.

Metcalf, Eddy, Tchobanoglous, G., Burton, F.L.and Stensel, H.D. 2003. Wastewater Engineering: Treatment and Reuse. 4 ed, McGraw-Hill. Boston.

Metcalf&EddyInc. 2003. Wastewater Engineering: Treatment and Reuse, 4th ed. **McGraw-Hill. New York**.

Nguyen, H.T.T., Le, V.Q., Hansen, A.A., Nielsen, J.L.and Nielsen, P.H. 2011. High diversity and abundance of putative polyphosphate-accumulating Tetrasphaera-related bacteria in activated sludge systems. *FEMS Microbiology Ecology*, 76(2), 256-267.

Nielsen, P.H., Mielczarek, A.T., Kragelund, C., Nielsen, J.L., Saunders, A.M., Kong, Y., Hansen, A.A.and Vollertsen, J. 2010. A conceptual ecosystem model of microbial communities in enhanced biological phosphorus removal plants. *Water Research*, 44(17), 5070-5088.

Osaka, T., Shirotani, K., Yoshie, S.and Tsuneda, S. 2008. Effect of carbon source on denitrification efficiency and microbial community structure in a saline wastewater treatment process. *Water Res*, 42, 3709-3718.

Osaka, T., Yoshie, S., Tsuneda, S., Hirata, A., Iwami, N.and Inamori, Y. 2006. Identification of acetate- or methanol-assimilating bacteria under nitrate-reducing condition by stable-isotope probing. *Microbial Ecol*, 52(2), 253-266.

Park, J., Ellis, T.G.and Lally, M. 2006. Evaluation of tire derived rubber particles for biofiltration media. *WEFTEC*, 6, 3217-3230.

Reysenbach, A.L., Ehringer, M.and Hershberger, K. 2000. Microbial diversity at 83°C in Calcite Springs, Yellowstone National Park: Another environment where the Aquificales and 'Korarchaeota' coexist. *Extremophiles*, 4(1), 61-67.

Rittmann, B.E.and McCarty, P.L. 2001. Environmental Biotechnology: Principles and Applications. *McGraw-Hill, Singapore*.

Rungkitwatananukul, P. 2010. Synthetic wastewater treatment by anaerobic fluidized bed system using rubber granule as a media: effect of organic loading rate. Master thesis. *Engineering. Chulalongkorn University.*

Sakai, S., Imachi, H., Hanada, S., Ohashi, A., Harada, H.and Kamagata, Y. 2008. Methanocella paludicola gen. nov., sp. nov., a methane-producing archaeon, the first isolate of the lineage 'Rice Cluster I', and proposal of the new archaeal order Methanocellales ord. nov. *International Journal of Systematic and Evolutionary Microbiology*, 58(4), 929-936.

Saravanane, R.and Muthy, D.V.S. 2000. Application of anaerobic fluidized bed reactors in wastewater treatment: a review. *Environmental Management and Health*, 11(2), 97-117.

Saravanathamizhan, R., Paranthaman, R., Balasubramanian, N.and Basha, C.A. 2008. Residence time distribution in continuous stirred tank electrochemical reactor. *Chemical Engineering Journal*, 142(2), 209-216.

Sauder, L.A., Engel, K., Stearns, J.C., Masella, A.P., Pawliszyn, R.and Neufeld, J.D. 2011. Aquarium nitrification revisited: Thaumarchaeota are the dominant ammonia oxidizers in freshwater aquarium biofilters. *PLoS ONE*, 6(8).

Savant, D.V., Shouche, Y., Prakash, S.and Ranade, D. 2002. Methanobrevibacter acididurans sp. nov., a novel methanogen from a sour anaerobic digester. *International Journal of Systematic and Evolutionary Microbiology*, 52, 1081-1087.

Sendhil, J., Muniswaran, P.K.A.and Ahmed Basha, C. 2012. Residence time distribution studies in flow through tubular electrochemical reactor. *International Journal of Engineering Research and Development*, 1(7), 52-62.

Shen, Z., Zhou, Y., Hu, J.and Wang, J. 2013. Denitrification performance and microbial diversity in a packed-bed bioreactor using biodegradable polymer as carbon source and biofilm support. *J Hazard Mater*, 250-251, 431-438.

Singh, K.S., Harada, H.and Viraraghavan, T. 1996. Low-strength wastewater treatment by a UASB reactor. *Bioresource Technology*, 55(3), 187-194.

Sirinukulwattana, T., Pungrasmi, W.and Puprasert, C. 2013. Treatment of low strength wastewater by rubber granule media AFB reactor without internal recirculation. *Journal of Water Sustainability*, 3(2), 97-106.

Šmilauer, P.and Lepš, J. 2014. *Multivariate analysis of ecological data using CANOCO* 5, Cambridge university press.

Sooria, P.M., Jyothibabu, R., Anjusha, A., Vineetha, G., Vinita, J., Lallu, K.R.and Jagadeesan, L. 2015. Plankton food web and its seasonal dynamics in a large monsoonal estuary (Cochin backwaters, India)-significance of mesohaline region. *Environmental monitoring and assessment*, 187(7), 427.

Speece, R.E. 1996. Anaerobic Biotechnology for Industrial Wastewaters. *Archae Press Nashville, Tennessee*.

Takayuki, K., M. 1994. *The anaerobic treatment of low strength soluble wastewater*. Wageningen Agricultural University, Wageningen, The Natherlands.

Thomson, T.R., Kong, Y.and Nielson, P.H. 2007. Ecophysiology of abundant denitrifying bacteria in activated sludge. *FEMS Microbiol Ecol*, 60, 370-382.

Tiedje, J.M. 1988. Ecology of denitrification and dissimilatory nitrate reduction to ammonium. *Biology of anaerobic microorganisms, Zehnder A.J.B. (ed)*, **John Wiley, New York**, 179-244.

van Lier, J.B., Mahmoud, N.and Zeeman, G. 2008. *Biological Wastewater Treatment: Principles Modeling and Design*. IWA Publishing, London, UK.

van Loosdrecht, M.C., Lyklema, J., Norde, W.and Zehnder, A.J. 1990. Influence of interfaces on microbial activity. *Microbiol Rev*, 54(1), 75-87.

Verstraete, W.and Vandevivere, P. 1999. New and Broader Applications of Anaerobic Digestion. *Crit Rev Environ Sei Technol*, 28(2), 151.

Wan, C.Y., De Wever, H., Diels, L., Thoeye, C., Liang, J.B.and Huang, L.N. 2011. Biodiversity and population dynamics of microorganisms in a full-scale

membrane bioreactor for municipal wastewater treatment. *Water Research*, 45(3), 1129-1138.

Wang, X., Hu, M., Xia, Y., Wen, X.and Ding, K. 2012. Pyrosequencing analysis of bacterial diversity in 1 4 wastewater treatment systems in china. *Applied and Environmental Microbiology*, 78(19), 7042-7047.

Weidler, G.W., Gerbl, F.W.and Stan-Lotter, H. 2008. Crenarchaeota and their role in the nitrogen cycle in a subsurface radioactive thermal spring in the Austrian Central Alps. *Appl Environ Microbiol*, 74(19), 5934-42.

Wen, J., Pan, L., Du, L.and Mao, G. 2003. The denitrification treatment of low C/N ratio nitrate-nitrogen wastewater in a gas-liquid-solid fluidized bed bioreactor. *Chemical Engineering Journal*, 94, 155-159.

Xie, L., Chen, J., Wang, R.and Zhou, Q. 2012. Effect of carbon sourse and COD/NO_3^- - N ratio on anaerobic simultaneous denitrification and methanogenesis for high-strength wastewater treatment. *Journal of Bioscience and Bioengineering*, 113(6), 759-764.

Zhang, T., Shao, M.F.and Ye, L. 2012. 454 Pyrosequencing reveals bacterial diversity of activated sludge from 14 sewage treatment plants. *ISME Journal*, 6(6), 1137-1147.

Zheng, M.X., Wang, K.J., Zuo, J.E., Yan, Z., Fang, H.and Yu, J.W. 2012. Flow pattern analysis of a full-scale expanded granular sludge bed-type reactor under different organic loading rates. *Bioresource Technology*, 107, 33-40.

APPENDIX

Appendix A

Microbial Community Analysis

A.1. DNA Extraction

FastDNA SPIN Kit for soil Protocol

1. Add up to 500 mg of sludge sample to a Lysing Matrix E tube.
2. Add 978 µl Sodium Phosphate Buffer to sample in Lysing Matrix E tube.
3. Add 122 µl MT Buffer. Shack vigorously to mix, then vortex 10-15 seconds.
4. Homogenize in the FastPrep® Instrument for 40 seconds at a speed setting of 6.0.
5. Centrifuge at 14,000 xg for 5-10 minutes to pellet debris.

   NOTE: Extending centrifugation to 15 minutes can enhance elimination of excessive debris from large samples, or from cells with complex cell walls.
6. Transfer supernatant to a clean 2.0 ml microcentrifuge tube. Add 250 µl PPS (Protein Precipitation Solution) and mix by shaking the tube by hand 10 times.
7. Centrifuge at 14,000 x g for 5 minutes to pellet precipitate. Transfer supernatant (600-800 µl) to a clean 2.0 µl (or 15 ml) tube. Add an equal amount of Binding Matrix to the microcentrifuge tube. Shake gently by hand mix, then place on a rocker or invert by hand for 3-5 minutes to allow binding of DNA to matrix.

   NOTE: While a 2.0 ml microcentrifuge tube may be used at this step, better mixing and DNA binding will occur in a larger tube.
8. Mix the solution by pipetting up and down several times. Transfer 800 µl of the solution to a SPIN™ Filter tube. Centrifuge at 14,000 x g for 5 minute. Empty the catch tube. Repeat mixing, transferring and centrifuging for the remaining solution to the SPIN™ Filter tube. Discard the flow-through.
9. Add 500 µl prepared SEWS-M to the SPIN™ Filter tube. Shake gently by hand or flick the tube to mix.

10. Centrifuge at 14,000 x g for 5 minute. Empty the catch tube and centrifuge again for 5 minutes to remove the residual ethanol.
11. Transfer the SPIN™ Filter to a clean 2.0 ml catch tube. Air dry the SPIN™ Filter for 5 minutes at room temperature.
12. Add 50-100 µl DES to the SPIN™ Filter tube and gently re-suspend the pellet by finger flicking.

    NOTE: Yields may be increased by incubation for 5 minutes at 55°C in a heat block or water bath.
13. Centrifuge at 14,000 x g for 2 minute to eluted DNA into the clean catch tube. Discard the SPIN filter. DNA is now ready for PCR and other downstream applications.

    Store at -20°C for extended periods or 4°C until use.

A.2. Polymerase Chain Reaction (PCR)

1. PCR solution for amplification

Primer 515F (10 µM)	1 µl
Primer 806R (10 µM)	1 µl
DNA template (10 ng/µL)	2 µl
Ex. Taq*	10 µl
MQ water	6 µl
Total volume	20 µl

* Ex.Taq included dNTP, Taq Polymerase, $MgCl_2$ and buffer.

2. PCR amplification condition

- Stage 1 Incubation

  94.0 °C for 3:00 min

- Stage 2 Annealing (25 cycles)

  94.0 °C for 0:45 min

  50.0 °C for 1:00 min

72.0 °C for 1:30 min

- Stage 3 Extension

72.0 °C for 10 min

- Stage 4 Keeping

4.0 °C until use

3. Electrophoresis for PCR product checking

- 2% agarose gel is prepared from 1g of agarose in SYBR 1X TAE 50 ml.
- Load 5 µl of PCR product on the well of agarose gel with 1 µl of 6X dye loading buffer.
- Run the gel on electrophoresis at 135V, 20 minutes.
- Check DNA bands with UV light on Gel Doc machine.

A.3. PCR Purification

1. Add 5 volumes of Buffer PB to 1 volume of the PCR sample and mix. It is not necessary to remove mineral oil or kerosene. For example, add 500 µl of Buffer PB to 100 µl PCR sample (not including oil).
2. Place a QIAquick spin column in a provided 2 ml collection tube.
3. To bind DNA, apply the sample to the QIAquick column and centrifuge for 30–60 s.
4. Discard flow-through. Place the QIAquick column back into the same tube. Collection tubes are re-used to reduce plastic waste.
5. To wash, add 0.75 ml Buffer PE to the QIAquick column and centrifuge for 30–60 s.
6. Discard flow-through and place the QIAquick column back in the same tube. Centrifuge the column for an additional 1 min at maximum speed. IMPORTANT: Residual ethanol from Buffer PE will not be completely removed unless the flow-through is discarded before this additional centrifugation.

7. Place QIAquick column in a clean 1.5 ml microcentrifuge tube.
8. To elute DNA, add 16 µl Buffer TE to the center of the QIAquick membrane, let the column stand for 1 min and then centrifuge the column for 1 min.

IMPORTANT: Ensure that the elution buffer is dispensed directly onto the QIAquick membrane for complete elution of bound DNA. The average eluate volume is 48 µl from 50 µl elution buffer volume, and 28 µl from 30 µl elution buffer. Elution efficiency is dependent on pH. The maximum elution efficiency is achieved between pH 7.0 and 8.5. When using water, make sure that the pH value is within this range, and store DNA at –20°C as DNA may degrade in the absence of a buffering agent. The purified DNA can also be eluted in TE (10 mM Tris·Cl, 1 mM EDTA, pH 8.0), but the EDTA may inhibit subsequent enzymatic reactions.

Appendix B

Low strength anaerobic wastewater treatment: Process parameter analysis

COD

OLR 18.6 g COD/L-d				
Date	Days	Influent	Effluent	Efficiency
8/3/2015	1	521	388	26
8/7/2015	5	532	384	28
8/11/2015	9	436	157	64
8/12/2015	10	538	346	36
8/14/2015	12	474	336	29
8/15/2015	13	538	307	43
8/17/2015	15	508	291	43
8/18/2015	16	463	345	25
8/19/2015	17	472	345	27
8/25/2015	23	509	254	50
8/27/2015	25	522	376	28
8/28/2015	26	403	198	51
8/31/2015	29	461	211	54
9/1/2015	30	423	154	64
9/5/2015	34	523	215	59
9/11/2015	40	510	275	46
9/15/2015	44	480	202	58
9/19/2015	48	588	212	64
9/20/2015	49	463	174	62
9/25/2015	54	510	255	50
9/30/2015	59	449	150	67
10/3/2015	62	412	182	56
10/4/2015	63	460	153	67
10/7/2015	66	448	190	58
10/8/2015	67	520	200	62
10/11/2015	70	530	120	77
10/19/2015	78	500	190	62
10/23/2015	82	621	168	73
10/24/2015	83	605	192	68
10/27/2015	86	554	121	78
10/29/2015	88	452	115	75

OLR 18.6 g COD/L-d				
Date	Days	Influent	Effluent	Efficiency
10/31/2015	90	538	144	73
11/2/2015	92	424	101	76
11/4/2015	94	645	111	83

OLR 9.4 g COD/L-d				
Date	Days	Influent	Effluent	Efficiency
11/5/2015	95	224	100	55
11/6/2015	96	290	193	33
11/10/2015	100	229	153	33
11/13/2015	103	207	99	52
11/14/2015	104	275	38	86
11/17/2015	107	255	103	60
11/18/2015	108	260	130	50
11/21/2015	111	250	100	60
11/22/2015	112	250	100	60
11/24/2015	114	280	120	57
11/26/2015	116	240	140	42
11/29/2015	119	250	70	72
12/3/2015	123	267	105	61
12/4/2015	124	313	71	77
12/10/2015	130	275	46	83
12/14/2015	134	249	74	70
12/16/2015	136	283	61	78
12/19/2015	139	248	91.7	63
12/22/2015	142	228	52.7	77
12/24/2015	144	279	72.2	74
12/28/2015	148	220.4	92	58
12/29/2015	149	220	64	71
1/1/2016	152	217	87.8	60
1/3/2016	154	273	70.2	74
1/5/2016	156	283	80	72

OLR 5.6 g COD/L-d				
Date	Days	Influent	Effluent	Efficiency
1/9/2016	160	150	33	78

OLR 5.6 g COD/L-d				
Date	Days	Influent	Effluent	Efficiency
1/11/2016	162	170	27.1	84
1/12/2016	163	129	27.3	79
1/13/2016	164	188	7.8	96
1/14/2016	165	137	27.3	80
1/16/2016	167	131	17.6	87
1/19/2016	170	138	12	91
1/22/2016	173	119	12	90
1/25/2016	176	138	35	
1/28/2016	179	178	19.4	89
2/4/2016	186	160	27.3	83
2/10/2016	192	160	29.3	82
2/16/2016	198	150	13	91

Profiling of COD concentration

OLR 18.6 g COD/L-d					
Reactor height (cm)	Sampling port	10/6/2015	10/10/2015	Average	SD
238	Eff	162	240	201	55.2
220	P10	162	295	229	94.0
198	P9	219	242	231	16.3
176	P8	143	316	230	122.3
154	P7	238	316	277	55.2
132	P6	190	358	274	118.8
110	P5	257	347	302	63.6
88	P4	276	379	328	72.8
66	P3	257	337	297	56.6
44	P2	362	379	371	12.0
22	P1	295	337	316	29.7
0	Inf	448	550	499	72.1

OLR 9.4 g COD/L-d					
Reactor height (cm)	Sampling port	10/6/2015	10/10/2015	Average	SD
238	Eff 250	100	130	115	21.2
220	P10	135	141	138	4.2
198	P9	139	176	158	26.2
176	P8	143	161	152	12.7
154	P7	139	172	156	23.3
132	P6	139	187	163	33.9
110	P5	131	168	150	26.2
88	P4	135	176	156	29.0
66	P3	162	161	162	0.7
44	P2	154	176	165	15.6
22	P1	166	237	202	50.2
0	Inf 250	224	260	242	25.5

OLR 9.4 g COD/L-d					
Reactor height (cm)	Sampling port	10/6/2015	10/10/2015	Average	SD
238	Eff 150	20	30	25	7.1
220	P10	20	30	25	7.1
198	P9	25	30	28	3.5
176	P8	39	37	38	1.4
154	P7	50	39	45	7.8
132	P6	56	47	52	6.4
110	P5	62	51	57	7.8
88	P4	77	78	78	0.7
66	P3	81	68	75	9.2

OLR 9.4 g COD/L-d					
Reactor height (cm)	Sampling port	10/6/2015	10/10/2015	Average	SD
44	P2	80	84	82	2.8
22	P1	135	98	117	26.2
0	Inf 150	155	160	158	3.5

VFA and alkalinity

OLR 18.6 g COD/L-d							
Date	Days	VFA (mg/L)		Alkalinity (mg/L)		VFA/ALK	
		Inf.	Eff.	Inf.	Eff.	Inf.	Eff.
8/4/2015	2	10	100	550	535	0.02	0.19
8/5/2015	3	65	135	520	550	0.13	0.25
8/7/2015	5	100	160	405	460	0.25	0.35
8/11/2015	9	80	95	425	425	0.19	0.22
8/12/2015	10	70	140	530	505	0.13	0.28
8/13/2015	11	30	65	495	495	0.06	0.13
8/14/2015	12	105	115	360	510	0.29	0.23
8/15/2015	13	110	170	625	761	0.18	0.22
8/17/2015	15	35	155	580	505	0.06	0.31
8/19/2015	17	140	175	562.5	525	0.25	0.33
8/25/2015	23	55	120	570	515	0.10	0.23
8/27/2015	25	60	110	565	750	0.11	0.15
8/30/2015	28	105	200	575	610	0.18	0.33
8/31/2015	29	70	125	565	575	0.12	0.22
9/2/2015	31	170	200	590	540	0.29	0.37
9/8/2015	37	130	210	495	580	0.26	0.36
9/16/2015	45	100	190	630	570	0.16	0.33
9/19/2015	48	75	225	610	605	0.12	0.37
9/20/2015	49	130	300	500	725	0.26	0.41

OLR 18.6 g COD/L-d							
Date	Days	VFA (mg/L)		Alkalinity (mg/L)		VFA/ALK	
		Inf.	Eff.	Inf.	Eff.	Inf.	Eff.
9/30/2015	59	110	160	675	650	0.16	0.25
10/1/2015	60	55	130	490	550	0.11	0.24
10/2/2015	61	160	168	738	813	0.22	0.21
10/6/2015	65	40	120	650	650	0.06	0.18
10/8/2015	67	170	150	845	845	0.20	0.18
10/10/2015	69	50	80	650	420	0.08	0.19
10/13/2015	72	120	100	1100	1090	0.11	0.09
10/16/2015	75	180	230	840	1090	0.21	0.21
10/19/2015	78	70	60	1090	1200	0.06	0.05
10/26/2015	85	30	80	640	600	0.05	0.13
10/28/2015	87	60	35	535	370	0.11	0.09
10/31/2015	90	80	100	800	780	0.10	0.13
11/3/2015	93	270	220	1170	1110	0.23	0.20

OLR 9.4 g COD/L-d							
Date	Days	VFA (mg/L)		Alkalinity (mg/L)		VFA/ALK	
		Inf.	Eff.	Inf.	Eff.	Inf.	Eff.
11/5/2015	95	100	110	405	455	0.25	0.24
11/6/2015	96	85	125	475	532.5	0.18	0.23
11/10/2015	100	150	160	500	550	0.30	0.29
11/13/2015	103	100	110	405	455	0.25	0.24
11/14/2015	104	85	125	475	1065	0.18	0.12
11/17/2015	107	100	170	650	690	0.15	0.25
11/18/2015	108	175	175	765	880	0.23	0.20
11/22/2015	112	50	90	600	650	0.08	0.14

11/24/2015	114	100	150	550	575	0.18	0.26
11/26/2015	116	100	170	650	690	0.15	0.25
11/27/2015	117	175	175	1530	1760	0.11	0.10
11/29/2015	119	40	80	600	760	0.07	0.11
12/1/2015	121	50	90	600	650	0.08	0.14
12/3/2015	123	40	100	1350	1410	0.03	0.07
12/5/2015	125	80	70	500	530	0.16	0.13
12/6/2015	126	50	80	570	650	0.09	0.12
12/8/2015	128	100	90	780	820	0.13	0.11
12/11/2015	131	120	200	850	1000	0.14	0.20
12/14/2015	134	80	70	1000	1060	0.08	0.07
12/15/2015	135	10	50	720	720	0.01	0.07
12/18/2015	138	50	100	680	800	0.07	0.13
12/21/2015	141	15	85	630	750	0.02	0.11
12/23/2015	143	130	50	720	640	0.18	0.08
12/26/2015	146	30	50	300	350	0.10	0.14
12/28/2015	148	100	110	500	750	0.20	0.15
1/3/2016	154	60	40	350	350	0.17	0.11
1/6/2016	157	50	100	680	800	0.07	0.13

OLR 5.6 g COD/L-d							
Date	Days	VFA (mg/L)		Alkalinity (mg/L)		VFA/ALK	
		Inf.	Eff.	Inf.	Eff.	Inf.	Eff.
1/12/2016	163	80	60	400	450	0.20	0.13
1/13/2016	164	35	37.5	285	200	0.12	0.19
1/17/2016	168	70	75	570	400	0.12	0.19
1/18/2016	169	55	70	475	490	0.12	0.14
1/21/2016	172	50	75	490	525	0.10	0.14
1/22/2016	173	100	75	490	410	0.20	0.18
1/26/2016	177	50	40	500	550	0.10	0.07

OLR 5.6 g COD/L-d							
Date	Days	VFA (mg/L)		Alkalinity (mg/L)		VFA/ALK	
		Inf.	Eff.	Inf.	Eff.	Inf.	Eff.
1/30/2016	181	35	30	450	625	0.08	0.05
2/2/2016	184	45	25	455	550	0.10	0.05
2/5/2016	187	50	20	525	600	0.10	0.03
2/10/2016	192	30	25	460	480	0.07	0.05
2/18/2016	200	35	30	425	500	0.08	0.06

pH

OLR 18.6 g COD/L-d							
Date	Days	Influent	Effluent	Date	Days	Influent	Effluent
8/3/2015	1	8.35	7.26	9/2/2015	31	7.6	6.84
8/4/2015	2	8.29	6.95	9/8/2015	37	6.72	6.7
8/5/2015	3	8.11	7.4	9/10/2015	39	6.92	7.03
8/6/2015	4	6.27	6.92	9/13/2015	42	6.54	7.65
8/11/2015	9	6.7	7.16	9/16/2015	45	6.99	7.47
8/12/2015	10	8.07	6.65	9/19/2015	48	8.05	7.34
8/14/2015	12	6.23	6.96	9/20/2015	49	6.26	7.47
8/15/2015	13	8.11	7.61	9/24/2015	53	8.29	7.59
8/17/2015	15	8.12	6.83	9/30/2015	59	7.81	7.13
8/18/2015	16	7.19	7.42	10/1/2015	60	8.08	7.64
8/19/2015	17	7.04	7.52	10/2/2015	61	7.31	8.09
8/25/2015	23	8.03	7.55	10/3/2015	62	7.96	6.79
8/26/2015	24	6.82	6.99	10/4/2015	63	7.92	7.83
8/27/2015	25	8.08	7.34	10/5/2015	64	6.25	6.77
8/28/2015	26	7.22	6.99	10/6/2015	65	7.91	7.18
8/31/2015	29	8.09	7.2	10/7/2015	66	8.1	7.75
9/1/2015	30	7.75	7.02	10/8/2015	67	7.16	8.02

OLR 9.4 g COD/L-d							
Date	Days	Influent	Effluent	Date	Days	Influent	Effluent
11/5/2015	95	7.56	6.98	12/6/2015	126	7.74	7.09
11/6/2015	96	6.74	7.56	12/12/2015	132	7.95	7.33

OLR 9.4 g COD/L-d							
Date	Days	Influent	Effluent	Date	Days	Influent	Effluent
11/10/2015	100	8.23	7.66	12/13/2015	133	8.11	7.68
11/16/2015	106	7.9	7.21	12/14/2015	134	6.92	7.49
11/17/2015	107	8.07	7.49	12/16/2015	136	6.69	7.63
11/18/2015	108	7.02	7.66	12/17/2015	137	7.11	6.83
11/19/2015	109	7.84	7.47	12/18/2015	138	7.04	6.87
11/20/2015	110	8.13	7.53	12/20/2015	140	7.54	7.37
11/21/2015	111	6.7	7.17	12/21/2015	141	7.68	7.22
11/22/2015	112	7.99	7.5	12/29/2015	149	6.75	7.64
11/23/2015	113	8.12	7.33	12/30/2015	150	6.77	7.64
11/24/2015	114	7.21	7.53	1/2/2016	153	7.78	7.68
11/27/2015	117	8.1	7.29	1/3/2016	154	6.63	7.58
11/28/2015	118	8.11	7.77	1/5/2016	156	7.39	7.11
11/29/2015	119	7.22	7.88	1/6/2016	157	6.55	7
12/2/2015	122	7.06	7.86	1/8/2016	159	7.78	7.89
12/5/2015	125	7.03	7.94				

OLR 5.6 g COD/L-d							
Date	Days	Influent	Effluent	Date	Days	Influent	Effluent
1/9/2016	160	-	7.82	1/21/2016	172	8.00	8.05
1/11/2016	162	7.55	7.83	1/22/2016	173	6.87	7.78
1/12/2016	163	7.57	8.14	1/27/2016	178	6.75	7.59
1/13/2016	164	7.97	7.16	1/28/2016	179	7.78	7.94
1/14/2016	165	7.44	7.2	2/3/2016	185	6.95	7.8
1/16/2016	167	7.17	7.58	2/5/2016	187	6.95	7.8
1/17/2016	168	7.82	7.32	2/10/2016	192	7.53	7.81
1/18/2016	169	7.55	7.89	2/14/2016	196	7.2	7.8
1/19/2016	170	7.05	7.57	2/17/2016	199	7.05	7.75
1/20/2016	171	6.73	7.79				

ORP

Date	Influent	Effluent	Date	Influent	Effluent
8/27/2015	-171.2	-170.4	10/5/2015	-126.2	-138.6
8/28/2015	-166.1	-169	10/6/2015	-138	-147.8
8/31/2015	-245.4	-238.2	10/7/2015	-76.5	-135.8
9/1/2015	-136.5	-142.5	10/8/2015	-145.3	-177.4
9/2/2015	-128.9	-134.6	10/12/2015	-175.3	-192.5
9/8/2015	-281.4	-299.7	10/13/2015	-185	-191.1
9/10/2015	-90.7	-107.4	10/16/2015	-123.4	-178.7
9/13/2015	-95.8	-167.7	10/19/2015	-167.7	-174
9/16/2015	-77.6	-144.2	10/20/2015	-140.1	-139.6
9/19/2015	-73.6	-107.5	10/26/2015	-145	-148.9
9/20/2015	-99.6	-129.6	10/28/2015	-117.8	-146.3
9/24/2015	-91.4	-97.3	10/30/2015	-136.5	-156.2
9/30/2015	-81.5	-155.5	10/31/2015	-122.7	-172.2
10/1/2015	-91.8	-168.5	11/1/2015	-119.7	-142.5
10/2/2015	-147.6	-180.4	11/3/2015	-127.9	-140.6
10/3/2015	-131.5	-158.7	11/4/2015	-131.1	134.7
10/4/2015	-81.7	-150.6			

Total suspended solid

OLR 18.6 g COD/L-d		
Date	Day	Suspended solid (mg/L)
8/3/2015	1	60
8/12/2015	10	16
8/14/2015	12	33
8/15/2015	13	18
8/17/2015	15	10.5
8/18/2015	16	37
8/19/2015	17	25
8/25/2015	23	6
8/27/2015	25	92
8/28/2015	26	35
8/31/2015	29	28
9/6/2015	35	36

9/11/2015	40	33
9/21/2015	50	22
9/29/2015	58	28
10/8/2015	67	84.7
10/15/2015	74	76
10/21/2015	80	82
10/27/2015	86	69
11/3/2015	93	92

OLR 9.4 g COD/L-d		
Date	Day	Suspended solid (mg/L)
11/9/2015	99	92
11/14/2015	104	35
11/19/2015	109	28
11/24/2015	114	26
11/27/2015	117	63.7
12/2/2015	122	48.7
12/4/2015	124	32.0
12/10/2015	130	26.3
12/23/2015	143	27.3
12/28/2015	148	30.2
1/5/2016	156	28.5

OLR 5.6 g COD/L-d		
Date	Day	Suspended solid (mg/L)
1/9/2016	160	13.5
1/17/2016	168	9.7
1/23/2016	174	12.3
1/29/2016	180	18.0
2/4/2016	186	10.2
2/11/2016	193	6.5
2/17/2016	199	8
2/20/2016	202	7.5

MiSeq Illumina sequencing data

	OLR 5.6 g COD/L-d			
#OTU ID	P1	P2	P6	P10
denovo6969	18.1%	17.5%	17.3%	21.7%
denovo8885	20.0%	18.8%	5.5%	6.5%
denovo11390	3.0%	3.4%	5.7%	4.6%
denovo7595	2.7%	2.8%	3.0%	4.0%
denovo11911	10.5%	7.6%	5.0%	4.6%
denovo1122	4.4%	6.4%	4.6%	7.9%
denovo4894	0.5%	0.3%	0.0%	0.1%
denovo1991	2.2%	2.5%	6.4%	4.3%
denovo1168	0.1%	0.1%	4.6%	2.3%
denovo4848	1.5%	1.4%	1.2%	1.4%
denovo6967	3.5%	3.3%	0.9%	1.0%
denovo6010	2.7%	2.9%	2.1%	1.5%
denovo1169	1.1%	1.3%	2.5%	2.1%

	OLR 9.4 g COD/L-d			
#OTU ID	P1	P2	P6	P10
denovo6969	38.3%	33.7%	21.5%	22.3%
denovo8885	11.8%	10.6%	11.4%	18.6%
denovo11390	5.2%	4.9%	12.9%	13.1%
denovo7595	13.3%	13.2%	4.6%	4.1%
denovo11911	3.9%	5.0%	9.5%	5.0%
denovo1122	0.4%	1.8%	4.1%	3.6%
denovo4894	7.4%	6.3%	1.9%	1.6%
denovo1991	0.5%	0.5%	2.0%	2.4%
denovo1168	0.4%	0.3%	1.0%	1.3%
denovo4848	1.8%	3.8%	3.2%	2.6%
denovo6967	0.8%	1.2%	1.3%	1.1%
denovo6010	0.0%	0.0%	0.0%	0.0%

	OLR 9.4 g COD/L-d			
#OTU ID	P1	P2	P6	P10
denovo1169	0.1%	0.3%	0.5%	0.6%

	OLR 18.6 g COD/L-d			
#OTU ID	P1	P2	P6	P10
denovo6969	13.5%	9.6%	13.1%	13.5%
denovo8885	25.2%	32.7%	19.0%	15.1%
denovo11390	9.1%	10.5%	22.1%	23.2%
denovo7595	11.1%	10.8%	2.3%	2.2%
denovo11911	8.4%	3.9%	3.5%	3.2%
denovo1122	0.6%	0.2%	4.7%	5.1%
denovo4894	6.5%	7.2%	3.8%	4.2%
denovo1991	0.9%	0.6%	2.1%	2.4%
denovo1168	0.1%	0.1%	1.0%	2.0%
denovo4848	1.0%	0.7%	3.0%	2.0%
denovo6967	0.0%	0.1%	0.5%	0.6%
denovo6010	0.0%	0.0%	0.1%	0.0%
denovo1169	0.0%	0.0%	0.4%	0.3%

OTU sequences

#OTU ID	Sequences
denovo6969	ACGTAGGTGGCAAGCGTTGTCCGGATTTACTGGGCGTAAAGGGTGCGTAGGCGGACC TTTAAGTGAGATGTGAAATCCCCGAGCTTAACTTGGGGGCTGCATTTCAAACTGGAG GTCTAGAGTGCAGGAGAGGAGAGTGGAATTCCTAGTGTAGCGGTGAAATGCGTAGAG ATTAGGAAGAACACCAGTGGCGAAGGCGACTCTCTGGACTGTAACTGACGCTGAGGC ACGAAAGCGTGGGGAGCAAACAG
denovo8885	ACCGGCAGCTCTAGTGGTAGCCATTTTTATTGGGCCTAAAGCGTTCGTAGCCGGTTT AATAAGTCTCTGGTGAAATCCCGTAGCTTAACTATGGGAATTGCTGGAGATACTATTA GACTTGAGGTCGGGAGAGGTTAGAGGTACTCCCAGGGTAGGGGTGAAATCCTGTAAT CCTGGGAGGACCACCTGTGGCGAAGGCGTCTAACTGGAACGAACCTGACGGTGAGG GACGAAAGCTAGGGGCGCGAACCG
denovo11390	ACGTAGGGGGCAAGCGTTGTCCGGAATGATTGGGCGTAAAGGGCGCGTAGGCGGCC TGGTAAGTCTGGAGTGAAAGTCCTGCTTTTAAGGTGGGAATTGCTTTGGATACTGTC GGGCTTGAGTGCAGGAGAGGTAAGTGGAATTCCCGGTGTAGCGGTGAAATGCGTAGA GATCGGGAGGAACACCAGTGGCGAAGGCGACTTACTGGACTGTAACTGACGCTGAGG CGCGAAAGTGTGGGGAGCAAACAG
denovo7595	ACGGAGGGTGCAAGCGTTAATCGGAATTACTGGGCGTAAAGCGCACGCAGGCGGTTG GATAAGTCAGATGTGAAAGCCCCGGGCTCAACCTGGGAACTGCATTTGAAACTGTTC GACTAGAGTCTTGTAGAGGGGGGTAGAATTCCAGGTGTAGCGGTGAAATGCGTAGAG ATCTGGAGGAATACCGGTGGCGAAGGCGGCCCCCTGGACAAAGACTGACGCTCAGGT GCGAAAGCGTGGGGAGCAAACAG
denovo11911	ACGGAGGGTGCAAGCGTTAATCGGAATCACTGGGCGTAAAGCGCGCGTAGGCCGTCT TTTAAGTCGGACGTGAAAGCCCTCGGCTCAACCGGGGAACTGCGTTCGATACTGGGA GACTTGAGTCCTGGAGAGGGTGGCGGAATTCCGGGTGTAGGAGTGAAATCCGTAGAT ATCCGGAGGAACACCGGTGGCGAAGGCGGCCACCTGGACAGGTACTGACGCTGAGG CGCGAAAGCGTGGGGAGCAAACAG
denovo1122	ACGTAGGATCCGAGCGTTATCCGAATTTACTGGGCGTAAAGCGCGTGCAGGCGGTTT GGCAAGTTGGATGTAAAAGCTCCTGGCTCAACTGGGAGAGGCCGTTCAAAACTACCA GACTAGAGGGCGACAGAGGGAGGTGGAATTCCCGGTGTAGTGGTGAAATGCGTAGAT ATCGGGAGGAACACCTGTGGCGAAAGCGGCCTCCTGGGTCGTACCTGACGCTCAGAC GCGAAAGCTAGGGGAGCGAACGG
denovo4894	ACGGAGGGTGCAAGCGTTAATCGGAATTACTGGGCGTAAAGCGCACGCAGGCGGTCT GTCAAGTCGGATGTGAAATCCCCGGGCTCAACCTGGGAACTGCATTCGAAACTGGCA GGCTAGAGTCTTGTAGAGGGGGGTAGAATTCCAGGTGTAGCGGTGAAATGCGTAGAG ATCTGGAGGAATACCGGTGGCGAAGGCGGCCCCCTGGACAAAGACTGACGCTCAGGT GCGAAAGCGTGGGGAGCAAACAG

#OTU ID	Sequences
denovo1991	ACGTAGGGGGCAAGCGTTGTTCGGAATTACTGGGCGTAAAGGGCATGTAGGCGGCCTTGTAAGCTTGGCGTGAAAGTCCACGGCTTAACCGTGGGATTGCGTTGAGAACTGCGAGGCTTGAGTGACGGAGAGGGAGCTAGAATTCCTGGTGTAGGGGTGGAATCTGTAGAGATCAGGAAGAATACCAATGGCGAAGGCAAGCTCCTGGCCGATGACTGACGCTGAGGTGCGAAAGTGTGGGGATCAAACAG
denovo1168	ACAGGGGTGGCAAGCGTTGTCCGGATTTACTGGGTGTAAAGGGTGCGCAGGCGGATCAATAAGTCGGGGGTTAAATCCATGTGCTTAACACATGCACGGCTTCCGATACTGTTGATCTAGAGTCTCGAAGAGGAAGGTGGAATTTCCGGTGTAACGGTGGAATGTGTAGATATCGGAAAGAACACCAGTGGCGAAGGCAGCCTTCTGGTCGAGTACTGACGCTCATGCACGAAAGCGTGGGGAGCAAACAG
denovo4848	ACGTAAGGGGCGAGCGTTGTTCGGAATTATTGGGCGTAAAGGGCGCGTAGGCGGTCCTGTAAGCCCGGCGTGAAAACCTGGAGCTCAACTCCGGGCCTGCGCTGGGAACTGCGGGACTAGAGTCATGGAAGGGAAGTTGGAATTCCAGGTGTAGGGGTGAAATCTGTAGATATCTGGAAGAACACCGGTGGCGAAGGCGAACTTCTGGCCAATGACTGACGCTGAGGCGCGAAAGTGCGGGGAGCAAACAG
denovo6967	ACGGAGGGTGCAAGCGTTGTTCGGAATCACTGGGCGTAAAGGGCGCGTAGGCGGTTTGATAAGTCAGATGTGAAAGCCCACGGCTTAACCGTGGAAGTGCATTTGAAACTGTCAGACTTGAGTATCAGAGGGGAAAGTGGAATTCCCGGTGTAGAGGTGAAATTCGTAGATATCGGGAGGAATACCGGTGGCGAAGGCGACTTTCTGGCTGAATACTGACGCTGAGGCGCGAAAGCGTGGGGAGCAAACAG
denovo6010	ACGGAGGATGCGAGCGTTATCCGGATTTATTGGGTTTAAAGGGTGCGTAGGCGGATTGATAAGTCAGTGGTGAAAACCTGCAGCTTAACTGTAGACTTGCCGTTGATACTGTCAGTCTTGAGTGTGGTCAAGGTAGGCGGAATGTGTAATGTAGCGGTGAAATGCTTAGATATTACACAGAACACCGATTGCGAAGGCAGCTTACTGGGCCATTACTGACGCTGATGCACGAAAGCGTGGGGATCGAACAG
denovo1169	ACGTAGGGGGCGAGCGTTGTCCGGAATCACTGGGCGTAAAGCGCACGTAGGCGGGCTGCCAAGTCGGCCGTGAAAGGCACTGGCTCAACCGGTGCATGTCGGTCGATACTGGCAGTCTGGAGTATGGGAGAGGGAACTGGAATTCCCGGTGTAGCGGTGAAATGCGTAGATATCGGGAGGAACACCAGTGGCGAAGGCGGGTTCCTGGCCCATGACTGACGCTGAGGTGCGAAAGCCGGGGGAGCGAACGG

Appendix C

Parameter analysis results in denitrification

C.1. Nitrate reduction at different COD to nitrate ratios

- COD

COD:NO_3^- - N ratio = 1:1

Date	COD (mg/L)		Efficiency (%)	Date	COD (mg/L)		Efficiency (%)
	Influent	Effluent			Influent	Effluent	
3-Feb-15	81.4	29.8	63.4	3-Mar-15	106.1	15.9	85.0
4-Feb-15	108.2	15.4	85.8	4-Mar-15	116.1	15.0	87.1
7-Feb-15	76.0	8.0	89.5	5-Mar-15	97.3	7.9	91.9
8-Feb-15	84.5	15.4	81.8	6-Mar-15	97.3	9.9	89.8
9-Feb-15	88.6	22.6	74.4	7-Mar-15	125.0	25.8	79.4
11-Feb-15	80.7	9.8	87.8	8-Mar-15	103.2	16.9	83.6
12-Feb-15	96.4	20.7	78.6	10-Mar-15	103.5	8.8	91.5
13-Feb-15	81.9	11.4	86.1	11-Mar-15	101.5	9.8	90.4
17-Feb-15	76.2	7.6	90.0	16-Mar-15	101.6	17.7	82.6
18-Feb-15	78.1	13.3	82.9	19-Mar-15	97.2	13.2	86.4
25-Feb-15	89.6	10.8	88.0	20-Mar-15	113.7	22.1	80.6
28-Feb-15	90.7	6.5	92.9	21-Mar-15	99.4	11.0	88.9
1-Mar-15	76.7	4.3	94.4	26-Mar-15	109.8	10.6	90.4
2-Mar-15	70.4	10.9	84.5				

$COD:NO_3^-$ - N ratio = 2:1

Date	COD (mg/L)		Efficiency (%)	Date	COD (mg/L)		Efficiency (%)
	Influent	Effluent			Influent	Effluent	
3-Feb-15	148.9	35.7	76.0	5-Mar-15	208.3	19.8	90.5
4-Feb-15	192.0	46.1	76.0	6-Mar-15	196.5	25.8	86.9
7-Feb-15	160.0	30.0	81.3	7-Mar-15	206.3	32.7	84.1
8-Feb-15	143.0	36.5	74.5	8-Mar-15	205.3	39.7	80.7
9-Feb-15	157.4	29.5	81.3	10-Mar-15	204.0	15.6	92.3
11-Feb-15	159.4	23.6	85.2	11-Mar-15	205.0	18.5	91.0
12-Feb-15	190.9	31.5	83.5	16-Mar-15	223.0	11.0	95.0
13-Feb-15	175.2	9.5	94.6	19-Mar-15	209.8	11.0	94.7
17-Feb-15	152.3	17.1	88.7	20-Mar-15	205.3	13.2	93.5
18-Feb-15	164.7	17.1	89.6	21-Mar-15	216.4	13.2	93.9
3-Mar-15	207.3	16.9	91.8	26-Mar-15	204.9	16.9	91.8
4-Mar-15	207.3	41.7	79.9				

$COD:NO_3^-$ - N ratio = 3:1

Date	COD (mg/L)		Efficiency (%)	Date	COD (mg/L)		Efficiency (%)
	Influent	Effluent			Influent	Effluent	
14-May-15	363.0	181.0	50.1	11-Jun-15	307.2	30.7	90.0
19-May-15	457.0	102.0	77.7	12-Jun-15	288.0	103.7	64.0
20-May-15	394.0	15.7	96.0	16-Jun-15	298.1	14.3	95.2
21-May-15	362.0	31.5	91.3	17-Jun-15	332.0	44.2	86.7
22-May-15	394.0	23.6	94.0	19-Jun-15	402.7	44.0	89.1
24-May-15	328.0	31.2	90.5	23-Jun-15	311.0	13.4	95.7
25-May-15	362.0	19.5	94.6	26-Jun-15	276.5	30.7	88.9
26-May-15	342.0	84.0	75.4	2-Jul-15	286.0	6.6	97.7

Date	COD (mg/L)		Efficiency (%)	Date	COD (mg/L)		Efficiency (%)
	Influent	Effluent			Influent	Effluent	
27-May-15	342.0	107.0	68.7	3-Jul-15	347.6	18.8	94.6
28-May-15	305.0	72.4	76.3	6-Jul-15	264.0	23.0	91.3
6-Jun-15	265.0	23.0	91.3	8-Jul-15	323.0	13.7	95.8
7-Jun-15	121.0	14.0	88.4				

COD:NO_3^- - N ratio = 5:1

Date	COD (mg/L)		Efficiency (%)	Date	COD (mg/L)		Efficiency (%)
	Influent	Effluent			Influent	Effluent	
10-Sep-2014	480.0	120.0	75.0	19-Oct-2014	566.0	21.0	96.3
27-Sep-2014	563.0	120.0	78.7	21-Oct-2014	414.0	47.0	88.6
29-Sep-2014	499.0	137.0	72.5	23-Oct-2014	520.0	50.0	90.4
2-Oct-2014	480.0	148.0	69.2	8-Jan-2015	352.0	42.0	88.1
8-Oct-2014	616.0	91.0	85.2	20-Jan-2015	480.0	48.0	90.0
9-Oct-2014	486.0	95.0	80.4	22-Jan-2015	440.0	92.0	79.1
12-Oct-2014	440.0	80.0	81.8	24-Jan-2015	500.0	38.0	92.4
17-Oct-2014	557.0	126.0	77.4				
18-Oct-2014	515.0	61.0	88.2				

COD:NO_3^- - N ratio = 10:1

Date	COD (mg/L)		Efficiency (%)	Date	COD (mg/L)		Efficiency (%)
	Influent	Effluent			Influent	Effluent	
13-May-2015	944.0	91.6	90.3	9-May-2015	965.0	286.0	70.4
16-May-2015	953.0	129.0	86.5	11-May-2015	1114.0	220.8	80.2
20-May-2015	650.0	130.0	80.0	12-May-2015	691.0	152.0	78.0
21-May-2015	670.0	39.4	94.1	16-May-2015	1145.6	440.3	61.6
22-May-2015	690.0	118.1	82.9	17-May-2015	1124.5	341.4	69.6
24-May-2015	1113.0	242.0	78.3	19-May-2015	870.0	200.0	77.0
25-May-2015	1210.0	285.0	76.4	26-May-2015	998.4	307.2	69.2
26-May-2015	1124.0	285.6	74.6	27-May-2015	1152.0	307.2	73.3
27-May-2015	1238.0	182.0	85.3	2-May-2015	979.0	265.0	72.9
28-May-2015	1199.0	442.0	63.1	3-May-2015	1081.0	280.0	74.1
6-Jun-2015	998.4	230.4	76.9	6/-May-2015	914.0	250.0	72.6
7-May-2015	861.0	127.0	85.2				

- Nitrate

COD:NO_3^- - N ratio = 1:1

Date	Nitrate (mg/L)		Efficiency (%)	Date	Nitrate (mg/L)		Efficiency (%)
	Influent	Effluent			Influent	Effluent	
4-Feb-15	105.5	54.86	48.0	5-Mar-15	104	84.55	18.7
8-Feb-15	75.31	45.56	39.5	6-Mar-15	91.18	65.4	28.3
9-Feb-15	100	58.5	41.5	7-Mar-15	94.15	67.97	27.8
10-Feb-15	98.96	58.21	41.2	10-Mar-15	111.7	82.5	26.1
12-Feb-15	89.63	67.59	24.6	11-Mar-15	100.7	84.84	15.7
16-Feb-15	88.29	77.57	12.1	13-Mar-15	90.95	66.68	26.7
17-Feb-15	90.59	79.81	11.9	14-Mar-15	86.12	59.52	30.9
18-Feb-15	90.98	77.54	14.8	17-Mar-15	73.93	57.54	22.2
21-Feb-15	117.6	101.5	13.7	18-Mar-15	80.57	56.98	29.3
28-Feb-15	101.2	85.28	15.7	21-Mar-15	92.23	64.85	29.7
1-Mar-15	100	81.74	18.3	24-Mar-15	92.39	64.53	30.2
2-Mar-15	102	78.81	22.7	26-Mar-15	91.95	64.07	30.3
4-Mar-15	105	67.94	35.3				

COD:NO_3^- - N ratio = 2:1

Date	Nitrate (mg/L)		Efficiency (%)	Date	Nitrate (mg/L)		Efficiency (%)
	Influent	Effluent			Influent	Effluent	
9-Feb-15	87.4	43	50.8	5-Mar-15	108.7	48.3	55.6
14-Feb-15	110	76.47	30.5	6-Mar-15	96.24	39.86	58.6
15-Feb-15	81.5	72.54	11.0	7-Mar-15	98.47	48.9	50.3
17-Feb-15	94.8	63.72	32.8	13-Mar-15	102.7	44.78	56.4
18-Feb-15	90.94	61.3	32.6	14-Mar-15	90.33	37.58	58.4
21-Feb-15	95.9	62.22	35.1	16-Mar-15	94.73	44.48	53.0
24-Feb-15	118.5	70.1	40.8	17-Mar-15	73.8	39.31	46.7
26-Feb-15	112.9	68.05	39.7	18-Mar-15	80.3	41.02	48.9
28-Feb-15	97.53	78.62	19.4	21-Mar-15	107.9	45.67	57.7
1-Mar-15	98.1	65.07	33.7	24-Mar-15	99.66	44.79	55.1
2-Mar-15	99.08	57.09	42.4	26-Mar-15	89.24	42.48	52.4
4-Mar-15	88.47	46.64	47.3				

COD:NO_3^- - N ratio = 3:1

Date	Nitrate (mg/L)		Efficiency (%)	Date	Nitrate (mg/L)		Efficiency (%)
	Influent	Effluent			Influent	Effluent	
12-May-2015	120	78.67	34.4	11-June-2015	103.3	28.15	72.7
13-May-2015	120	61.18	49.0	13-June-2015	93.97	28.07	70.1
15-May-2015	73.34	20.29	72.3	15-June-2015	97.25	25.25	74.0
16-May-2015	105.5	50.21	52.4	16-June-2015	94.29	6.35	93.3
18-May-2015	104.3	42.62	59.1	21-June-2015	99.48	7.26	92.7
19-May-2015	104.9	35.26	66.4	22-June-2015	99.48	8.62	91.3
20-May-2015	107.9	49.2	54.4	23-June-2015	102.2	7.17	93.0
21-May-2015	101	30.53	69.8	27-June-2015	99.48	7.26	92.7
24-May-2015	84.21	16.81	80.0	29-June-2015	99.63	7.87	92.1
25-May-2015	100.4	34.27	65.9	30-June-2015	92.67	7.78	91.6
30-May-2015	101	30.53	69.8	2/July/2015	87.35	5.085	94.2
2-June-2015	100.5	31.08	69.1	3 July 2015	103.3	2.05	98.0
4-June-2015	98.16	30.5	68.9	6 July 2015	107.8	1.124	99.0
5-June-2015	96.21	30.19	68.6	10 July 2015	102.5	0.112	99.9
6-June-2015	91.17	19.21	78.9	15 July 2015	111.7	0.794	99.3
9-June-2015	96.15	28.39	70.5	16 July 2015	102.5	0.855	99.2
10-June-2015	95.13	33.47	64.8				

COD:NO_3^- - N ratio = 5:1

Date	Nitrate (mg/L)		Efficiency (%)	Date	Nitrate (mg/L)		Efficiency (%)
	Influent	Effluent			Influent	Effluent	
25 July 2015	100	20	80.0	29-Aug-2014	103.5	1.58	98
26 July 2015	100	20	80.0	1-Sep-2014	98.2	1.02	99

Date	Nitrate (mg/L)		Efficiency (%)	Date	Nitrate (mg/L)		Efficiency (%)
	Influent	Effluent			Influent	Effluent	
27 July 2015	100	20	80.0	3-Sep-2014	95.7	3.21	97
28 July 2015	100	20	80.0	6-Sep-2014	102.5	2.12	98
29 July 2015	100	20	80.0	8-Sep-2014	99.9	5.21	95
30 July 2014	101.2	19.63	81	19-Sep-2014	113.6	9.52	92
1-Aug-2014	91.81	12.16	87	22-Sep-2014	91.55	3.21	96
2-Aug-2014	96.5	0.8	99	23-Oct-/2014	104.5	7.46	93
10-Aug-2014	101.6	3.55	97	13-Nov-2014	125.5	4.17	97
11-Aug-2014	102.5	2.25	98	15-Nov-2014	108.7	2.06	98
12-Aug-2014	107.3	1.38	99	20-Nov-2014	105	1.21	99
15-Aug-2014	101.4	1.33	99	24-Nov-2014	109.9	2.35	98
17-Aug-2014	109	1.79	98	15-Dec-2014	100.1	1.032	99
20-Aug-2014	99.8	1.57	98	10-Jan-2015	91.47	0.79	99
22-Aug-2014	97.88	3.98	96	15-Jan-2015	108.7	2.06	98
26-Aug-2014	107.5	2.35	98	22-Jan-2015	109.9	2.2	98

COD:NO_3^- - N ratio = 10:1

Date	Nitrate (mg/L)		Efficiency (%)	Date	Nitrate (mg/L)		Efficiency (%)
	Influent	Effluent			Influent	Effluent	
8-May-2015	99.83	1	99.0	13-Jun-2015	99.22	0.045	99.9
11-May-2015	105.3	11.07	89.5	15-Jun-2015	95.36	0.016	99.9
14-May-2015	95.84	0.295	99.7	17-Jun-2015	105.5	0.005	99.9
16-May-2015	100.3	10.72	89.3	18-Jun-2015	106.5	0.081	99.9
23-May-2015	96.2	1.274	98.7	19-Jun-2015	103.7	0.064	99.9
24-May-2015	99.17	0.329	99.7	23-Jun-2015	99.7	0.005	99.9
25-May-2015	116	0.417	99.6	27-Jun-2015	100.8	0.032	99.9
26-May-2015	106.1	1.241	98.8	30-Jun-2015	102	2.504	97.5
27-May-2015	104.3	0.783	99.2	6-Jul-2015	108.4	0.261	99.8
28-May-2015	97.15	0.252	99.7	7-Jul-2015	105.1	0.001	99.9
2-Jun-2015	100	16	84.0	8-Jul-2015	95.05	0.351	99.6
6-Jun-2015	101.3	9.635	90.5	9-Jul-2015	108.6	0.001	99.9
9-Jun-2015	96.65	6.929	92.8	10-Jul-2015	98.7	0.048	99.9
10-Jun-2015	107.2	10.31	90.4	11-Jul-2015	108.6	0.07	99.9
11-Jun-2015	110	0.097	99.9	13-Jul-2015	95.04	0.006	99.9
12-Jun-2015	99.86	0.021	99.9				

- Profile of COD and nitrate concentration

- pH

COD:NO_3^- - N ratio = 1:1

Date	Influent	Effluent	Date	Influent	Effluent
3-Feb-15	7.61	8.12	3-Mar-15	8.4	8.4
4-Feb-15	7.2	7.3	4-Mar-15	8.1	8.07
7-Feb-15	7.71	8.26	5-Mar-15	8.32	8.27
8-Feb-15	8.19	8.31	6-Mar-15	8.12	8.24
10-Feb-15	7.5	7.99	11-Mar-15	8.26	8.24
12-Feb-15	8.13	7.88	12-Mar-15	8.32	8.28
14-Feb-15	7.9	8.04	13-Mar-15	8.47	8.41
16-Feb-15	7.62	7.8	14-Mar-15	7.99	7.97
17-Feb-15	7.43	8.14	16-Mar-15	8.1	8.27
18-Feb-15	7.22	7.4	17-Mar-15	8.14	8.11
19-Feb-15	7.32	7.32	18-Mar-15	8.32	8.29
21-Feb-15	8.2	8.18	19-Mar-15	8.22	8.15
24-Feb-15	7.26	7.36	21-Mar-15	8.05	8.18
26-Feb-15	8.21	8.34	24-Mar-15	7.94	8.25
28-Feb-15	8.33	8.43	25-Mar-15	8.28	8.31
1-Mar-15	7.54	8.2	26-Mar-15	7.83	7.65

COD:NO_3^- - N ratio = 2:1

Date	Influent	Effluent	Date	Influent	Effluent
27-Mar-15	7.22	8.02	24-Apr-15	8.19	7.56
28-Mar-15	7.2	7.2	25-Apr-15	8.12	8.04
31-Mar-15	7.82	7.88	26-Apr-15	8.24	8.06
1-Apr-15	8.31	7.82	27-Apr-15	8.34	8.32
3-Apr-15	7.81	7.65	2-May-15	8.2	8.02
5-Apr-15	7.94	7.74	3-May-15	8.48	8.32
7-Apr-15	7.53	7.9	4-May-15	8.63	8.24
9-Apr-15	7.45	8.06	5-May-15	8.06	7.94
10-Apr-15	7.48	8.14	7-May-15	8.23	8.14
11-Apr-15	7.45	7.04	8-May-15	8.13	7.98
12-Apr-15	7.39	7.39	9-May-15	8.34	8.32
14-Apr-15	8.15	8.14	10-May-15	8.21	7.82
17-Apr-15	7.32	7.37	12-May-15	8.26	7.89
19-Apr-15	8.05	8.24	15-May-15	8.41	8.3
21-Apr-15	8.35	8.33	16-May-15	8.42	8.08
22-Apr-15	7.73	8.2	17-May-15	7.73	7.47

COD:NO_3^- - N ratio = 3:1

Date	Influent	Effluent	Date	Influent	Effluent
19-May-15	8.37	8.04	24-Jun-15	8.32	8.28
22-May-15	8.33	8.15	25-Jun-15	8.37	7.98
23-May-15	7.74	8.33	26-Jun-15	8.35	7.8

Date	Influent	Effluent	Date	Influent	Effluent
24-May-15	8.16	8.33	27-Jun-15	8.36	7.93
25-May-15	8.38	8.02	28-Jun-15	8.2	7.9
26-May-15	8.46	8.46	29-Jun-15	8.31	8.14
27-May-15	8.38	8.2	30-Jun-15	8.31	8.08
29-May-15	8.45	8.16	7-Jul-15	8.43	8.21
30-May-15	8.31	8.11	8-Jul-15	7.55	8.23
31-May-15	8.45	8.31	10-Jul-15	8.24	7.86
1-Jun-15	8.33	8.33	11-Jul-15	8.35	7.78
3-Jun-15	8.22	8.13	12-Jul-15	7.72	7.83
4-Jun-15	7.81	8.15	13-Jul-15	8.04	7.94
5-Jun-15	8.34	8.06	14-Jul-15	8.1	8.18
6-Jun-15	8.37	8.22	17-Jul-15	7.37	8.23
7-Jun-15	8.35	8.17	18-Jul-15	8.15	8.04
8-Jun-15	8.32	7.94	19-Jul-15	8.25	8.26
9-Jun-15	8.51	8.11	20-Jul-15	8.04	8.02
13-Jun-15	8.03	8.11	21-Jul-15	8.21	8.01
16-Jun-15	7.44	7.46	22-Jul-15	8.22	8.2
17-Jun-15	7.44	7.42	23-Jul-15	7.7	8.2
19-Jun-15	7.47	8.12	24-Jul-15	8.21	8.22
20-Jun-15	8.42	8.2	26-Jul-15	8.31	8.32
21-Jun-15	8.35	8.33	27-Jul-15	8.28	8.27
22-Jun-15	8.36	8.34			
23-Jun-15	6.06	7.98			

COD:NO_3^- - N ratio = 5:1

Date	Influent	Effluent	Date	Influent	Effluent
29-Jul-15	7.98	7.94	5-Sep-15	8.07	8
5-Aug-15	7.74	7.41	6-Sep-15	6.28	6.19
6-Aug-15	7.25	7.68	7-Sep-15	7.53	8.1
7-Aug-15	7.96	7.97	8-Sep-15	7.66	7.4
8-Aug-15	7.9	7.87	9-Sep-15	7.99	8.1
10-Aug-15	7.83	7.85	10-Sep-15	7.55	7.86
15-Aug-15	7.9	7.81	11-Sep-15	8.03	7.65
16-Aug-15	7.94	8.04	12-Sep-15	8.05	7.9
17-Aug-15	7.53	7.57	13-Sep-15	7.84	7.6
18-Aug-15	7.65	7.63	14-Sep-15	-	7.45
19-Aug-15	7.65	7.53	15-Sep-15	7.91	8.1
20-Aug-15	7.94	7.74	16-Sep-15	7.67	-
21-Aug-15	7.82	7.52	19-Sep-15	8.17	8.16
22-Aug-15	7.16	7.00	20-Sep-15	8.16	7.96
23-Aug-15	7.52	7.00	21-Sep-15	7.84	7.75
24-Aug-15	7.72	7.85	22-Sep-15	7.5	6.98
25-Aug-15	7.38	6.5	24-Sep-15	8.29	7.59
26-Aug-15	8.02	7.94	30-Sep-15	7.81	7.13
27-Aug-15	8.15	8.05	1-Oct-15	8.08	7.64
28-Aug-15	7.92	8.13	2-Oct-15	7.31	8.09
29-Aug-15	7.2	7.5	3-Oct-15	7.96	6.79
30-Aug-15	7.84	7.91	4-Oct-15	7.92	7.83
31-Aug-15	7.84	8.2	5-Oct-15	6.25	6.77
1-Sep-15	8.12	8.05	6-Oct-15	7.91	7.18
2-Sep-15	8.21	8.1	7-Oct-15	8.1	7.75
3-Sep-15	8.27	8.1	8-Oct-15	7.16	8.02
4-Sep-15	7.27	7.05			

COD:NO_3^- - N ratio = 10:1

Date	Influent	Effluent	Date	Influent	Effluent
16-Oct-15	6.57	7.92	21-Nov-15	6.06	7.89
17-Oct-15	8.37	8.2	22-Nov-15	8.42	8.11
20-Oct-15	8.38	8.11	23-Nov-15	8.35	7.7
21-Oct-15	7.92	7.74	24-Nov-15	8.33	7.28
22-Oct-15	8.4	8.03	25-Nov-15	8.37	7.63
23-Oct-15	8.43	7.72	26-Nov-15	8.45	8.01
24-Oct-15	8.41	8.37	27-Nov-15	8.33	7.98
25-Oct-15	8.52	7.41	28-Nov-15	8.37	7.82
27-Oct-15	8.46	7.42	1-Dec-15	-	7.84
28-Oct-15	8.6	7.68	2-Dec-15	8.41	7.98
29-Oct-15	8.5	7.97	5-Dec-15	8.32	-
30-Oct-15	8.47	8.24	6-Dec-15	8.34	7.56
1-Nov-15	8.28	8.1	8-Dec-15	8.15	7.13
2-Nov-15	7.99	7.91	9-Dec-15	8.29	7.75
3-Nov-15	8.46	7.8	10-Dec-15	7.87	6.7
4-Nov-15	8.41	7.78	11-Dec-15	7.12	7.29
5-Nov-15	8.46	7.84	12-Dec-15	8.05	6.97
6-Nov-15	8.27	7.69	15-Dec-15	8.3	7.28
7-Nov-15	8.35	7.62	16-Dec-15	8.22	7.4
11-Nov-15	8.25	7.18	17-Dec-15	8.3	7.44
14-Nov-15	7.58	7.21	18-Dec-15	8.27	7.52
15-Nov-15	7.46	7.33	19-Dec-15	8.12	7.64
17-Nov-15	7.49	8.01	20-Dec-15	8.31	7.66
18-Nov-15	8.38	7.98	21-Dec-15	8.08	8.19
19-Nov-15	8.45	8.1	22-Dec-15	8.17	7.98
20-Nov-15	8.28	8.03			

- ORP

COD:NO_3^- - N ratio = 1:1

Date	Influent	Effluent	Date	Influent	Effluent
3-Feb-15	-150.2	-132.5	1-Mar-15	-128.6	-122.1
4-Feb-15	-127.8	-129.1	3-Mar-15	-218.1	-269.1
7-Feb-15	-196.3	-198.6	4-Mar-15	-245.5	-254.5
8-Feb-15	-162.2	-161.5	5-Mar-15	-301.1	-302.7
10-Feb-15	-120.2	-131.2	11-Mar-15	-195.1	-196.8
12-Feb-15	-171.8	-161.5	12-Mar-15	-171.2	-174.7
14-Feb-15	-176.2	-193.5	13-Mar-15	-165.8	-173.2
16-Feb-15	-193.3	-191.1	16-Mar-15	-176.8	-181.3
17-Feb-15	-143.2	-127.8	17-Mar-15	-163.7	-177.9
18-Feb-15	-132.6	-134.9	18-Mar-15	-166.5	-168.2
19-Feb-15	-141	-141.2	19-Mar-15	-171.4	-174
21-Feb-15	-178.4	-177	21-Mar-15	-164.7	-176
24-Feb-15	-138.8	-131.5	24-Mar-15	-149.7	-153.6
26-Feb-15	-153.6	-149.9	25-Mar-15	-172.5	-175.8
28-Feb-15	-147	-153.5	26-Mar-15	-160.9	-162.9

COD:NO_3^- - N ratio = 2:1

Date	Influent	Effluent	Date	Influent	Effluent
27-Mar-15	-142.2	-138.8	22-Apr-15	-127.2	-120.4
28-Mar-15	-130.7	-124.1	24-Apr-15	-260.7	-254.7
31-Mar-15	-200.1	-191.1	25-Apr-15	-248.7	-251.5
1-Apr-15	-161.7	-155.8	26-Apr-15	-279.8	-286.7
3-Apr-15	-108.6	-127.5	2-May-15	-180.1	-176.6
5-Apr-15	-172	-160.1	3-May-15	-173.8	-174
7-Apr-15	-175.9	-177.2	4-May-15	-165.8	-165.3
9-Apr-15	-188.5	-183.6	7-May-15	-182.2	-181.6
10-Apr-15	-143	-129.3	8-May-15	-175.7	-168.2

Date	Influent	Effluent	Date	Influent	Effluent
11-Apr-15	-134.9	-134.5	9-May-15	-171.4	-170
12-Apr-15	-139.8	-141.7	10-May-15	-178.2	-203.6
14-Apr-15	-180.8	-179.5	12-May-15	-171.3	-165.6
17-Apr-15	-144.7	-136.2	15-May-15	-154	-152.5
19-Apr-15	-155.2	-149.6	16-May-15	-173	-165.2
21-Apr-15	-147	-155	17-May-15	-165.5	-159.7

COD:NO_3^- - N ratio = 3:1

Date	Influent	Effluent	Date	Influent	Effluent
20-May-15	-129.7	-125.3	25-Jun-15	-100	-91.5
23-May-15	-93.9	-97.4	26-Jun-15	-176.1	-184.9
24-May-15	-87.2	-85.6	27-Jun-15	-188	-117.4
25-May-15	-169.8	-171.7	28-Jun-15	-158.5	-201.1
26-May-15	-95.2	-95.3	29-Jun-15	-77.9	-77.8
27-May-15	-121.7	-134.2	30-Jun-15	-76.6	-78
28-May-15	-85	-78.8	1-Jul-15	-168	-84
30-May-15	-84.2	-88.2	9-Jul-15	-81	-95.9
31-May-15	-57.5	-57.5	11-Jul-15	-79.5	-78.5
1-Jun-15	-112.2	-11.6	12-Jul-15	-78.5	-77.1
2-Jun-15	-91.4	-98.8	13-Jul-15	-103.7	-108.5
4-Jun-15	-92.3	-91.5	14-Jul-15	-78.6	-185.5
5-Jun-15	-105.6	-102.5	15-Jul-15	-152	-222.1
6-Jun-15	-80.8	-82.3	18-Jul-15	-89.4	-91.5
7-Jun-15	-85	-76	19-Jul-15	-194.9	-203.8
10-Jun-15	-90.3	-120	20-Jul-15	-232.1	-223
14-Jun-15	-96.3	-107	22-Jul-15	-97.1	-92.5
17-Jun-15	-128.8	-127	23-Jul-15	-153.2	-153.4
18-Jun-15	-149.2	-149.5	24-Jul-15	-96.9	-101.2
20-Jun-15	-177	-177.2	25-Jul-15	-106.7	-99.6

Date	Influent	Effluent	Date	Influent	Effluent
21-Jun-15	-79.4	-84.3	27-Jul-15	-115.9	-159
23-Jun-15	-91	-90.1	28-Jul-15	-117.3	-117.7
24-Jun-15	-94.7	-100.6			

COD:NO_3^- - N ratio = 5:1

Date	Influent	Effluent	Date	Influent	Effluent
2-Aug-15	-105.9	-121.4	2-Sep-15	-250.7	-244.3
3-Aug-15	-127	-126.4	3-Sep-15	-190.8	-195.2
4-Aug-15	-102.8	-104.6	4-Sep-15	-313.8	-290.6
5-Aug-15	-117.6	-120.9	5-Sep-15	-281	-264.9
6-Aug-15	-208.3	-206.5	6-Sep-15	-224.9	-218.1
7-Aug-15	-224	-225.6	7-Sep-15	-228.3	-227.4
8-Aug-15	-168.2	-161.9	9-Sep-15	-194.2	-196.3
9-Aug-15	-138.1	-133.8	13-Sep-15	-182.8	-182.5
10-Aug-15	-124	-122.2	14-Sep-15	-181.6	-183
11-Aug-15	-117.6	-118.5	16-Sep-15	-142.5	-144.2
12-Aug-15	-73.7	-78.7	17-Sep-15	-246.2	-243.6
16-Aug-15	-69.8	-67.2	20-Sep-15	-146.5	-131.3
17-Aug-15	-85.5	-87.9	21-Sep-15	-219	-227.8
18-Aug-15	-93.1	-92.3	23-Sep-15	-35.1	-49.5
19-Aug-15	-98.1	-98.9	24-Sep-15	-91.4	-97.3
20-Aug-15	-78.1	-81.3	30-Sep-15	-81.5	-155.5
21-Aug-15	-96.4	-99.3	1-Oct-15	-91.8	-168.5
22-Aug-15	-158.2	-161.8	2-Oct-15	-147.6	-180.4
23-Aug-15	-65.8	-69.1	3-Oct-15	-131.5	-158.7
24-Aug-15	-138.9	-97.6	4-Oct-15	-81.7	-150.6
25-Aug-15	-102.9	-110.4	5-Oct-15	-126.2	-138.6
26-Aug-15	-184.1	-181.5	6-Oct-15	-138	-147.8
27-Aug-15	-142.5	-144.2	7-Oct-15	-76.5	-135.8
28-Aug-15	-246.2	-243.6	8-Oct-15	-145.3	-177.4

29-Aug-15	-146.5	-131.3	11-Oct-15	-271.7	-276.6
30-Aug-15	-219	-227.8	12-Oct-15	-175.3	-192.5
31-Aug-15	-35.1	-49.5	13-Oct-15	-185	-191.9
1-Sep-15	-139.5	-137.7			

COD:NO_3^- - N ratio = 10:1

Date	Influent	Effluent	Date	Influent	Effluent
17-Oct-15	-167.7	-174	22-Nov-15	-87.4	-99.7
18-Oct-15	-126.6	-110.4	23-Nov-15	-101.8	-192.8
21-Oct-15	-103.1	-105.9	24-Nov-15	-177	-195.1
22-Oct-15	-85.6	-83.4	25-Nov-15	-193.1	-127.5
23-Oct-15	-169.2	-167.8	26-Nov-15	-141.4	-252.5
24-Oct-15	-96.1	-93.8	27-Nov-15	-80.9	-156.7
25-Oct-15	-122.7	-130	28-Nov-15	-79	-237
26-Oct-15	-81.8	-84.8	29-Nov-15	-165.6	-205.2
28-Oct-15	-84.4	-81.5	3-Dec-15	-90.7	-241
29-Oct-15	-55.7	-57.7	7-Dec-15	-93.2	-218.8
30-Oct-15	-106.1	-108.1	9-Dec-15	-92.1	-76.8
31-Oct-15	-92.1	-95.3	10-Dec-15	-77	-139.5
2-Nov-15	-89	-84.9	11-Dec-15	-105.9	-185.5
3-Nov-15	-106.6	-105.5	12-Dec-15	-114.2	-183.2
4-Nov-15	-82.3	-87.5	13-Dec-15	-154.7	-229.3
5-Nov-15	-83.3	-73.8	16-Dec-15	-86.5	-163.1
8-Nov-15	-91.3	-131	17-Dec-15	-193.5	-197.3
12-Nov-15	-94.9	-95.9	18-Dec-15	-234.7	-222.4
15-Nov-15	-130	-126	20-Dec-15	-95.4	-91.3
16-Nov-15	-148.3	-145.3	21-Dec-15	-154.7	-154.5
18-Nov-15	-177.3	-177	22-Dec-15	-97.3	-99.9
19-Nov-15	-77	-85.6	23-Dec-15	-102.9	-101.4

Date	Influent	Effluent	Date	Influent	Effluent
21-Nov-15	-114.9	-103.6			

- Volatile fatty acid and total alkalinity

COD:NO_3^- - N ratio = 1:1

Date	VFA (mg/L)		Alkalinity (mg/L)	
	Influent	Effluent	Influent	Effluent
8-Feb-15	50	40	595	740
24-Feb-15	20	10	465	470
26-Feb-15	20	20	440	550
1-Mar-15	20	10	200	390
7-Mar-15	30	35	240	250
10-Mar-15	20	10	240	270
11-Mar-15	10	20	220	270
13-Mar-15	20	20	300	340
14-Mar-15	20	20	200	280
16-Mar-15	20	20	250	320
18-Mar-15	20	20	360	450
20-Mar-15	20	20	180	300
23-Mar-15	20	15	240	290

COD:NO_3^- - N ratio = 2:1

Date	VFA (mg/L)		Alkalinity (mg/L)	
	Influent	Effluent	Influent	Effluent
1-Apr-15	25	25	670	790
17-Apr-15	20	15	213	610
19-Apr-15	20	20	460	650
22-Apr-15	10	10	390	450
28-Apr-15	45	55	400	525
1-May-15	30	10	270	490
2-May-15	10	20	370	450
4-May-15	20	40	440	500
5-May-15	20	35	380	470
7-May-15	20	20	410	480
9-May-15	20	30	410	520
11-May-15	20	20	330	520
14-May-15	15	15	360	440

COD:NO_3^- - N ratio = 3:1

Date	VFA (mg/L)		Alkalinity (mg/L)	
	Influent	Effluent	Influent	Effluent
27-May-15	50	200	535	780
28-May-15	20	20	1110	1315
4-Jun-15	75	230	900	1300
5-Jun-15	40	80	925	975
8-Jun-15	30	170	1000	1020
15-Jun-15	140	135	535	780
26-Jun-15	20	20	565	880
27-Jun-15	20	80	555	760

28-Jun-15	25	65	620	850
29-Jun-15	30	25	730	910
30-Jun-15	20	15	475	655
7-Jul-15	45	15	885	1085
11-Jul-15	60	85	525	750
13-Jul-15	40	50	510	725
14-Jul-15	20	18	605	800
20-Jul-15	30	25	540	830

COD:NO_3^- - N ratio = 5:1

Date	VFA (mg/L)		Alkalinity (mg/L)	
	Influent	Effluent	Influent	Effluent
26-Jul-15	30	20	315	650
30-Jul-15	30	65	675	1090
5-Aug-15	20	100	540	755
15-Aug-15	56.8	112.5	315	780
16-Aug-15	56.1	250.9	675	1090
19-Aug-15	100	100	650	691
20-Aug-15	37.5	100	689	651
21-Aug-15	37.5	62.5	256	275
23-Aug-15	56.8	98.4	244	512
24-Aug-15	80.2	85.2	350	556
25-Aug-15	210	140	370	391
26-Aug-15	56.3	93.8	370	520
28-Aug-15	59.6	150.2	375	875
30-Aug-15	56.5	87.5	456	681
1-Sep-15	60.5	185.2	651	688
3-Sep-15	75.8	135.7	1100	1013
8-Sep-15	130	210	875	951
16-Sep-15	100	190	795	877

Date	VFA (mg/L)		Alkalinity (mg/L)	
	Influent	Effluent	Influent	Effluent
19-Sep-15	75	225	495	580
20-Sep-15	10	60	630	570
30-Sep-15	110	160	610	605
1-Oct-15	55	130	500	725
4-Oct-15	40	160	675	650
6-Oct-15	40	120	490	550
8-Oct-15	170	250	600	910
11-Oct-15	50	80	650	650
13-Oct-15	120	100	1690	1690

COD:NO_3^- - N ratio = 10:1

Date	VFA (mg/L)		Alkalinity (mg/L)	
	Influent	Effluent	Influent	Effluent
16-Oct-15	180	230	650	420
19-Oct-15	70	60	1100	1090
20-Oct-15	10	60	840	1090
26-Oct-15	30	80	1090	1200
28-Oct-15	60	35	700	730
2-Nov-15	60	380	640	600
3-Nov-15	50	200	535	370
6-Nov-15	150	500	1390	1800
13-Nov-15	215	240	1190	1665
24-Nov-15	25	145	1310	1650
25-Nov-15	100	150	1225	1250
26-Nov-15	60	250	880	1275
27-Nov-15	75	255	855	1255
28-Nov-15	30	120	890	1160
5-Dec-15	50	200	860	1160

Date	VFA (mg/L)		Alkalinity (mg/L)	
	Influent	Effluent	Influent	Effluent
6-Dec-15	110	200	1145	1350
9-Dec-15	85	175	810	1105
11-Dec-15	55	100	865	1225
15-Dec-15	90	160	1145	1525
17-Dec-15	60	150	725	1000
18-Dec-15	65	195	825	1000

- Suspended solid

COD:NO_3^- - N ratio = 1:1

Date	Suspended solid (mg/L)
4-Feb-15	20
15-Feb-15	15
20-Feb-15	20
26-Feb-15	18
2-Mar-15	12
10-Mar-15	7.7
20-Mar-15	10

COD:NO_3^- - N ratio = 2:1

Date	Suspended solid (mg/L)
26-Mar-15	10
8-Apr-15	40
13-Apr-15	30
19-Apr-15	35
23-Apr-15	29
26-Apr-15	20

2-May-15	21
9-May-15	19

COD:NO_3^- - N ratio = 3:1

Date	Suspended solid (mg/L)
17-May-15	21
18-May-15	24
4-Jun-15	20
14-Jun-15	33
25-Jun-15	50
2-Jul-15	33
8-Jul-15	37
16-Jul-15	25
25-Jul-15	19

COD:NO_3^- - N ratio = 5:1

Date	Suspended solid (mg/L)
27-Jul-15	18
28-Jul-15	27.3
2-Aug-15	20
8-Aug-15	16
15-Aug-15	11
18-Aug-15	9
22-Aug-15	36
24-Aug-15	38
27-Aug-15	38
29-Aug-15	78
30-Aug-15	16
3-Sep-15	50
5-Sep-15	40
9-Sep-15	50
16-Sep-15	36

COD:NO_3^- - N ratio = 10:1

Date	Suspended solid (mg/L)	Date	Suspended solid (mg/L)
16-Oct-15	5	8-Nov-15	70
19-Oct-15	22	12-Nov-15	40
23-Oct-15	48	17-Nov-15	40
25-Oct-15	150	23-Nov-15	86
27-Oct-15	244	25-Nov-15	130
30-Oct-15	128	30-Nov-15	75
2-Nov-15	96	5-Dec-15	78
5-Nov-15	63	11-Dec-15	80

MiSeq Illumina sequencing data

#OTU ID	COD to nitrate ratio = 1:1				COD to nitrate ratio = 2:1			
	P1	P2	P6	P10	P1	P2	P6	P10
denovo14365	51.1%	50.9%	14.7%	19.7%	16.5%	31.8%	22.4%	9.6%
denovo6318	0.1%	0.7%	0.2%	1.2%	0.4%	0.7%	1.5%	0.2%
denovo11351	8.6%	3.5%	2.2%	2.5%	5.3%	2.3%	4.0%	3.0%
denovo11003	2.4%	5.0%	13.5%	1.6%	0.3%	0.1%	0.1%	0.9%
denovo9022	4.2%	1.8%	0.6%	1.2%	0.8%	1.3%	0.6%	0.5%
denovo833	0.0%	0.6%	0.0%	17.9%	0.0%	0.0%	0.0%	0.5%
denovo4478	0.1%	1.1%	0.3%	0.8%	3.4%	2.2%	3.5%	0.3%
denovo4848	0.1%	0.2%	0.1%	0.1%	1.0%	0.2%	0.6%	0.3%
denovo12807	0.0%	0.0%	13.0%	0.0%	0.0%	0.0%	0.0%	0.0%
denovo4113	0.4%	0.1%	0.1%	0.2%	0.1%	0.1%	0.0%	0.1%
denovo12733	0.0%	0.5%	0.3%	0.2%	5.9%	1.7%	5.1%	0.1%
denovo1122	0.0%	0.1%	0.0%	0.1%	2.8%	0.3%	2.6%	9.0%
denovo9866	3.4%	3.2%	4.8%	8.7%	2.0%	3.2%	1.8%	5.9%
denovo7595	1.5%	5.7%	0.1%	0.6%	6.0%	3.5%	6.7%	1.6%
denovo11289	0.1%	0.4%	0.3%	0.5%	7.6%	1.0%	6.5%	0.3%
denovo4894	1.0%	0.3%	0.1%	0.2%	0.3%	3.8%	0.3%	0.2%
denovo1578	0.5%	0.7%	6.0%	1.0%	1.0%	1.8%	0.8%	1.4%
denovo4334	0.1%	0.1%	0.3%	0.3%	1.7%	5.3%	1.6%	1.4%
denovo14365	19.9%	24.6%	20.5%	25.2%	9.5%	10.0%	9.4%	8.7%
denovo6318	2.8%	1.1%	6.5%	1.0%	3.3%	2.6%	2.4%	2.4%
denovo11351	11.1%	19.4%	9.5%	10.6%	31.9%	25.8%	18.8%	16.7%
denovo11003	0.1%	0.2%	7.9%	0.6%	13.0%	21.8%	27.4%	19.7%
denovo9022	14.2%	18.8%	2.7%	11.4%	3.1%	2.5%	2.6%	2.6%
denovo833	0.0%	0.0%	0.0%	0.3%	0.0%	0.0%	0.0%	0.0%
denovo4478	16.3%	3.3%	5.0%	3.8%	9.3%	8.9%	10.4%	9.1%
denovo4848	0.4%	0.2%	0.5%	0.6%	0.0%	0.0%	0.1%	0.1%
denovo12807	0.0%	0.0%	0.0%	0.0%	0.0%	0.0%	0.0%	0.0%
denovo4113	0.3%	0.6%	0.5%	0.2%	0.6%	0.6%	0.5%	0.4%
denovo12733	1.6%	0.5%	9.6%	0.4%	4.8%	3.8%	4.2%	1.8%
denovo1122	0.0%	0.0%	0.0%	0.0%	0.0%	0.0%	0.0%	0.0%
denovo9866	0.5%	0.6%	0.1%	2.3%	0.0%	0.0%	0.0%	0.1%

#OTU ID	COD to nitrate ratio = 1:1				COD to nitrate ratio = 2:1			
	P1	P2	P6	P10	P1	P2	P6	P10
denovo7595	1.8%	1.2%	4.9%	1.9%	2.8%	2.8%	1.3%	3.7%
denovo11289	0.3%	0.1%	0.5%	0.1%	0.3%	0.4%	0.9%	0.7%
denovo4894	2.1%	1.4%	2.5%	1.4%	6.6%	5.4%	4.4%	7.2%
denovo1578	0.1%	0.1%	1.8%	1.0%	0.0%	0.0%	0.1%	0.5%
denovo4334	0.0%	0.0%	0.0%	0.1%	0.0%	0.0%	0.0%	0.2%

#OTU ID	COD to nitrate ratio = 3:1				COD to nitrate ratio = 5:1			
	P1	P2	P6	P10	P1	P2	P6	P10
denovo14365	19.9%	24.6%	20.5%	25.2%	9.5%	10.0%	9.4%	8.7%
denovo6318	2.8%	1.1%	6.5%	1.0%	3.3%	2.6%	2.4%	2.4%
denovo11351	11.1%	19.4%	9.5%	10.6%	31.9%	25.8%	18.8%	16.7%
denovo11003	0.1%	0.2%	7.9%	0.6%	13.0%	21.8%	27.4%	19.7%
denovo9022	14.2%	18.8%	2.7%	11.4%	3.1%	2.5%	2.6%	2.6%
denovo833	0.0%	0.0%	0.0%	0.3%	0.0%	0.0%	0.0%	0.0%
denovo4478	16.3%	3.3%	5.0%	3.8%	9.3%	8.9%	10.4%	9.1%
denovo4848	0.4%	0.2%	0.5%	0.6%	0.0%	0.0%	0.1%	0.1%
denovo12807	0.0%	0.0%	0.0%	0.0%	0.0%	0.0%	0.0%	0.0%
denovo4113	0.3%	0.6%	0.5%	0.2%	0.6%	0.6%	0.5%	0.4%
denovo12733	1.6%	0.5%	9.6%	0.4%	4.8%	3.8%	4.2%	1.8%
denovo1122	0.0%	0.0%	0.0%	0.0%	0.0%	0.0%	0.0%	0.0%
denovo9866	0.5%	0.6%	0.1%	2.3%	0.0%	0.0%	0.0%	0.1%
denovo7595	1.8%	1.2%	4.9%	1.9%	2.8%	2.8%	1.3%	3.7%
denovo11289	0.3%	0.1%	0.5%	0.1%	0.3%	0.4%	0.9%	0.7%
denovo4894	2.1%	1.4%	2.5%	1.4%	6.6%	5.4%	4.4%	7.2%
denovo1578	0.1%	0.1%	1.8%	1.0%	0.0%	0.0%	0.1%	0.5%
denovo4334	0.0%	0.0%	0.0%	0.1%	0.0%	0.0%	0.0%	0.2%
denovo14365	0.0%	0.0%	0.0%	0.0%	0.0%	0.0%	0.0%	0.0%
denovo6318	0.1%	0.0%	0.1%	0.3%	0.4%	0.5%	0.8%	1.3%
denovo11351	2.3%	2.1%	3.7%	2.2%	0.0%	0.0%	0.0%	0.0%
denovo11003	1.6%	2.2%	0.2%	1.5%	0.4%	0.4%	0.4%	0.9%
denovo9022	3.1%	2.6%	0.3%	2.1%	0.0%	0.0%	0.0%	0.0%

#OTU ID	COD to nitrate ratio = 3:1				COD to nitrate ratio = 5:1			
	P1	P2	P6	P10	P1	P2	P6	P10
denovo833	0.1%	0.0%	0.1%	1.1%	0.0%	0.1%	0.1%	0.1%
denovo4478	2.0%	3.0%	0.5%	2.2%	0.5%	0.6%	0.7%	0.7%
denovo4848	1.3%	1.7%	0.7%	2.8%	0.0%	0.0%	0.0%	0.0%
denovo12807	0.0%	0.0%	0.1%	0.0%	0.0%	0.0%	0.0%	0.0%
denovo4113	19.9%	24.6%	20.5%	25.2%	9.5%	10.0%	9.4%	8.7%
denovo12733	2.8%	1.1%	6.5%	1.0%	3.3%	2.6%	2.4%	2.4%
denovo1122	11.1%	19.4%	9.5%	10.6%	31.9%	25.8%	18.8%	16.7%
denovo9866	0.1%	0.2%	7.9%	0.6%	13.0%	21.8%	27.4%	19.7%
denovo7595	14.2%	18.8%	2.7%	11.4%	3.1%	2.5%	2.6%	2.6%
denovo11289	0.0%	0.0%	0.0%	0.3%	0.0%	0.0%	0.0%	0.0%
denovo4894	16.3%	3.3%	5.0%	3.8%	9.3%	8.9%	10.4%	9.1%
denovo1578	0.4%	0.2%	0.5%	0.6%	0.0%	0.0%	0.1%	0.1%
denovo4334	0.0%	0.0%	0.0%	0.0%	0.0%	0.0%	0.0%	0.0%

#OTU ID	COD to nitrate ratio = 10:1			
	P1	P2	P6	P10
denovo14365	1.3%	2.3%	1.9%	2.1%
denovo6318	36.5%	18.8%	35.7%	25.6%
denovo11351	1.6%	2.7%	2.9%	2.6%
denovo11003	0.6%	2.8%	1.2%	2.1%
denovo9022	8.6%	10.3%	7.8%	5.6%
denovo833	0.0%	0.0%	0.0%	0.0%
denovo4478	11.0%	8.4%	13.5%	10.1%
denovo4848	5.5%	11.2%	7.9%	13.2%
denovo12807	0.0%	0.0%	0.0%	0.0%
denovo4113	5.2%	12.2%	6.7%	7.7%
denovo12733	0.2%	0.2%	0.1%	0.2%
denovo1122	0.1%	0.2%	0.0%	0.0%
denovo9866	0.0%	0.0%	0.0%	0.1%

denovo7595	8.5%	5.2%	4.3%	4.9%
denovo11289	0.0%	0.0%	0.0%	0.3%
denovo4894	0.3%	0.5%	0.6%	0.8%

-Denovo sequences

#OTU ID	Sequences
denovo14365	ACGTAGGGTGCGAGCGTTAATCGGAATTACTGGGCGTAAAGCGTGCGCAGGC GGTTTTGTAAGACAGAGGTGAAATCCCCGGGCTCAACCTGGGAACTGCCTTTG TGACTGCAAGGCTGGAGTGCGGCAGAGGGGGATGGAATTCCGCGTGTAGCAG TGAAATGCGTAGATATGCGGAGGAACACCGATGGCGAAGGCAATCCCCTGGG CCTGCACTGACGCTCATGCACGAAAGCGTGGGGAGCAAACAG
denovo6318	ACGTAGGGTGCGAGCGTTAATCGGAATTACTGGGCGTAAAGCGTGCGCAGGC GGTTGTGTAAGACAGATGTGAAATCCCCGGGCTCAACCTGGGAACTGCGTTTG TGACTGCACAACTAGAGTACGGCAGAGGGAGGTGGAATTCCGCGTGTAGCAG TGAAATGCGTAGAGATGCGGAGGAACACCGATGGCGAAGGCAGCCTCCTGGG CCAGTACTGACGCTCATGCACGAAAGCGTGGGGAGCAAACAG
denovo11351	ACGAAGGGGGCTAGCGTTGTTCGGAATTACTGGGCGTAAAGCGCATGTAGGC GGATATTTAAGTCAGGGGTGAAATCCCAGAGCTCAACTCTGGAACTGCCTTTG ATACTGGGTATCTTGAGTATGGAAGAGGTAAGTGGAATTCCGAGTGTAGAGGT GAAATTCGTAGATATTCGGAGGAACACCAGTGGCGAAGGCGGCTTACTGGTCC ATTACTGACGCTGAGGTGCGAAAGCGTGGGGAGCAAACAG
denovo11003	ACGTAGGTGGCAAGCGTTGTCCGGATTTATTGGGCGTAAAGCGAGCGCAGGC GGTTCCTTAAGTCTGATGTGAAAGCCCACGGCTTAACCGTGGAAGGTCATTGG AAACTGGGGAACTTGAGTGCAGAAGAGGAGAGTGGAATTCCATGTGTAGCGGT GAAATGCGTAGATATATGGAGGAACACCAGTGGCGAAGGCGACTCTCTGGTCT GTAACTGACGCTGAGGCTCGAAAGCGTGGGGAGCAAACAG
denovo9022	ACGGAGGGTGCAAGCGTTATCCGGATTTATTGGGTTTAAAGGGTCCGTAGGCG GACTTATAAGTCAGTGGTGAAAGCCTGTCGCTTAACGATAGAACTGCCATTGA TACTGTAAGTCTTGAGTATATTTGAGGTAGCTGGAATAAGTAGTGTAGCGGTG AAATGCATAGATATTACTTAGAACACCAATTGCGAAGGCAGGTTACCAAGATA TAACTGACGCTGAGGGACGAAAGCGTGGGTAGCGAACAG
denovo833	ACGTAGGAGGCGAGCGTTATCCGGATTCACTGGGCGTAAAGCGCGTGCAGGC GGTTCGGTAAGTTGGGCGTGAAATCTCCCGGCTCAACTGGGAGAGGTCGTTCA ATACTACCGGACTTGAGAGCGATAGAGGAAAATGGAATTCCCGGTGTAGTGGT

#OTU ID	Sequences
	GAAATGCGTAGATATCGGGAGGAACACCAGTGGCGAAAGCGATTTTCTGGATC GTTTCTGACGCTCAGACGCGAAAGCTAGGGTAGCAAACGG
denovo4478	ACGTAGGGTGCGAGCGTTAATCGGAATTACTGGGCGTAAAGCGTGCGCAGGC GGTTGTGTAAGACAGGCGTGAAATCCCCGGGCTCAACCTGGGAACTGCGCTTG TGACTGCACAGCTAGAGTACGGCAGAGGGGGGTGGAATTCCACGTGTAGCAG TGAAATGCGTAGAGATGTGGAGGAACACCGATGGCGAAGGCAGCCCCCTGGG CCGATACTGACGCTCATGCACGAAAGCGTGGGTAGCAAACAG
denovo4848	ACGTAAGGGGCGAGCGTTGTTCGGAATTATTGGGCGTAAAGGGCGCGTAGGC GGTCCTGTAAGCCCGGCGTGAAAACCTGGAGCTCAACTCCGGGCCTGCGCTG GGAACTGCGGGACTAGAGTCATGGAAGGGAAGTTGGAATTCCAGGTGTAGGG GTGAAATCTGTAGATATCTGGAAGAACACCGGTGGCGAAGGCGAACTTCTGGC CAATGACTGACGCTGAGGCGCGAAAGTGCGGGGAGCAAACAG
denovo12807	ACGTAGGTGGCAAGCGTTGTCCGGAATTATTGGGCGTAAAGCGCGCGCAGGC GGTTCCTTAAGTCTGATGTGAAAGCCCCCGGCTCAACCGGGGAGGGTCATTGG AAACTGGGGAACTTGAGTGCAGAAGAGGAGAGCGGAATTCCACGTGTAGCGG TGAAATGCGTAGAGATGTGGAGGAACACCAGTGGCGAAGGCGGCTCTCTGGT CTGTAACTGACGCTGAGGCGCGAAAGCGTGGGGAGCGAACAG
denovo4113	ACGTAGGTGGCAAGCGTTGTCCGGATTTACTGGGCGTAAAGGGTGCGTAGGC GGACCTTTAAGTGAGATGTGAAATCCCCGAGCTTAACTTGGGGGCTGCATTTC AAACTGGAAGGCTGGAGTGCAGGAGAGGAGGATGGAATTCCTAGTGTAGCAG TGAAATGCGTAGAGATTAGGAAGAACACCAATGGCGAAGGCGACTCTCTGGAC TGGAACTGACGCTGAGGCACGAAAGCGTGGGGGGCAAACAG
denovo12733	ACGTAGGGTGCGAGCGTTAATCGGAATTACTGGGCGTAAAGCGTGCGCAGGC GGTTTTGTAAGACAGCTGTGAAATCCCCGGGCTCAACCTGGGAACTGCGGTTG TGACTGCAAGACTGGAGTACGGCAGAGGGGGGTGGAATTCCTGGTGTAGCAG TGAAATGCGTAGATATCAGGAGGAACACCGATGGCGAAGGCAGCCCCCTGGG CCTGTACTGACGCTCATGCACGAAAGCGTGGGGAGCAAACAG
denovo1122	ACGTAGGATCCGAGCGTTATCCGAATTTACTGGGCGTAAAGCGCGTGCAGGCG GTTTGGCAAGTTGGATGTAAAAGCTCCTGGCTCAACTGGGAGAGGCCGTTCAA AACTACCAGACTAGAGGGCGACAGAGGGAGGTGGAATTCCCGGTGTAGTGGT GAAATGCGTAGATATCGGGAGGAACACCTGTGGCGAAAGCGGCCTCCTGGGT CGTACCTGACGCTCAGACGCGAAAGCTAGGGGAGCGAACGG
denovo9866	ACGTAGGGGGCAAGCGTTGTCCGGATTTACTGGGTGTAAAGGGCGCGCAGGC GGGATAACAAGTCAGAGGTGAAATCCTACAGCTTAACTGTAGAACTGCCTTTG

#OTU ID	Sequences
	ATACTGTTATTCTTGAGTTCGGAAGAGAGAGACGGAATTCCAGGTGTAGTGGT GAAATACGTAGATATCTGGAAGAACACCAGTTGCGAAGGCGGTCTCTTGGTCC GATACTGACGCTGAGGCGCGAAAGCGTGGGGAGCAAACAG
denovo7595	ACGGAGGGTGCAAGCGTTAATCGGAATTACTGGGCGTAAAGCGCACGCAGGC GGTTGGATAAGTCAGATGTGAAAGCCCCGGGCTCAACCTGGGAACTGCATTTG AAACTGTTCGACTAGAGTCTTGTAGAGGGGGGTAGAATTCCAGGTGTAGCGGT GAAATGCGTAGAGATCTGGAGGAATACCGGTGGCGAAGGCGGCCCCCTGGAC AAAGACTGACGCTCAGGTGCGAAAGCGTGGGGAGCAAACAG
denovo11289	ACGTAGGGTGCGAGCGTTAATCGGAATTACTGGGCGTAAAGCGTGCGCAGGC GGTTTGCTAAGACAGGTGTGAAATCCCCGGGCTTAACCTGGGAACTGCGCTTG TGACTGGCAGGCTAGAGTACGGCAGAGGGGGGTGGAATTCCTGGTGTAGCAG TGAAATGCGTAGAGATCAGGAGGAACACCGATGGCGAAGGCAGCCCCCTGGG CCTGTACTGACGCTCATGCACGAAAGCGTGGGGAGCAAACAG
denovo4894	ACGAAGGGGGCTAGCGTTGTTCGGAATTACTGGGCGTAAAGGGCGCGTAGGC GGTTTGTTAAGTCAGGCGTGAAAGCCCTGGGCTCAACCTGGGAGGTGCGCTTG ATACTGGCAGGCTTGAGTGCAGGAGAGGATGGTGGAATTCCCAGTGTAGAGGT GAAATTCGTAGATATTGGGAAGAACACCGGTGGCGAAGGCGGCCATCTGGACT GCAACTGACGCTGAGGCGCGAAAGCGTGGGGAGCAAACAG
denovo1578	ACGGAGGATGCAAGCGTTATCCGGATTCATTGGGTTTAAAGGGTGCGTAGGCG GACTATTAAGTCAGTGGTGAAATCCTGCAGCTTAACTGCAGAACTGCCATTGA TACTGATAGCCTTGAGTTTGGTTAAGGTAGGCGGAATGTGTAATGTAGCGGTG AAATGCTTAGATATTACACAGAACACCAATTGCGTAGGCAGCTTACTGAGCCG ACACTGACGCTGAGGCACGAAAGCGTGGGGATCGAACAG
denovo4334	ACGTAGGAAGCGAGCGTTATCCGGATTTACTGGGCGTAAAGCGTGTGTAGGCG GTTTGACAAGTTGGATGTGAAAGCTCCTGGCTTAACTGGGAGAGGTCGTTCAA AACTGTCAGACTTGAGAGTGGTAGAGGGAGGTGGAATTCCGGGTGTAGTGGT GAAATGCGTAGATATCCGGAGGAACACCAGTGGCGAAAGCGGCCTCCTGGCC CATTTCTGACGCTCAGACACGAAAGCTAAGGTAGCAAACGG

VITA

Name : Phatchariya Rungkitwatananukul

Birth date : January, 25, 1984

Birth place: Kanchanabury, Thailand

ACADEMIC BACKGROUND

2013 Ph.D. Candidate at Department of Environmental Engineering, Faculty of Engineering, Chulalongkorn University, Thailand.

2011 Master of Engineering, M.Eng. (Environmental Engineering), Department of Environmental Engineering, Faculty of Engineering, Chulalongkorn University, Thailand.

2007 Bachelor of Science, B.Sc. (Environmental Science), Department of Environmental Science, Faculty of Science and Technology, Thammasat University, Thailand.